Revisiting the roles of replicase complex proteins in tobamovirus replication and suppression of RNA silencing.

Inauguraldissertation

zur

Erlangung der Würde eines Doktors der Philosophie

vorgelegt der

Philosophisch-Naturwissenschaftlichen Fakultät

der Universität Basel

von

Hortensia Nachelli Malpica López

aus México

Basel, 2017

Originaldokument gespeichert auf dem Dokumentenserver der Universität Basel

edoc.unibas.ch

Genehmigt von der Philosophisch-Naturwissenschaftlichen Fakultät

auf Antrag von

Prof. Dr. Thomas Boller, PD Dr. Mikhail M. Pooggin und PD Dr. Todd Blevins.

Basel, den 20. Juni 2017

Prof. Dr. Martin Spiess

Dekan

CONTENTS

Acknowledgements

I would like to express my gratefulness to Prof. Thomas Boller and PD Dr. Mikhail Pooggin for giving me the opportunity to get involved as a PhD student in this project and to PD Dr. Todd Blevins for being part of my thesis committee. A special thanks to Dr. Pooggin for his valuable guidance as supervisor during the project's performance and completion, and for sharing with me his scientific knowledge through fruitful discussions that made the project so interesting and gratifying.

I also would like to thank the Botanical Institute of the University of Basel, the Swiss National Foundation and the "Freiwillige Akademische Gesellschaft Basel", for providing us with the necessary resources to develop and complete the present work.

My sincere thankfulness to my lab colleagues and friends that in different ways, were always supporting and accompanying me throughout this enterprise making it more satisfying and enjoyable. Thank you Rajesh, Anna, Jonathan, Victor and Silvia, as well as my recognition to all the lab guests from which I learned so much too. My acknowledgement also to the rest of my colleagues at the Botanical Institute and to our staff members Vaclav, Giacomo, Maura, Markus and Franziska for their exceptional support.

My deep gratitude to Prof. Thomas Hohn and Prof. Barbara Hohn for accepting me in the lab when I was quite new in Switzerland, for sharing their deep knowledge, and for motivating new generations to be curious, analytical and passionate while doing science.

Specially, I would also like to profoundly thank my parents for their endless love and encouragement, and for being my first instructors in life. Thanks also to my beloved sisters for always being there.

Finally and with all my love, I would like to deeply thank my husband Ulrich and my children, Santiago and Isabel, for their infinite patience and unconditional support and love throughout this journey. This work belongs also to them.

Preface

Just as other organisms, plants are also susceptible to bacterial, fungal or viral diseases. Recently, deeper knowledge on the different mechanisms by which plants defend themselves against pathogens has come to light, but further research needs to be done to clearly understand the plant defense complete network.

The present work had the aim to gain insight on the molecular events that take place in plants during viral infection, particularly related to RNA silencing, that is one of the most important plant defense mechanisms against viruses and that is present also in animals. One particular interest was also to understand more clearly the molecular strategies that some viruses display, like the RNA *Oilseed rape mosaic tobamovirus* (ORMV) in this case, to counteract this type of plant defense response. Oilseed rape infection by ORMV causes large losses in oilseed rape crops, one of the most important sources for vegetable oils all around the world.

Along the introduction of the present work, updated information on what is currently known about the RNA silencing pathways in plants will be briefly mentioned, including the biogenesis of endogenous miRNAs and siRNAs and their function, as well as the production of viral siRNAs in infected hosts. The replication mechanism of tobamoviruses in plant cells will be described, as well as the production of double stranded RNA viral replication intermediates, responsible of triggering the RNA silencing machinery against the virus. Some of the currently known strategies employed by different viruses to counteract the RNA silencing machinery will also be discussed. Among them, the production of viral silencing suppressors and their effect on the plant's defense response at different layers.

Our findings bring new knowledge about the interaction between plants and viruses during infection, and raise new questions about ORMV as plant pathogen, related to its effects on the RNA silencing machinery and the immune responses of the host plant, and to the mechanisms the virus employs to neutralize them.

Abstract

Tobamoviral replicase possesses an RNA-dependent RNA polymerase (RDR) domain and is translated from genomic (g)RNA via a stop codon readthrough mechanism at a one-to-ten ratio relative to a shorter protein lacking the RDR domain. The two proteins share methyltransferase and helicase domains and form a heterodimer implicated in gRNA replication. The shorter protein is also implicated in suppressing RNA silencing based antiviral defenses. Using a stop codon mutant of Oilseed rape mosaic tobamovirus (ORMV), we demonstrate that the readthrough replicase (p182) is sufficient for gRNA replication and for subgenomic RNA transcription during systemic infection in *Nicotiana benthamiana* and *Arabidopsis thaliana*. However, the mutant virus displays milder symptoms and does not interfere with HEN1-mediated methylation of viral short interfering (si)RNAs or plant small (s)RNAs. The mutant virus tends to revert the stop codon, thereby restoring expression of the shorter protein (p125), even in the absence of plant Dicer-like activities that generate viral siRNAs. Plant RDR activities that generate endogenous siRNA precursors do not prevent replication or movement of the mutant virus, and double-stranded precursors of viral siRNAs representing the entire virus genome are likely synthesized by p182. Transgenic expression of p125 partially recapitulates the ORMV disease symptoms associated with overaccumulation of plant sRNAs. Taken together, the readthrough replicase p182 is sufficient for viral replication and transcription but not for silencing suppression. By contrast, the shorter p125 protein suppresses silencing, provokes severe disease symptoms, causes overaccumulation of unmethylated viral and plant sRNAs but it is not an essential component of the viral replicase complex.

Section I. RNA silencing pathway

1.1. RNA silencing

Viruses are obligate intracellular pathogens which have the capacity to infect most living organisms, by taking advantage of the molecular mechanisms that take place in the host cells, in order to replicate and spread from cell to cell, and eventually cause disease. Viruses trigger defense responses in the host upon infection, once their DNA, RNA or proteins are detected by the infected organism. These mechanisms range from RNA interference (RNAi), a mechanism mainly used to eliminate viruses by plants and other eukaryotes including protozoa (*Trypanosoma*), yeast (*Candida albicans*), nematodes (*Caenorhabditis elegans*), flies (*Drosophila melanogaster*) and even mammals (mouse embryonic stem cells), to the sophisticated interferon-regulated gene response which conforms part of the immunological and antiviral response in higher animals (Ding 2010; Csorba et al., 2009; Ding and Voinnet 2007; Maillard et al., 2013).

RNAi, also known as RNA silencing, is an eukaryotic gene regulation mechanism. In plants, it plays an important role in many biological processes including plant development, maintenance of the genome integrity against mobile transposons, stress response and notably in antiviral defense. In *Arabidopsis,* RNAi is initially triggered by double-stranded RNAs that are processed by one of the four RNAse III-like DICER enzymes (DCL1, DCL2, DCL3 and DCL4), into 21-24 nucleotide small RNAs that are divided into two different classes: small interfering RNAs (siRNAs) that are produced from sequential dicing of perfect or near perfect long dsRNA, and microRNAs (miRNAs) which are excised from imperfectly folded precursor RNAs (Baulcombe, 2004; Bernstein et al., 2001; Bartel, 2004). As a particular feature, all plant siRNAs and miRNAs have a 5' phosphate and a 3'-terminal 2'-*O*-methyl group added by the enzyme HUA ENHANCER 1 (HEN1) (Yu et al., 2005; Zhai et al., 2012) in order to confer them stability.

Besides the production of endogenous small RNAs like trans-acting siRNAs (tasi-RNAs), miRNAs, and natural antisense transcripts siRNAs (NAT-siRNAs) among others, also viral siRNAs (viRNAs) can be generated by the RNA silencing machinery, once the dsRNAs derived from DNA or RNA viruses are recognized by DICER enzymes in infected plants (Blevins et al., 2006).

Upon DCLs processing, endogenous and viral sRNAs are incorporated into one of ten AGO proteins in *Arabidopsis* to form the RNA induced silencing complex (RISC), which by complementarity can target messenger RNAs and induce their post transcriptional gene silencing (PTGS) by endonucleolytic cleavage (slicing) or translational repression (Almeida and Allshire 2005; Brodersen et al., 2008; Kim et al., 2014). RISC can also induce transcriptional gene silencing (TGS) through DNA methylation or chromatin modifications of the targeted genes (Law et al., 2010; Creamer and Partridge 2011).

A more detailed description of the RNA silencing process and some of the its main components such as proteins and small RNAs are explained below.

1.2. DICER-like proteins

Dicer RNase-III are endoribonucleases that process long double stranded RNA (dsRNA) into small RNA duplexes bearing a 2 nucleotide (nt) 3' overhang and a 5' monophosphate. These enzymes possess a DEXD box helicase domain at the N terminus, a domain of unknown function (DUF283), a PIWI/ARGONAUTE/ZWILLE (PAZ) domain, two RNAse III domains and one or two dsRNA binding domains (dsRBD) (Margis et al., 2006; Fukudome and Fukuhara, 2016). It is believed that their small RNA product size are determined by the distance separating the PAZ and catalytic domains of each Dicer-like protein (Park et al., 2011), and by the availability of a determined DCL in a specific tissue or cells.

Arabidopsis thaliana encodes four DICER paralogues with specialized functions (Baulcombe 2004). Dicer-like 1 (DCL)-1 produces miRNAs from non coding, imperfect stem-loop precursor RNAs (Voinnet, 2009), while 21,22 and 24 nt long short interfering (si)RNAs are produced from long, perfectly or nearly perfectly paired double stranded RNAs through the action of DCL4, DCL2, and DCL3, respectively (Brodersen and Voinnet, 2006; Vazquez, 2006; Chapman and Carrington, 2007). DCL4 and DCL2 are redundant and recent reports suggest that DCL2 also stimulates the production of secondary siRNAs as well as transitivity, which refers to the production of new siRNAs corresponding to sequences located outside the primary targeted region of a transcript, while DCL4 is more efficient in synthesizing primary siRNAs (Parent et al., 2015). DCL3 mainly produces 24-nt repeat associated siRNAs derived from transposons and repetitive elements and is involved in TGS.

Double stranded RNA intermediates derived from DNA or RNA viruses are also accessible to DCLs, and a strong hierarchy can be observed among these enzymes regarding viral small RNAs production. DCL4 and DCL2 are involved in the production of 21- and 22-nt siRNAs from RNA viruses (Deleris et al., 2006; Donaire et al., 2008; García-Ruíz et al., 2010; Qu et al., 2008), while all four DCLs produce 21-nt (DCL4 and DCL1) , 22-nt (DCL2) and 24-nt (DCL3) from DNA viruses (Akbergenov et al., 2006, Blevins et al., 2006).

1.3. AGO proteins

The AGO family received its name after AGO1 in *Arabidopsis thaliana*, because the loss of this gene leads to a plant exhibiting tubular shaped leaves that resemble small squids (*Argonautus*) (Bohmert et al.,1998). AGO proteins are present in bacteria, archae and eukaryotes and it has been observed that the number of AGO family members varies greatly among different species. For example, it is known that only one AGO protein is present in the yeast *Schizosaccharomyces pombe,* while there are four AGOs and four PIWIs in humans, 15 in poplar and 10 in *Arabidopsis* (Carmell et al., 2002; Morel et al., 2002).

AGO proteins are effectors of RNA interference in eukaryotes (Meister, 2013). They bind small RNAs and guide them to silence target RNA and DNA at a post-transcriptional or transcriptional level, respectively. In plants, it is believed that duplication events may have given functional diversification of AGOs defining their particular biochemical activities (Havecker et al., 2010; Mi et al., 2008). Studies have shown that some of them have a slicer activity since they show similarity to RNase H, as is the case of AGO1, AGO2, AGO4, AGO7 and AGO10 in *Arabidopsis* (Baumberger and Baulcombe 2005; Qi et al., 2005; Song et al., 2004; Liu et al., 2004; Carbonell et al., 2012; Qi et al., 2006; Tomari and Zamore 2005; Höck and Meister 2008; Montgomery et al., 2008; Takeda et al., 2008; Ji et al., 2011). AGO-sRNA

compexes target endogenous and exogenous genes/transcripts to regulate plant development, as well as plant defense against diverse pathogens like bacteria and viruses, and some of them seem to be programmed with virus derived siRNAs to directly target viral RNA (Schuck et al., 2013, Omarov et al., 2007, Pantaleo et al., 2007).

1.3.1. AGOs domains and loading

Argonautes in eukaryotes have 4 disctinct domains: a variable amino-terminal (N) domain and 3 conserved domains including PAZ (PIWI-ARGONAUTE-ZWILLE), MID (middle) and PIWI (Tolia and Joshua-Tor, 2007). While the function of the N domain is not yet clear, the PAZ domain harbors an oligonucleotide binding fold that allows AGO proteins to bind single stranded nucleic acids (Lingel et al., 2003; Song et al., 2003; Yan et al., 2003). By binding the 3' end of the guide strand into a specific binding pocket, the PAZ domain anchors sRNAs (Lingel et al., 2004; Ma et al., 2004). The PAZ domain also contributes to the unwinding of the duplexes (Gu et al., 2012).

The MID domain specifically recognizes the 5' nucleotide of small RNA and is responsible for the binding preferences of different AGO proteins for small RNAs with different 5' nucleotides (Frank et al., 2010, Frank et al., 2012). Indeed, in order to work properly, small RNAs need to be correctly sorted into specific AGO complexes and in plants, the identity of the 5' nucleotide plays a key role in this process (Mi et al., 2008; Montgomery et al., 2008; Takeda et al., 2008). *Arabidopsis* AGO1 preferentially will bind sRNAs with a 5'U, AGO2 sRNAs with a 5'A and AGO5 sRNAs with a 5'C. AGO4 primarily will associate with sRNAs beginning with a 5'A.

The PIWI domain, on the other hand, enables some AGO proteins, but not all, to cleave the target RNAs complementary to the bound sRNAs (Song et al., 2004; Rivas et al., 2005).

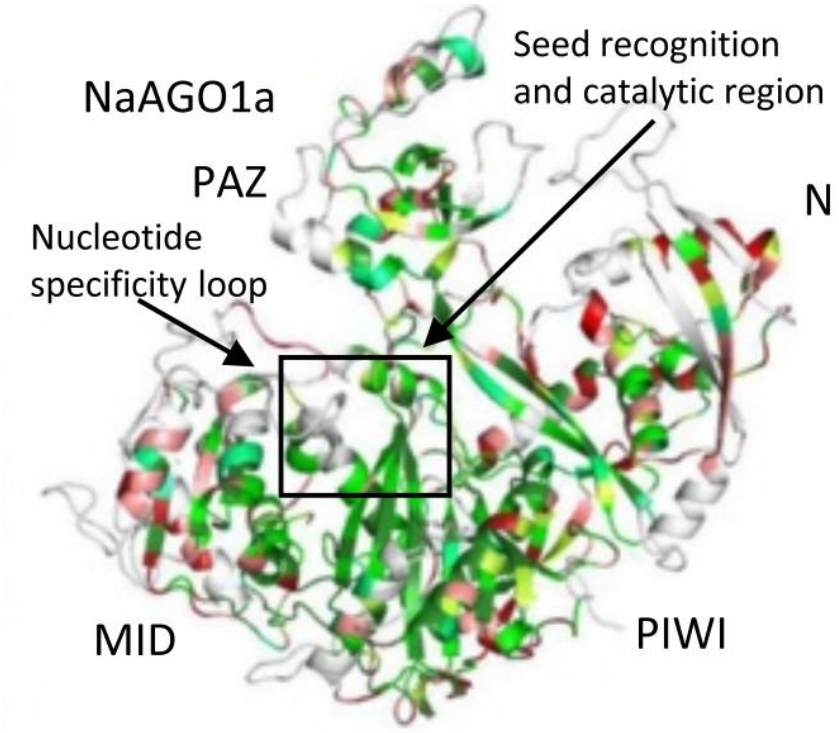

Singh et al., 2015

Figure 1.1. Model structure of *Nicotiana attenuata* AGO1 showing the different domains: N, PAZ, MID, PIWI.

Once the sRNA duplex has been loaded in the AGO protein, the passenger strand of the duplex is selectively displaced and degraded while the guide strand is retained to form the mature RNA-induced silencing complex (RISC). However, in some cases it has been shown that also the passenger strand can be retained in the AGO complex making RISC still functional (Manavella et al., 2012; Zhang X. et al., 2011).

Based on phylogenetic relationships, plant AGO proteins are grouped in three major clades: AGO1/5/10, AGO2/3/7 and AGO4/6/8/9.

1.3.2. The AGO1/5/10 clade

Arabidopsis AGO1 is the effector protein that bound to miRNAs and ta-siRNAs regulates the expression of genes involved in numerous developmental and physiological processes. Additionally, AGO1 also functions in defense against some viruses upon loading viral siRNAs (Morel et al., 2002; Zhang[b] et al., 2006; Takeda et al., 2008; Wang et al., 2011). Indeed, studies identified AGO1 as the major antiviral AGO against suppressor-defective *Turnip crinkle virus* (TCV) in *Arabidopsis* (Qu et al., 2008), as well as against *Brome mosaic virus* (BMV) (Dzianott et al., 2012), *Cucumber mosaic virus* (CMV) (Wang et al., 2011) and *Turnip mosaic virus* (TuMV) (García-Ruíz et al., 2015).

AGO1 is similar to AGO10 but both have a different pattern of expression. For example, in contrast with the ubiquitous expression of AGO1, AGO10 is expressed in provasculature, adaxial leaf primordial and the meristem (Moussian et al., 1998; Lynn et al., 1999), playing

an important role in the maintenance of undifferentiated stem cells present at the shoot apical meristem. AGO10 can also bind viral siRNAs and cooperate with AGO1 to have a modest antiviral effect in influorescences as shown in *Arabidopsis* for *Turnip mosaic virus* (TuMV) (García-Ruíz et al., 2015).

AGO 5 is confined to megaspore mother cells and promotes megagametogenesis (Tucker et al., 2012). It has been shown to bind viral siRNAs of *Cucumber mosaic virus,* mainly those starting with a 5' cytosine (CMV) (Takeda et al., 2008), and its is induced by *Potato virus* X (PVX) infection. Together with AGO2 it is able to restrict PVX infection (Brosseau and Moffett 2015).

1.3.3. The AGO2/3/7 clade

Together with AGO1, *Arabidopsis* AGO2 plays an important role in antiviral defense and has been shown to be required for resistance to a broad spectrum of plant viruses (Harvey et al., 2011; Jaubert et al., 2011; Wang et al., 2011; Carbonell et al., 2012; Zhang X. et al., 2012; García-Ruíz et al., 2015). Its antiviral activity has also been reported in *Nicotiana benthamiana* (Scholthof et al., 2011). AGO2 binds viral siRNAs beginning with a 5' terminal A and its catalytic activity is essential for its role in antiviral defense (Carbonell et al., 2012). Supporting the former, Schuck et al., (2013) demonstrated that synthetic viral siRNAs loaded on AGO2 and AGO3 could target *in vitro* viral RNAs for cleavage, thereby inhibiting viral replication. Other studies have shown that AGO1 and AGO7 work together to ensure efficient clearance of viral RNAs, where AGO1 mainly targets viral RNAs containing complex structures, whereas AGO7 favors less structured RNA targets (Qu et al., 2008).

1.3.4. The AGO4/6/8/9 clade

Arabidopsis AGO4 is the effector protein that bound to 24nt long hc-siRNAs directs DNA methylation of the genome through the RNA-directed DNA methylation (RdDM) pathway (Pontes et al., 2006; Qi et al., 2006). AGO4 is also thought to be involved in plant defense against DNA viruses, since its presence is required in tissues that have recovered from infection and where the *Beet curly top virus* (BCTV) *L2* mutant, a L2 RNA silencing suppressor mutant, has been found to be hypermethylated (Raja et al., 2008). While AGO4 is expressed throughout the plant, AGO6 is expressed in shoots and apical meristems (Zheng at el 2007; Havecker et al., 2010; Eun et al., 2011), but both are required for DNA methylation at most of their target loci. AGO4 and AGO6 have non-redundant roles and it has been suggested that they may act sequentially to mediate DNA methylation (Duan et al., 2015).

1.4. RDRs

In plants there are two classes of siRNAs that can be identified: the primary siRNAs that are produced by the cleavage of an initial double stranded RNA trigger by DCLs, and the secondary siRNAs which require an RDR enzyme for their biogenesis (Ruíz-Ferrer et al.,. 2009; Donaire et al., 2008; Qu F, 2010; Wang et al., 2010; Wassenegger et al., 2006; García Ruíz et al., 2010). RDRs convert single-stranded RNAs into dsRNAs by primer independent (Tang et al., 2003; Curaba and Chen 2008) or primer dependent mechanisms using a small RNA as a primer (Moissiard et al., 2007; Voinnet, 2008; Devert et al., 2015). The dsRNA products of RDRs are sliced by DCLs into secondary 20-24 nt siRNA duplexes.

RDRs own a conserved RNA dependent RNA polymerase catalytic domain and are found in RNA viruses, plants, fungi, protists and some lower animals, but are absent in *Drosophila*, mice and humans (Willmann et al., 2011). *Arabidopsis thaliana* contains six RDRs (Wassenegger and Krczal, 2006). RDR1, RDR2 and RDR6 share the C-terminal canonical DLDGD motif present in eukaryotes, and RDR3, RDR4 and RDR5 share an atypical DFDGD domain whose function has not been determined yet.

Arabidopsis RDR2 is involved in the production of the 24-nt heterochromatic siRNAs and it has been associated to transgene silencing, genome maintanence and female gamete formation. RDR6, together with its partner SUPPRESSOR OF GENE SILENCING 3 (SGS3), is involved in the biogenesis of endogenous ta-siRNAs (Rajeswaran and Pooggin., 2012) and NAT-siRNAs and has been associated with stress responses, pathogen resistance, leaf development, self incompatibility, female gamete formation and transgene silencing. Like RDR2 and RDR6, RDR1 also has effects on the endogenous populations of *Arabidopsis* small RNAs but still studies need to be done to clarify its function (Kasschau et al., 2007). So far, the principle role of RDR1 has been defined in the production and amplification of exogenous, virus-derived siRNAs in infected plants. Studies in *Arabidopsis rdrd* mutants infected with mutant viruses deficient in silencing suppression proteins, have recently shown that resistance to different positive-strand RNA viruses depends on the production of viral secondary siRNAs by RDR1, RDR2 or RDR6 that amplify the antiviral response (Donaire at al 2008, García-Ruíz et al., 2010, Wang et al., 2010). In RNA virus-infected *Arabidopsis*, RDR1 is induced to produce siRNAs from multiple genes; (Yu et al., 2003; Wang XB et al., 2010).

1.5. HEN1

The stability and function of small RNAs is affected by various modifications, such as methylation, uridylation, adenylation, and RNA editing (Kim et al., 2010, Ji and Chen 2012). In plants, the HEN1 protein has been shown to work as a methyltransferase which is specific for double stranded sRNAs and whose function is to add a 2'-*O*-methyl group on the 3'-terminal nucleotide of template miRNAs and siRNAs (Yu et al., 2005; Yang et al., 2006) . Even though HEN1 orthologs are present in other organisms like bacteria and animals (Mui Chan et al., 2009), these can only methylate single stranded RNA, in contrast with HEN1 from plants which methylates only dsRNA duplexes (Yang et al., 2006). In *Arabidopsis* it was was shown that full methylation of the duplex (guide and passenger strand) is achieved via intermediate hemi-methylated states, where the successive methylation of the two strands occurs in a non-processive manner (Plotnikova et al., 2013).

The loss of HEN1 can have a widespread impact on small RNAs, especially in plants in which all known silencing pathways include the methylation activity of HEN1. In contrast to animals, it has been observed that nearly all plant miRNA/miRNA* duplexes are methylated at their 3′-termini by HEN1, which protects them from the nucleotidyl transferase HEN1 SUPPRESSOR (HESO1) mediated 3′-end uridylation and subsequent degradation (Zhao Y et al., 2012). Studies have shown that HESO1 interacts with AGO1 to uridylate AGO1-bound miRNAs *in vitro* (Ren et al., 2014). It is thought that this U tailing could be the result of deprotection, due to the fact that the addition of uridine (U) nucleotide at the 3' end of sRNAs in *hen1* mutants by HESO1 has been observed together with increased rates of degradation (Li et al., 2005; Yu et al., 2005). Interestingly, RNA gel blot analysis of miRNAs in a *hen1* background, have shown that they display a laddering of length reflecting the 3' tails, while sizes shorter than the wild type have also been detected, suggesting that 3' truncation also occurs. Deep sequencing analysis of miRNAs in a *hen1* background have confirmed both conditions (Zhai J et al., 2013). On the other hand, the presence of one or few post-transcriptionally added adenylic residues at the 3' end of plant miRNAs has also been observed and experiments *in vitro* showed that 3' adenylation reduces miRNA degradation rate (Lu et al., 2009).

It has been suggested that the methylation of miRNAs and siRNAs by HEN1 could also prevent the action of RNA-dependent RNA polymerases (RdRPs) from using the small RNAs as primers. The effect of the methyl group on the ability of RdRPs to use the small RNAs as primers would however need to be experimentally evaluated (Li et al., 2005). Within this context, Devert and his collaborators recently showed that recombinant and purified RDR2 and RDR6 can initiate dsRNA synthesis either by elongation of 21- to 24- nucleotides RNAs hybridized to complementary RNA template or by elongation of self-primed RNA template (Devert et al., 2015).

Section II. Endogenous and viral small RNAs

2.1. Primary and secondary siRNAs

In plants, endogenous siRNAs of different size classes are processed by DCL4 (21-nt), DCL2 (22-nt) or DCL3 (24-nt) from perfect dsRNA precursors produced by RDRs or from overlapping sense and antisense Pol II transcripts. While the RDR6/DCL4-dependent 21-nt secondary siRNAs (tasiRNAs and phased siRNAs) silence genes post-transcriptionally, the RDR2/DCL3-dependent 24-nt heterochromatic siRNAs silence repetitive DNA sequences or transposons by a mechanism known as transcriptional gene silencing (TGS) (Henderson et al., 2006; Pontes et al., 2006; Xie et al., 2004).

Secondary siRNAs are produced when an initiating small RNA (a miRNA or another secondary small RNA) targets and cleaves a primary transcript, leading to the recruitment of RDR6 that synthesizes the complementary RNA strand, so that DCL4 processes the dsRNA into secondary siRNAs. Secondary siRNAs are phased due to the succesive catalytic processing by DCL4 from a consistent dsRNA terminus, defined by the initial cleavage by a small RNA of the primary transcript. Studies support the idea that both 21-nt and 22-nt miRNAs are able to cleave their target but that only the 22-nt miRNAs are the ones able to trigger the production of secondary siRNAs (Cuperus et al., 2010). It has been shown for example, that *Arabidopsis* miR168, miR173 and miR472 are able to trigger the production of

phased siRNAs from their targets, in their 22 nt form, but not in their 21 nt form (Chen et al., 2010).

Secondary siRNAs that are able to act in *trans* to silence different mRNA targets are called *trans*-acting siRNAs (tasiRNAs) (Allen et al., 2005; Yoshikawa et al., 2005) (Figure 2.1). *Arabidopsis* tasiRNAs biogenesis is initiated by AGO-mediated cleavage of non-coding TAS transcripts generated from four families of TAS genes. TAS1a/b/c/ and TAS2 transcripts undergo an initial AGO1/miR173 mediated cleavage at their 5' end after which the 3' fragment is converted to dsRNA by RDR6 and sequentially processed by DCL4 to produce 21-nt siRNA duplexes. TAS1 and TAS2 tasiRNAs target genes encoding pentatricopeptide repeats (PPR) proteins (Peragine et al., 2004; Vazquez et al., 2004; Allen et al., 2005), which are RNA binding proteins involved in post-transcriptional processes such as RNA editing and splicing in mitochondria and chloroplasts (Schmitz-Linneweber and Small 2008). Through this process, TAS1 and TAS2 tasiRNAs coordinate the repression of this large gene family.

TAS 4 siRNAs are produced in a similar way as TAS1 and TAS2 siRNAS but the transcripts cleavage is guided by AGO1/miR828. In *Arabidopsis*, it has been shown that tasiRNA TAS4-3'-D4(−) (an antisense species 4 registers downstream from the miR828 trigger) targets the set of MYB transcription factors PRODUCTION OF ANTHOCYANIN PIGMENT1 (PAP1/MYB75), PAP2/MYB90, and MYB113, that regulate the anthocyanin and lignin biosynthesis pathways (Bhargava et al., 2010; Borevitz et al., 2000).

In the case of TAS3 transcripts, 2 sites are targeted by AGO7/miR390 in order to produce the TAS3 siRNAs. One is cleaved at the 3' end while the other one remains uncleaved at the 5' end (Axtell et al., 2006; Montgomery et al., 2008; Rajeswaran and Pooggin., 2012), and finally the action of RDR6 and DCL4 on the 3' end leads to the tasiRNAs production. TAS3 tasiRNAs target the mRNAs of *Arabidopsis* AUXIN RESPONSE FACTORs (ARF3 and ARF4), which work together as the tasiR-ARF regulatory module to regulate phase transition and lateral root growth (Fahlgren at al 2006; Marin et al., 2010).

It has also been observed that extensive secondary siRNAs are produced from disease resistance genes belonging to the nucleotide-binding site-leucine-rich repeat (NBS-LRR) superfamily, triggered by the miR482/miR2118 superfamily of miRNAs in multiple plant species, including miR472 in *Arabidopsis* (Li et al., 2012; Shivaprasad et al., 2012; Zhai et al., 2011). As high expression of NBS-LRRs can have fitness costs and can be lethal to the plant cells, it is believed that this miR482/miR2118/miR472 superfamily has the function of regulating them by reducing their expression (Tian et al., 2003, Stokes et al., 2002, Boccara et al., 2014-2015). During infection, on the other hand, they would be expressed to protect the plant. Indeed, studies confirming the latter showed a slightly reduction of miR482 in tomato plants infected with *Turnip crinkle virus* (TCV), that led to the reduction of secondary siRNAs synthesis and an increment in the accumulation of NBS-LRR mRNAs, that after translation eventually would protect the plant against disease (Shivaprasad et al., 2012).

2.2. Heterochromatic siRNAs

Heterochromatic siRNas are produced from intergenic and/or repetitive genomic regions, they are typically 23-24 nt long, and they play an important role in TGS mainly affecting transposons, chromosomal repeats and transgenic inserts (Nishimura et al., 2012). Most depend on RDR2 and DCL3 for their biogenesis and on plant-specific RNA polymerases Pol

IV and Pol V for their production, amplification and action (Haag and Pikaard, 2011). The current model suggests that when one of the short RNA strands from the duplex is loaded in an AGO protein from the AGO4 clade (AGO4, AGO6 or AGO9 in *Arabidopsis*) and recognizes a cognate complementary DNA strand, directed RNA dependent DNA methylation of the DNA target takes place, through cytosine or H3K9 histone methylation, leading to chromatin repression (Figure 2.1).

2.3. NAT-siRNAs

The dsRNA precursors of NAT-siRNAs are thought to arise from the hybridization of separately transcribed, complementary RNAs. The complementarity between the RNA strands could be the result of transcription from opposite strands of the same locus, called *cis*-NAT-siRNAs, or transcription from opposite strands present in different locus, called *trans*- NAT-siRNAs. They are 21- 24 nt long and so far, only *cis*-NAT-siRNAs have been described in plants. The biogenesis pathways responsible for their production are quite heterogenous (Borsani et al., 2005; Zhang et al., 2012) because they require individualized subsets of RDRs, DCLs and other factors for their accumulation (Axtell, 2013). Even though studies in *Brassica rapa* have shown that some NAT-siRNAs are responsive to heat stress and that in *Arabidopsis* some regulate salt tolerance (Borsani et al., 2005), their way of action and the identification of their targets still require further investigation.

2.4. miRNAs

As mentioned before, miRNAs are non coding RNAs of 21-22 nucleotides that regulate, through sequence specific recognition, gene expression in diverse eukaryotes. miRNAs elicit silencing at the post transcriptional level by several modes of action: mRNA cleavage, mRNA decay or degradation and translational repression (Bartel 2004).

In animals, miRNA genes are transcribed in the nucleus to primary miRNAs (pri-miRNAs) by RNA polymerase II (Lee at al., 2004) and therefore, they can be capped by 7-methyl guanosine at its 5' end and added a polyadenylated tail at its 3' end (Cai et al., 2004). The transcripts are at least 1000 nt long, containing single or clustered double stranded hairpins that bear single stranded 5' and 3' terminal overhangs and ~10 nt distal loops (Saini et al., 2007). Pri-miRNAs are cropped by the microprocessor complex comprising Drosha (RNase III endonuclease) and DGCR8 (DiGeorge syndrome critical region gene 8) where the latter, by recognition of the pri-miRNA's junction of stem and single stranded RNA, helps Drosha to be positioned to perform the asymmetrical endonucleolytic cleavage on both strands of the stem, releasing the 60-70 nt pre-miRNA containing a 5' phosphate and a 3' 2 nt overhang (Denli et al., 2004; Gregory et al., 2004; Han et al., 2006; Landthaler et al., 2004). Pre-miRNAs are then transported to the cytoplasm by Exportin-5 and Ran GTP (Yi et al., 2003; Lund et al., 2006) where they are processed by Dicer, starting from the end of the hairpin structure stem and in a sequential and processive way, 20-22 nt duplexes (mirRNA:miRNA *) that are incorporated and unwound into AGO proteins to form a mature and active RISC complex, where one strand of the duplex (guide strand) is bound to Argonaute to direct silencing while the other strand is discarded (passive or star strand) (Wilson and Doudna, 2013).

In plants, also MIR genes are transcribed to pri-miRNAs by RNA pol II in the nucleus. The pri-miRNA transcripts form one or more stem loop structures through extensive intra-molecular base pairs that are processed by DCL1, which interacts with HYPONASTIC LEAVES 1 (HYL1) for recognition and accurate cleavage of the pri-miRNAs into miRNA/miRNA* duplexes (Kurihara et al., 2006). It is assumed that the duplexes are then methylated by the nuclear methyltransferase HEN1 at the 3' terminal nucleotide on its 2'-OH group and then exported to the cytosol by HASTY (HST), a member of the importin *beta* family of nucleocytoplasmic transporters (Bollman et al., 2003). Finally, the duplex is unwound into a single stranded mature miRNA that enters the RISC complex containing AGO1 (or other AGOs), cleaving the target mRNA or inhibiting its translation (Bartel 2004; Kidner and Martienssen, 2005; Jones-Rhoades et al., 2006; Mallory and Vaucheret, 2006) (Figure 2.1 and Figure 2.2). The presence of mature miRNAs and their complementary miRNA (miRNA*) sequences in phloem plant material, suggests that miRNA duplexes, just as proposed for siRNAs, can move over long distances before final loading into AGO proteins (Buhtz et al., 2008).

Even though mRNA cleavage and translational repression seem to be present in both animal and plants, genetic and biochemical studies suggest that the mechanisms involving miRNA mediated silencing are different in the two kingdoms. As AGO proteins have a domain homologous to RNase H, when the small RNA is perfectly or almost perfectly complementary to the mRNA target, RISC cleaves the target mRNA between the 10 and 11 nucleotide positions of the small RNA. This mode of cleavage by RISC is seen in plants in which most of the microRNAs are nearly complementary to a single or few mRNAs, predominantly within the ORF regions (Jones-Rhoades et al., 2006). In contrast, animal miRNAs recognize their target mRNAs through partial base pairing generally at 3' UTRs, especially within the seed region at nucleotides 2-7 or 2-8 of the miRNA (Ameres et al., 2013; Bartel et al., 2009).

Imperfect miRNA-mRNA hybrids with central bulges (nucleotides 9–12) generally account for regulation that occurs mostly through translational inhibition and only rarely by slicing. Due to these relaxed base-pairing requirements, individual metazoan miRNAs may have dozens of target transcripts (Voinnet, 2009). Partial complementarity prevents the cleavage activity of animal RISC but it can still silence target genes by recruiting additional proteins, which induce translational repression and/or mRNA decay in a manner independent of endonucleolytic cleavage (Iwakawa and Tomari 2013, 2015).

Animal mRNAs can promote mRNA destabilization by recruiting deadenylases to the target mRNA (Wu et al., 2006; Braun et al., 2012), through the interaction of AGO1 with the protein GW182, a hub protein that is present in animals but not in plants, with the capacity of recruiting several factors to the target mRNA including the poly(A) binding protein (PABP) and two deadenylase complexes called CCR4-NOT and PAN2-PAN3. This interaction takes place due to the recognition of the tryptophan residues present in the N terminal glycine-tryptophan repeat domain of GW182 by the tryptophan binding pockets present in the PIWI domain of AGO (Till et al., 2007; Takimoto et al., 2009). After deadenylation, target mRNAs undergo decapping and degradation in the 5' to 3' mRNA decay pathway by XRN1 (Behm-Ansmant et al., 2006).

In contrast to animal miRNAs, plant miRNAs cannot promote deadenylation. Instead, they direct target cleavage through AGO1 that has a catalytic tetrad in its PIWI domain that cleaves the target mRNA with fully or nearly fully complementary sequence to the microRNA. In *Arabidopsis*, after the miRNA mediated endonucleolytic cleavage has taken place, the 5'

fragment is urylidated at its 3' end by HEN1 suppresor 1 (HESO1), followed by a probable 5' to 3' exonucleolytic degradation by XRN4 (Ren et al., 2014), and the 3' cleaved fragment is degraded by the 5' to 3' endoribonuclease XRN4 (Souret et al., 2004), that is the homolog of XRN1 in animals.

Due to the high complementarity between miRNAs and their targets in plants, it was initially thought that their way of action on messenger RNAs was through cleavage. However, later studies showed that even when they present high complementarity to their targets, plant miRNAs can also repress mRNAs translation (Ma X. et al., 2013). Aukerman and Sakai proved for example that overexpression of *Arabidopsis* miR172, with almost perfect complementarity to its target, inhibited APETAL2 (AP2) protein accumulation without affecting *AP2* mRNA abundance (Aukerman and Sakai, 2003). In *Arabidopsis* it was also reported that mir156/157 target the 3' UTR of the SQUAMOSA promoter-binding protein (SBP) box gene SPL3, inhibiting SPL3 expression at the protein although not at the RNA level, preventing early flowering by translational inhibition in seedlings (Gandikota et al., 2007). Recent studies in *Nicotiana benthamiana* also showed that AGO2 seems to be able to silence gene expression in a slicing independent way, where mismatches between the 3' end of the loaded miRNA guide strand and the 5' end of the target site, enhance gene silencing (Fátyol et al., 2016). However, the degree of miRNA-target complementarity necessary to support the translational repression activity by plant miRNAs remains unknown.

Translational repression has been correlated with the presence of miRNAs and AGO1 in polysomes (Lanet et al., 2009), supporting the view that plant RISC can remain bound on target mRNAs in order to block ribosomes. Recent experiments suggest that target cleavage and translational repression by AGO1-RISC in *Arabidopsis*, may be taking place at the same time augmenting the general silencing efficiency (Iwakawa and Tomari 2013). Interesting results were obtained by Várallyay et al., (2013) who observed, that the presence of the carnation Italian ringspot virus (CIRV) p19 RNA-silencing suppressor triggered the accumulation of miR168 in *Nicotiana benthamiana*, as well as the induction of AGO1 mRNA as part of the plant antiviral defense response. However, despite AGO1 mRNA accumulation, the protein production was reduced, implying a translational control mechanism on AGO1 mRNA mediated by miR168 and suggesting that plant viruses can inhibit the translational capacity of AGO1 mRNA by modulating the endogenous miR168 level to alleviate the anti-viral function of the AGO1 protein. The clear mechanism, however, has not been elucidated.

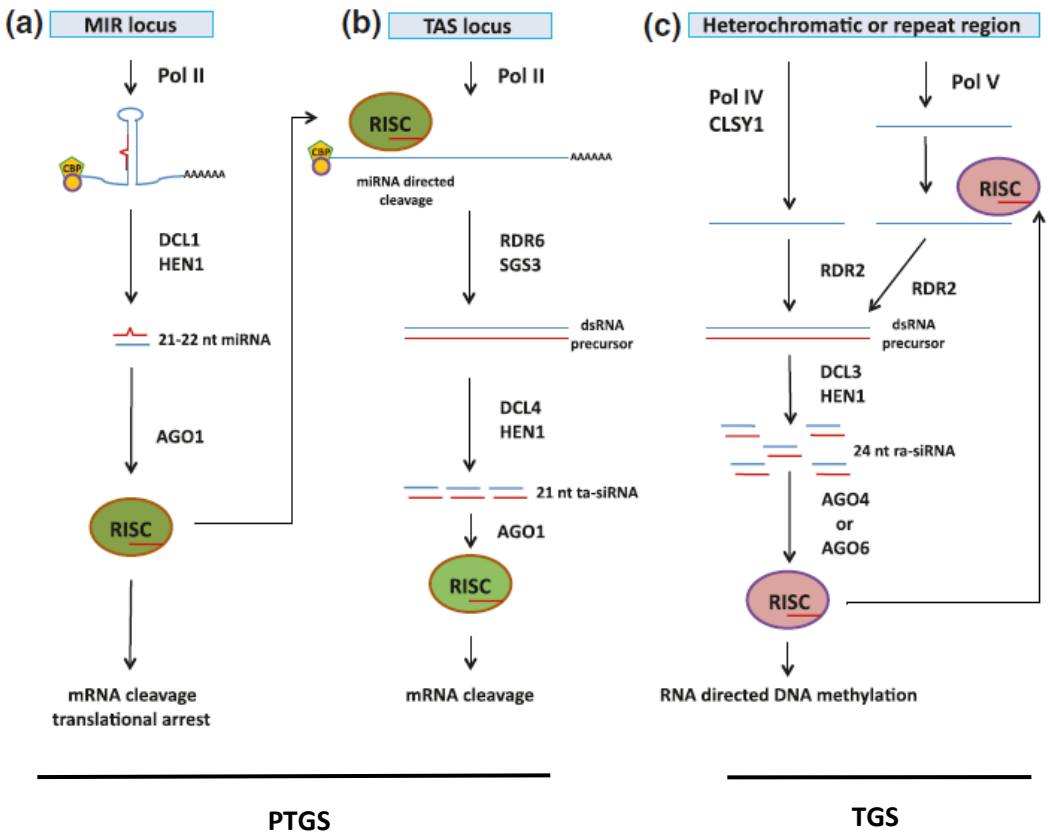

modified from Szittya and Burgyan 2013

Figure 2.1. Endogenous small RNA pathways. PTGS involves the production of miRNAs (21, 22nt long from imperfect RNA duplexes) and trans-acting siRNAs including the production of secondary siRNAs (21 nt long from perfect RNA duplexes) to silence a gene at the RNA level. TGS involves the production of heterochromatic siRNAs (24 nt) that through RISC and RNA directed DNA methylation, silence a gene at the DNA level.

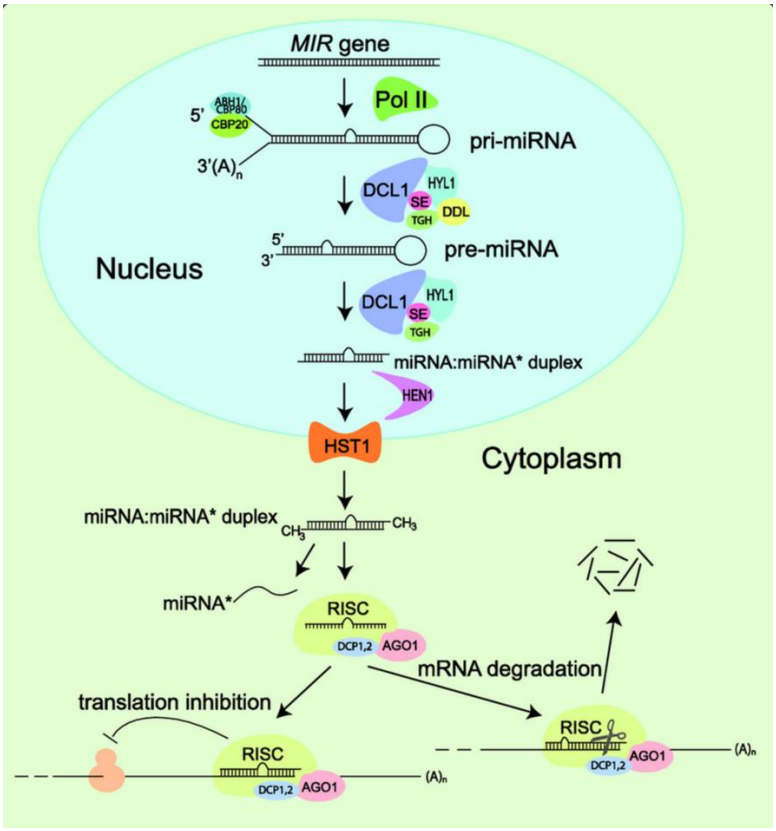

Yang and Li, 2012. Biology

Figure 2.2. miRNA genes are transcribed by RNA polymerase II. These transcripts are capped, spliced and polyadenylated. As the mature miRNA is located in a hairpin structure within the primary transcript or pri-miRNA, this last one needs to be processed in 2 steps by DCL1. The resulting miRNA:miRNA* duplex is then methylated by HEN1 and exported to the cytoplasm by HASTY1. Once there, the mature miRNA is loaded into RISC to guide the cleavage or translational repression of its target by base pairing.

2.5. Viral siRNAs

Evidence supports the role of RNA silencing as an antiviral defense mechanism in plants mainly by two reasons. First, because a large number of virus-derived small RNAs are found in the infected host plants, indicating that the plant RNA silencing mechanism can target viral RNA (Ding and Voinnet, 2007) and second, due to the fact that many plant viruses encode silencing suppressors to counteract the host antiviral defense mechanisms based on RNA silencing (Burgyán, 2008).

Current research indicates that viral siRNAs can be produced from viral double stranded RNA replication intermediates recognized by DCLs (Blevins et al., 2006; Bouche et al., 2006; Deleris et al., 2006) and that are able to guide an antiviral RISC to promote the cleavage of more viral transcripts (Pantaleo et al., 2007).The production of siRNAs in *Arabidopsis* from plant RNA viruses is mainly catalyzed first under the action of DCL4 and then DCL2, where DCL4 is mainly responsible for the processing of 21-nt long viral siRNAs. In case DCL4 is absent or its activity is reduced, DCL2 produces 22-nt long vsiRNAs (Ruíz-Ferrer et al., 2009; Cuperus et al., 2010; Deleris et al., 2006; Fusaro et al., 2006). Studies have also proved the production of viral secondary siRNAs by multiple host RDR pathways in *Arabidopsis* infected by different positive-strand RNA viruses (Díaz Pendon et al., 2007;

Donaire et al., 2008; García Ruíz et al., 2010; Wang et al., 2010). These secondary siRNAs are DCL products and therefore structurally indistinguishable from primary siRNAs (Voinnet, 2008). Viral siRNAs may also be produced from the processing of highly structured regions of viral RNA, rather than from perfectly paired dsRNA intermediates (Molnár et al., 2005; Koukiekolo et al., 2009; Szittya et al., 2010), meaning that sometimes, one of the strands, positive or minus, will be more efficiently targeted than the other one, suggested by a strand bias in the production of viral siRNAs (Pantaleo et al., 2007).

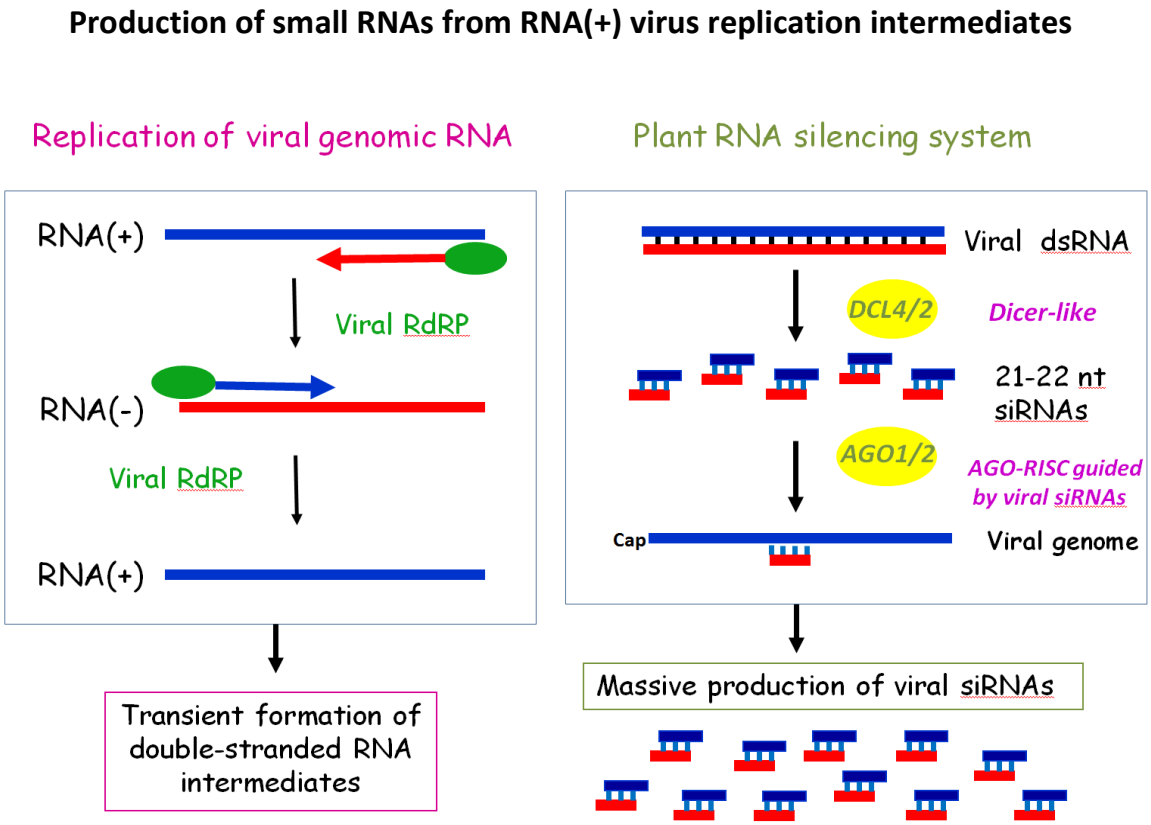

Figure 2.3. The RNA (+) virus replicase gives place to the minus strand using the genomic RNA positive strand as a template to form transient double stranded RNA replication intermediates. The negative strand will then become a template for the replicase to form new positive RNA strands, promoting also the transient formation of dsRNA intermediates. The replication intermediates are substrate for Dicer enzymes that will produce primary viral siRNAs, that when loaded in RISC, have the potential to target and cleave the viral genome to generate secondary viral siRNAs.

The replication intermediates belong to RNA viruses (Alquist, 2002) but not to DNA viruses. In the case of DNA geminiviruses, it has been proposed that the dsRNA structures may be formed formed by the annealing of converging sense/antisense readthrough transcripts (Chellappan et al., 2004; Aregger et al., 2012).

Infection with DNA viruses induces more abundant production of 24-nt viral siRNAs than 21- and 22-nt siRNAs in plants through the action of DCL3 (Akbergenov et al., 2006; Blevins et al., 2006, 2011; Aregger et al., 2012). It has been hypothesized that these 24-nt viral siRNAs

could potentially be involved in TGS through DNA and histone methylation, and some studies have confirmed this hypothesis. For example, Raja et al., showed in *Arabidopsis* that histone H3K9 methyltransferase or cytosin methyl transferases (*drm1,2,cmt3,met1*) mutated plants were more susceptible to infection by the DNA geminivirus *Cabbage leaf curl virus* than the wild-type plants (Raja et al., 2008), and Rodríguez-Negrete et al., (2013) showed that the geminivirus replication protein (Rep) can suppress TGS, by reducing CG methylation through the decreased expression of the maintenance methyltransferases MET1 and CMT3 in *Arabidopsis*.

Studies have shown that RNA silencing spreads from the site of initiation to the surrounding 10-15 neighboring cells and that this cell to cell movement occurs through plasmodesmata. The process can be amplified through conversion of target RNAs into dsRNA, by RDR6 and the production of secondary siRNAs (Melnyk et al., 2011, Schwach et al., 2005; Wassenegger and Krczal 2006), resulting in a more extensive cell to cell spread of silencing. Although studies suggest that both 21nt long and 24nt long small RNA duplexes can move between plant cells through plasmodesmata and the phloem, and that the 21nt small RNAs are effective over short ranges and the 24 nt small RNAs over longer ones, there may be circumstances in which the 21-nt long siRNAs could have a role in long-range spreading of silencing and the 24-nt-long siRNAs in short-range transfer.

One hypothesis for the function of small RNAs considers the idea that their ability to move between cells may help to target the spread of viruses within the plant. By allowing the viral small RNAs to reach uninfected cells, in a quick way the plant could eventually limit the spread of the virus throughout healthy cells (Sarkies and Miska, 2014). It is also assumed that the cleavage of viral RNAs by Dicers is by itself not sufficient to suppress virus replication and that other components of silencing, such as AGO and RDR are required for effective virus silencing (Wang et al., 2011). Indeed, Dunoyer et al., (2005) proposed that primary 21 nt siRNAs are short-range silencing signals while secondary 21 nt siRNAs generated by RDR6-mediated amplification are long-range silencing signals that are responsible for the efficient silencing of the virus at a systemic level.

Even though studies have shown that there are regions along the viral genomes referred as hot spots, from which high amounts of redundant viral siRNAs are produced, this does not necessarily mean that these viral siRNAs have an efficient antiviral function in the RNA silencing pathway. For example, the viral siRNAs produced from the leader region of the *Cauliflower mosaic virus* (CaMV) in infected plants, mainly have a decoy function to divert the silencing machinery from targeting the virus (Blevins et al., 2011). A similar example is the one of *Cymbidium ringspot virus* (CymRSV) where the viral siRNAs produced, most of them primary siRNAs, are inefficient to further downregulate the accumulation of viral RNAs due to the presence of the p19 viral suppressor that sequesters them (Pantaleo et al., 2007).

Section III. Viral RNA silencing suppressors

3.1. RNA silencing suppressors

Viruses have developed different mechanisms to avoid the plant antiviral defense. For example, those RNA and DNA viruses that carry out their genome replication and transcription in the cytoplasm, protect their genome from host defenses within replication complexes or organelle-like compartments made out of sheltering membranes, viral replication proteins and proteins belonging to the host (den Boon et al., 2010; Ishibashi et al., 2012). Additionally, to specifically counteract RNA silencing as the main plant antiviral defense, viruses have evolved to produce different types of silencing suppressors (VSR) that can interfere with the silencing machinery at different levels (Lakatos et al., 2006). For example, plant DNA viruses which replicate in the nucleus of the host and that are targeted by TGS, can encode suppressors that target the S-adenosyl methionine (SAM) pathway or RdDM pathway to alter the DNA/histone methylation processes in the host (Raja et al., 2008, Buchmann et al., 2009, Raja et al., 2010). On the other hand, RNA viruses which replicate in the cytoplasm can encode suppressors that bind dsRNAs of different sizes to interfere with the DCL processing of viral siRNA precursors and AGO-viral siRNA complex assembly steps, or bind and inactivate the protein components of the RNA silencing machinery. As most of the known viral silencing suppressors function at the same time as coat proteins, movement proteins, proteases or transcriptional regulators, they can be difficult to identify because their mutation can be lethal to the virus.

A general strategy that is used by several silencing suppressors encoded by different viruses is dsRNAs sequestration. P14 is a size-independent dsRNA-binding protein while P19 binds predominantly 21-nucleotide ds-sRNAs (Merai et al., 2005). Besides P14, other viral suppressors like P38 (*Turnip crinkle carmovirus*), NSs (*Tomato spotted wilt tospovirus*, *Groundnut bud necrosis virus*) and NS3 (*Rice hoja blanca tenuivirus, Rice stripe virus*) have been found to bind dsRNA (Merai et al., 2006; Zhai et al., 2014; Shen M. et al., 2010), presumably to prevent DCL-mediated production of viral siRNAs duplexes. Besides P19, other viral suppressors that can bind siRNAs are Hc-Pro (*Tobacco etch potyvirus*, *Turnip mosaic potyvirus Potato Y potyvirus,),* P21 (*Beet yellows closterovirus*), p15 (*Peanut* clump virus), p130/p126/p122 (Tobacco Mosaic Virus), NS3 which also binds microRNAs (*Rice hoja blanca tenuivirus*), 2b (*Cucumber mosaic cucumovirus, Tomato aspermy cucumovirus*) and PNS10 (*Rice dwarf phytoreovirus*) (Merai et al., 2006; Sahana et al., 2014; Harries et al., 2008; Hemmes et al., 2007; Goto et al., 2007; Ren at el 2010; Ding et al., 2004). Some of these siRNA-binding suppressors also interfere with the siRNAs 3' methylation by HEN1 as is the case of Hc-Pro from Potyvirus, P19 from Tombusvirus, P21 from Closterovirus and P126 from Tobamovirus (Lozsa et. al 2008).

Interestingly, christallographic studies have shown that p19 sequesters siRNA duplexes in a size dependent, but sequence independent manner, preventing RISC assembly (Silhavy et al., 2002, Vargason et al., 2003). And, although p19 has been shown to bind microRNA duplexes in p19 transgenic plants, miRNA binding by p19 seems not to be efficient during viral infection (Kontra et al., 2016).

AGO proteins are essential in antiviral defense against both RNA and DNA viruses (Azevedo et al., 2010; Pantaleo et al., 2007; Qu et al., 2008; Raja et al., 2008, 2014; Carbonell et al., 2012; Harvey et al., 2011; Wang et al., 2011). The effector step of post transcriptional silencing against RNA viruses in plants depends mainly on AGO1 and AGO2 activities that are required to restrict virus replication and spread. Other AGOs acting in PTGS, such as AGO5, AGO7 and AGO 10, have been also implicated in antiviral defense but with minor roles. On the other hand, genetic and biochemical evidences support that AGO4, functioning in TGS, plays a role against several RNA and DNA viruses (Wang et al., 2011; Carbonell and Carrington, 2015). As a counter defense, some viruses have therefore also developed silencing suppressors that interfere for example with small RNA loading on AGO1, AGO1 mRNA translation, AGO1 protein stability, or AGO1 activity (Chapman et al., 2004; Lakatos et al., 2006; Zhang X. et al., 2006; Baumberger et al., 2007; Bortolamiol et al., 2007; Csorba et al., 2007; Azevedo et al., 2010; Chiu et al., 2010; Várallyay et al., 2010). The best described silencing suppressor targeting AGOs is P0 from poleroviruses.

P0 proteins are divergent among poleroviruses and display diverse levels of RNA silencing suppression activity. These proteins do not posses RNA binding activity but they enhance the degradation of multiple AGOs (AGO1,2, 4-6,9) through the interaction of their F-Box motif with the family of E3 ubiquitin ligases (SKP1-Cullin-F-box complex) for ubiquitination of AGOs (Pazhouhandeh et al., 2006). The ubiquitinated AGOs might be then degraded in the autophagosome, avoiding the RISC complex to be assembled. Regarding their divergency, studies have shown that P0 proteins from *Turnip yellow virus* (TuYV), *Cucurbit Aphid-Borne Yellows Virus* (CABYV), *Potato leafroll virus* PLRV (European isolate), *Melon aphid-borne yellow virus* (MABYV) and *Beet mild yellowing virus* (BMYV) are all silencing suppressor proteins of local, but not systemic RNA silencing (Han et al., 2010; Kozlowska-Makulska et al., 2010; Pfeffer et al., 2002). On the other hand, the P0 proteins of *Sugarcane yellow leaf virus* (SCYLV), PRLV (Australian isolate), *beet yellow dwarf virus-GPV* (BYDV-GPV) and *pea enation mosaic virus-1* (PEMV-1, *Enamovirus* genus) are suppressors of both local and systemic RNA silencing (Fusaro et al., 2012; Liu et al., 2012; Mangwende et al., 2009), while no suppression activity has been found in the P0 proteins of 2 isolates of *beet yellow dwarf virus* (BMYV) and of 6 isolates of beet chlorosis virus (BChV).

Among other suppressors affecting AGOs, the *Sweet potato mild mottle ipomovirus* (SPMMV) P1 has been shown to interact directly with loaded AGO1 through GW/WG-motifs (AGO-hook) present at the N-terminal part of P1, necessary for binding and suppressing AGO1 function (Giner et al., 2010). The TCV coat protein P38 and CMV 2b, besides binding dsRNAs, can also bind to AGO1 and to AGO2 in the case of P38, interfering with their function (Azevedo et al., 2010, Zhang et al., 2006, Duan et al., 2012).

Recent studies have also shown that some silencing suppressors repress the translation of AGO1. From the 10 *Arabidopsis* AGOs only AGO1 and AGO2 seem to be regulated by miRNAs. Both miR168 and miR403 target AGO1 and AGO2 mRNA, respectively, and these regulations occur though their association with AGO1 (Rhoades et al., 2002; Vaucheret et al., 2004; Allen et al., 2005). Induction of AGO1 mRNA accumulation is believed to be a general response to viral infection (Zhanget al., 2006; Csorba et al., 2007; Havelda et al., 2008). However, this induction is generally not accompanied by an increase in AGO1 protein accumulation or activity due to the presence of viral suppressors that upregulate miR168. For example, the upregulation of miR168 in *Arabidopsis* has been observed in the presence of suppressors like 2b, Hc-Pro, P19, P38 and P126/P130/P122, that leads to the

downregulation of AGO1, through translational repression of AGO1 mRNA (Várallyay et al., 2010). In parallel, induction of AGO2 mRNA and AGO2 protein accumulation in response to viral infection has also been reported, presumably as a consequence of AGO1 viral inactivation (Lewsey et al., 2010; Endres et al., 2010, Harvey et al., 2011), where AGO1/miR403 mediated regulation of AGO2 mRNA would be impaired, leading to AGO2 protein accumulation.

The inactivation or inhibition by viral suppressors of other important proteins from the RNA silencing pathway like SGS3 and RDR6, both important for the production of secondary small RNAs, has also been documented. It is known that the V2 protein of *Tomato yellow leaf curl virus* (TYLCV) and the P2 protein of *Rice stripe virus* (RSV) interact with SGS3 interfering with RNA silencing (Du et al., 2011; Glick et al., 2008), and that the P6 protein of *Rice yellow stunt virus* binds RDR6 to interfere with the production of secondary siRNAs and systemic RNA silencing (Guo et al., 2013). Evidence has also showed that the RNA-silencing component double-stranded RNA-binding protein 4 (DRB4), which is a partner of DCL4 to produce siRNAs and that also plays an important role against bacterial infection, can be bound and inhibited by the Cauliflower Mosaic Virus (CaMV) suppressor P6 (Love et al., 2007; Shivaprasad et al., 2008; Haas et al., 2008; Zhu et al., 2013).

Other more complex mechanisms developed by viruses to avoid the plant antiviral response include for example the deployment of decoy vsiRNAs et al., that distract the RNA silencing machinery by keeping it working, but without effectively targeting the viral genome, so that the viral replication or coding regions are not affected at all, as in the case of CaMV and Rice tungro bacilliform virus (RTBV) (Blevins et al., 2011; Rajeswaran et al., 2014).

Section IV. Tobamoviruses

4.1. Tobamoviruses and ORMV

The *Tobamovirus* genus, part of the alphavirus-like superfamily (Hirashima and Watanabe 2003), includes positive sense single stranded RNA viruses whose genome contain closely packed open reading frames (ORFs) as is the case of *Tobacco Mosaic Virus* (TMV), *Tomato Mosaic Virus* (ToMV) and *Oilseed rape mosaic virus* (ORMV). The genomic RNA serves as template for both translation and negative-strand RNA synthesis for replication (Chujo et al., 2015; Figures 4.1 and 4.2). The genome is around 6300 nt long and at its 5' end a m^7Gppp cap is attached to the first nucleotide to protect the genomic RNA from degradation by the host exonucleases and to facilitate its translation. The 5' untranslated leader sequence (5'UTR) of 69 nucleotides, also known as omega sequence (Ω sequence), promotes the efficient translation of the genome (Galliet and Walbot 1992). The tRNA-like structure at its 3' end serves as anchor for the viral replicase to form the negative strand which will become a template to form new positive strands during the replication of the virus (Figure 4.2).

Oilseed rape mosaic virus (ORMV) genome

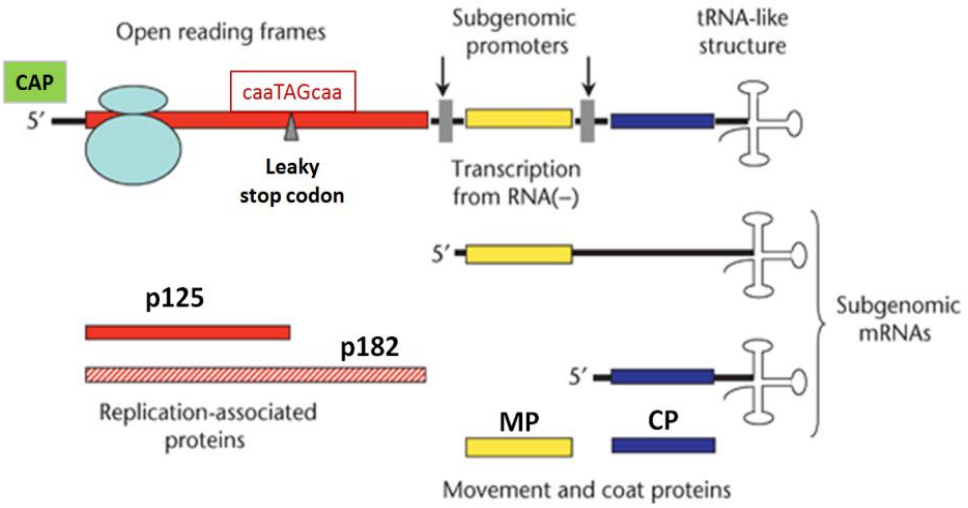

Fig 4.1. ORMV genome. The capped genomic RNA is the template for the 125 and 182 kDa replicase proteins. The movement protein (MP) and the coat protein (CP) respectively, are expressed from two separate 3' coterminal subgenomic mRNA (modified from Rybicki, 2015).

In case of ORMV, the genomic RNA encodes at least 4 proteins (NC_004422.1., Aguilar et al., 1996; Figure 4.1). The 125 kDa and the 182 kDa proteins are translated directly from the genomic RNA, whereas the 28 kDa movement protein (MP) and the 18 kDa protomers of the coat or capsid protein (CP) are synthesized from the respective subgenomic RNAs that are 3'-co-terminal with the genomic RNA (Grdzelishvili et al., 2000). Just as it has been described for TMV, it is believed that p125 and p182 are involved in the replication of the virus and p28 or MP in its movement throughout the cells. The capsid made out of several 18 kDa protomers, wraps the genomic RNA in order to protect it from the host ribonucleases and is elongated, rod shaped, straight, and exhibits helical symmetry.

Model for ORMV replication and translation

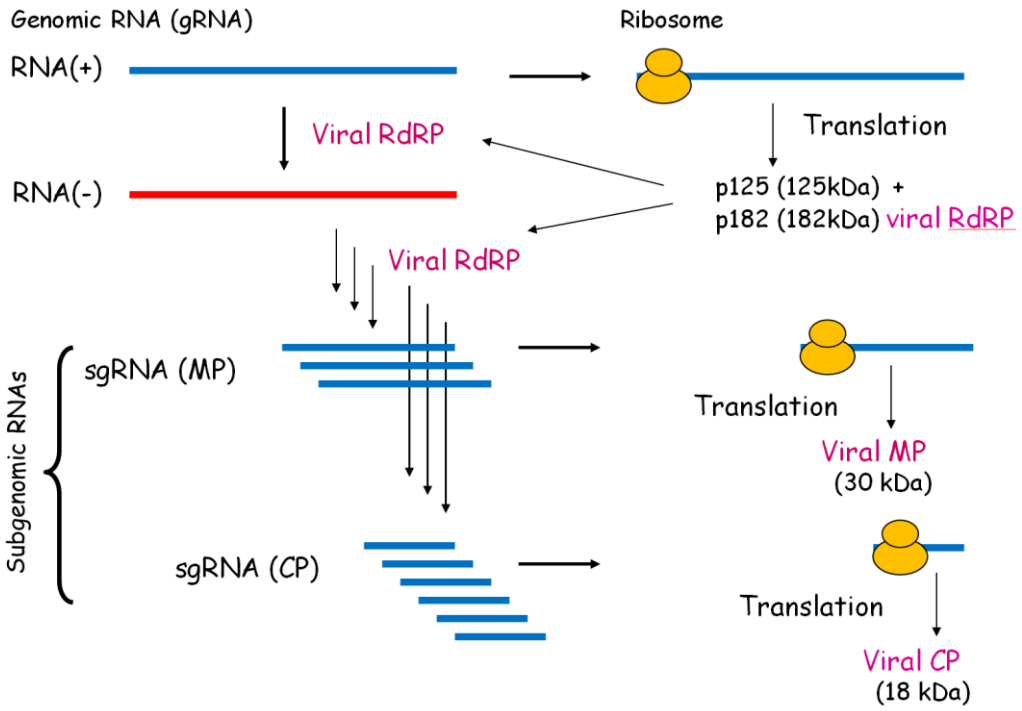

Figure 4.2. During replication, the RNA positive strand is used as a template to produce the minus strand by the viral replicase. The minus strand contains the promoters recognized by the replicase to produce the subgenomic RNAs for the movement (MP) and coat (CP) proteins. During translation, the genomic and subgenomic RNAs are translated by the host ribosomes.

The 125 kDa protein coding sequence has a leaky stop codon (UAG) that 1 in 10 times leads to the translation of the larger readthrough protein of 182 kDa, which constitutes the replicase of the virus since it contains the polymerase domain, as observed in other positive RNA viruses (Buck, 1996). It is believed that the ORMV p125 contains a methyltransferase -guanylyltransferase- like domain (MET) involved in the viral RNA 5' capping in its N- terminal region due to its similarity with the p126 of TMV where these functions have been already described (Merits et al., 1999). Studies in other alphaviruses have shown that the methyltransferase protein is membrane-bound protein that methylates GTP, dGTP and GpppG, but not capped RNAs, whereas the eukaryotic capping enzyme is soluble and readily methylates capped RNAs, but not GTP or dGTP (Laakkonen et al., 1996; Ahola et al., 1999). In agreement with the former, Merits' study showed that the p126 of TMV is able to form a p126-m^7GMP complex in presence of S-Adenosyl methionine (AdoMet) as the methyl donor in order to constitute the viral cap structure.

Studies suggest that contemporary DNA ligases, RNA ligases and RNA capping enzymes have evolved by fusion of effector domains from an ancestral catalytic module involved in RNA repair (Shuman and D Lima, 2004). As all eukaryotic mRNAs contain a cap structure, it seems probable that the strong selective pressure from the host defense responses has

forced viruses without a 5' cap to develop different strategies to cap their RNA or even repair it in order to keep on spreading further in the host (Ramanathan et al., 2016; Ho and Shuman, 2002, Yin et al., 2003; Nandakumar et al., 2006).

TMV p126 also contains an helicase domain which is thought to unwind the duplexed or structured RNA that is formed during RNA replication. Interestingly, the direct interaction of this helicase - like (HEL) domain with the ATP-bound N resistance protein (TIR-NBS-LRR) in *Nicotiana tabacum* has also been reported (Ueda et al., 2006). This fact deserves attention as it is known that plant resistance proteins (NBS-LRR) and the products of avirulence (Avr) genes present in diverse plant pathogens, are predicted to interact directly or indirectly with each other, leading to programmed cell death around the site of interaction, also termed hypersensitive response (HR), to restrict further spread of the pathogen in the host (Morel and Dangl, 1997).

4.2. Tobamovirus replication organelles

It is known that during infection, all positive-sense RNA viruses remodel host membranes into specialized membranous structures called viral replication organelles or viral replication factories. The viral genome is replicated in the lumen of these organelles, which together with viral and host proteins create the proper environment to facilitate the replication and protection of viral RNAs against degradation by cellular RNases, or detection by cytosolic RNA sensors that could trigger antiviral responses (Nagy et al., 2016). Host membrane proteins like Tobamovirus multiplication 1 (TOM1) and ADP-ribosylation factor-like 8 (ARL8) for example, have shown to be necessary for ToMV replication, suggesting that both are part of the replication complex (Ishibashi et al., 2012).

So far, two classes of host membrane rearrangements have been proposed to be induced by the alpha viruses: the invaginated vesicle/spherule type and the double membrane vesicle type. In the spherule type model studies have shown that the viral replicases reside in the invaginated membrane so that RNA replication takes place in the spherule lumen where a neck-like connection to the cytoplasm allows import of the required ribonucleotides and export of the newly synthesized RNA destined for translation or packaging into the capsid. The double membrane vesicles, on the other hand, are sealed and no connection to the cytosol is obvious. As replication still takes place inside these double membrane vesicles, it is believed that protein channels or transporters might be involved to link the vesicles interior to the cytosol (Paul and Bartenschlager 2013; Figure 4.3).

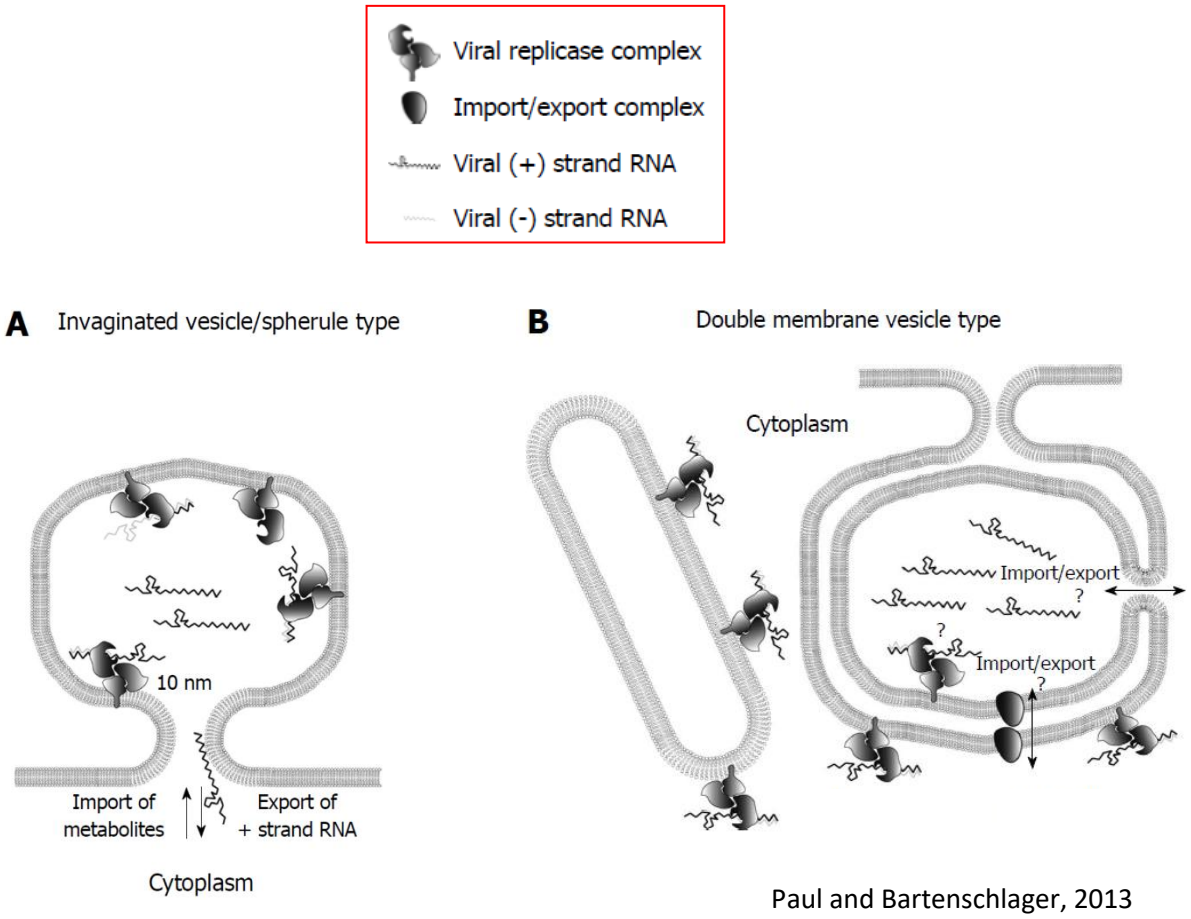

Figure 4.3. Membrane rearrangements proposed for the replication organelles of positive-sense ssRNA viruses in the host. A) Vesicle with a neck-like connection to the cytoplasm that allows import of the required ribonucleotides and export of the newly synthesized RNA destined for translation or packaging into the capsid. B) Closed double membrane vesicle where protein channels or transporters might be involved to link the vesicles interior to the cytosol.

Studies in infected plants have shown that TMV p126 and p182 form heterodimers in a 1:1 ratio to constitute viral replicase complexes that are bound to the membrane of vesicles derived from the endoplasmic reticulum (Watanabe et al., 1999; Buck,1999). Besides the viral polymerase complex, these vesicles also contain ribosomes and host proteins so that both, replication and protein synthesis are taken place in the same site. In addition to the heterodimers, a large excess of free p126 has been identified in the plant extracts but its biological function has not been yet defined (Watanabe, 1999). Using a TMV p126 mutant virus, it was previously shown that p126 is not essential for replication of the virus (Ishikawa et al., 1986). Therefore, it was concluded that p126 could control the heterodimer formation and that it could be needed at a step in transcription and/or replication after the synthesis of the minus RNA strand.

It is likely that during the early stages of replication of TMV, the positive strands that are already acting as translational templates for synthesis of the virus encoded proteins, also serve as templates for amplification of the negative strands. During infection, it is known that the synthesis of negative strands stops before the synthesis of positive strands (Ishikawa et al., 1991), and that later in the replication cycle, once synthesis of the negative strands has stopped and much coat protein has been synthesized, most of the progeny positive strands

become encapsidated to form virions (Aoki and Takebe, 1975; Palukaitis et al., 1983). As mentioned before, the genomic negative strand also serves as template for synthesis of the subgenomic mRNAs that code for the movement and coat proteins of the virus.

Isolated intermediates of replication in TMV infected plants have shown the presence of a completely double stranded RNA or replicative form (RF) and a partly double-stranded and partly single-stranded RNA or replicative intermediate form (RI) (Buck et al.,1999). If these two replicative forms are present *in vivo* is still unclear.

Section V. Resistance and immunity in plants

The plant immune system by which plants detect and fight a microbial pathogen relies initially on a first layer of defense known as pattern triggered immunity (PTI), where conserved pathogen associated or microbe associated molecular patterns (PAMPs or MAMPs) are recognized by surface receptors better known as pattern recognition receptors (PRR) (Jones and Dangl 2006; Boller et al., 2009). It is via this process, for example, that the bacterial protein flagellin, through a 22 amino acid peptide, can be recognized by the flagellin receptor FLS2 from *Arabidopsis* (Gómez-Gómez and Boller 2000) and initiate the innate immune MAP kinase signaling cascade (MEKK1, MKK4/MKK5 and MPK3/MPK6) that induces the expression of several defense genes in the host, resulting in enhanced resistance against pathogens (Zipfel et al., 2004). As a counter-defense to avoid PTI, bacteria secrete effector proteins in their hosts through the type III secretion system, that allow them to survive and further succeed with the infection (Deslandes et al., 2012; Feng et al., 2012). However, these effectors can also be recognized and neutralized by the plant's counter-counter defense response, constituted by a large class of disease resistance proteins referred as nucleotide binding leucine rich repeat receptors (NB-LRRs) for the reason that they contain a nucleotide binding domain (NB) and a leucine rich repeat domain (LRR).

Innate Immunity- Silencing Zig Zag Model

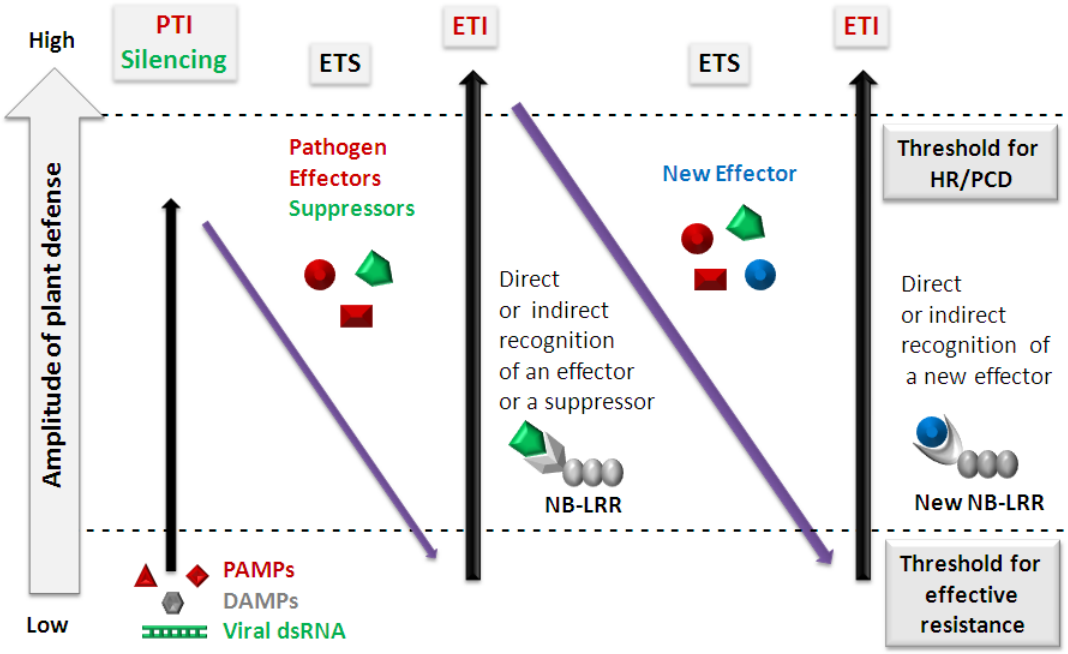

Fig. 5.1. Zig-zag model for evolution of innate immunity- and silencing-based plant defense against viral and non-viral pathogens (adopted and extended from Jones and Dangl 2006 [10]). In phase 1, plants detect pathogen-associated molecular patterns (PAMPs) and host danger-associated molecular patterns (DAMPs) via pattern-recognition receptors (PRRs) to induce pattern-triggered immunity (PTI) and, in the case of viral pathogens, plants additionally detect viral double-stranded RNA (dsRNA) to trigger RNA silencing. In phase 2, successful viral and non-viral pathogens deliver effectors/suppressors that interfere with both PTI and silencing, resulting in effector-triggered susceptibility (ETS). In phase 3, one effector or suppressor is recognized directly or indirectly by an NB-LRR protein, activating effector-triggered immunity (ETI), an amplified version of PTI that often passes a threshold for induction of hypersensitive response (HR) and programmed cell death (PCD). In phase 4, pathogen isolates are selected that have lost or modified the specifically recognized effector/suppressor, and perhaps gained a new effector that can help the pathogen to suppress ETI. A new plant NB-LRR allele is then evolved and selected that can recognize the newly acquired effector, resulting again in ETI.

Zvereva & Pooggin 2012, adapted from Jones and Dangl 2006.

The activation of such NB-LRR proteins results in an amplified or potent immune response, known as effector-triggered immunity (ETI), that frequently is followed by a kind of programmed cell death in plants called hypersensitivity response (HR) (Jones and Dangl 2006; Zipfel et al., 2004). HR has the goal of avoiding further spread of the pathogen within the host (Levine at al 1996). Interestingly it has been observed that the overexpression of NB-LRRs frequently leads to a constitutive immune response and HR (Zhang Y. et al., 2004), even in the absence of the effectors that activate NB-LRRs.

One of the best characterized host responses to viral infection by a NB-LRR protein is the one shown by the gene N derived from *Nicotiana glutinosa*, which as mentioned before, recognizes sequences within the helicase domain of the replicase protein of *Tobacco mosaic virus* (TMV) (Abbink et al., 1998; Erickson et al., 1999; Padgett and Beachy 1993) leading to a cascade of defense responses (Baker et al., 1997; Dixon et al., 1994).). Plants that carry the N resistance gene display after 48 hours, localized HR at the site of virus infection and the lesions are less than 5mm in diameter. On the other hand, plants which lack the N gene, allow TMV to replicate and spread systematically, developing the characteristic mosaic phenotype after some days of infection.

An interesting result was obtained by Cole et al., (2004) (Figure 5.2) after infecting with TMV two diferent varieties of *Nicotiana edwardsonii* (*N. edwardsonii* and *N. edwardsonii* cv. Columbia) which contained an identical sequence of the N resistance gene. They observed that the *N. edwardsonii* cv. Columbia variety was resistant and able to develop a normal HR response against TMV inducing also premature leaf senescence, while the susceptible *N. edwardsoni* variety had an initial HR response but failed to contain the virus, allowing its systemic spread accompanied with systemic necrosis. They concluded that the systemic movement of TMV in the susceptible plants and the development of systemic necrosis indicated that the N gene by itself might not prevent infection in some cases, either because some additional defense responses were absent in *N. edwardsonii* compared to Columbia, or because the N gene itself was defective. Further studies showed that the cv Columbia exhibited enhanced resistance to infection by *Pseudomonas tabaci* and *Pseudomonas phaseolica*, consistent with the idea of a general enhancement of plant defenses in this variety. On the other hand, Dinesh-Kumar et al., (2000) showed that point mutations in the P-loop motif of the N gene 216GMGGVGKT223 in *Nicotiana tabacum* TMV resistant plants, interfered with the wild type N function and that any substitution in the invariant G216 and K222 led to loss of resistance to TMV. Interestingly, the substitution of T223S, a conservative substitution, led to a partial loss of N function phenotype, where an initial HR could be initially detected after TMV infection, but that continued to spread throughout the plant together with the virus, resulting in plant death within 5-7 days. It is worth to mention that in these experiments the expression of the N protein was never assessed. Further studies have also showed that the K207R mutation in the P loop of the resistance protein I-2 from *Lycopersicon esculentum*, failed to induce the HR (Tameling et al., 2006).

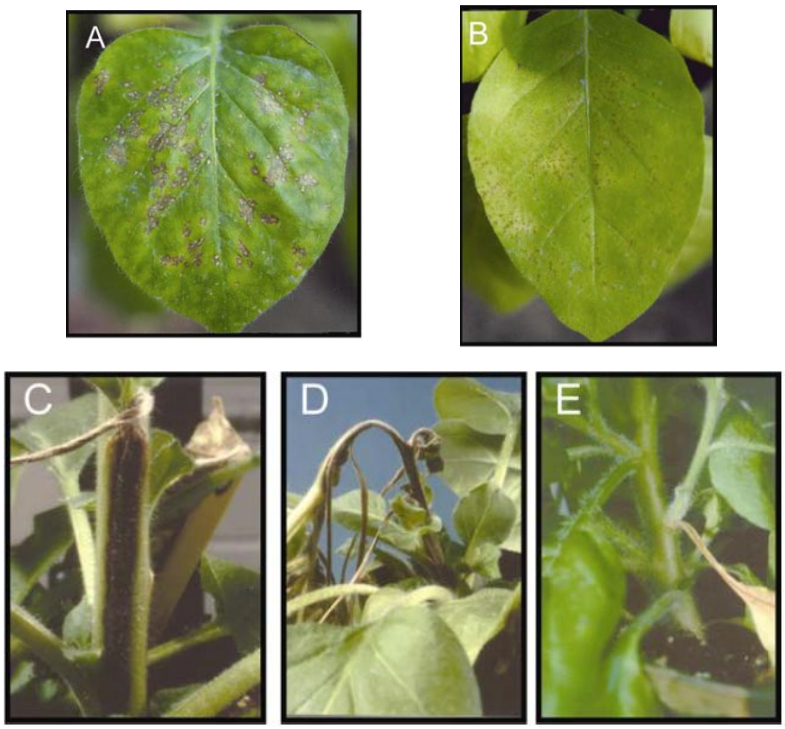

MPMI Cole et al., 2004.

Figure 5.2. A. Necrotic local lesions induced by TMV in a *N. edwardsonii* leaf (susceptible). B. Necrotic local lesions induced by TMV in a "Columbia" leaf (resistant). C. Necrosis associated with the systemic movement of TMV in *N. edwardsonii* from the petiole of the inoculated leaf into the vascular tissue. D. Further systemic movement of TMV in *N. edwardsonii* surrounding the stem, resulting in death of the meristem. E. Senescence of a "Columbia" leaf (resistant) inoculated with TMV.

NB-LRR proteins also own an N-terminal domain that can be either a Toll/interleukin 1 receptor domain (TIR) or a coiled-coiled domain (CNL) (Meyers et al., 2003). Among the NB-LRRs carrying a coiled-coiled domain are RESISTANT TO P. SYRINGAE 2 (RPS2), RESISTANCE TO P. SYRINGAE PV MACULICOLA 1 (RPM1), RESISTANT TO P. SYRINGAE 5 (RPS5), Potato virus X resistance protein (Rx) and Tomato Mi-1 resistance protein (Mi). On the other hand, RESISTANT TO P. SYRINGAE 4 (RPS4), RECOGNITION OF PERONOSPORA PARASITICA 1 (RPP1), RECOGNITION OF PERONOSPORA PARASITICA 5 (RPP5), and Tobacco Mosaic Virus resistance protein (N), contain a TIR domain (Dangl and Jones 2001; Staskawicz et al., 1995) (Figure 5.3). Studies have shown that the three domains, TIR, NB and LRR, are indispensable for the N-mediated resistance response against TMV (Dinesh-Kumar et al., 2000).

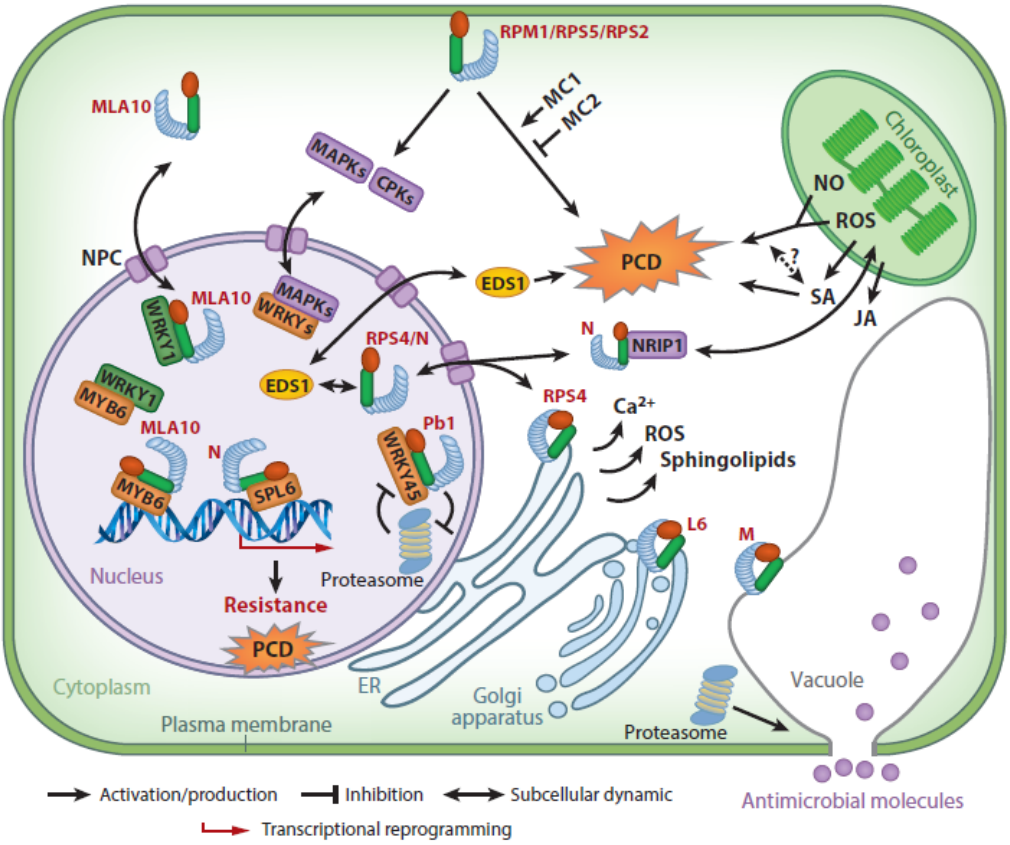

Cui et al., 2015

Figure.5.3. Activated nucleotide-binding/leucine-rich-repeat receptors (NB-LRR labeled in bold red) trigger Ca^{2+}- dependent protein kinases and mitogen-activated protein kinases (MAPK) cascades, reactive oxygen species and nitric oxide production, accumulation of the phytohormones salicylic acid (SA) and jasmonic acid (JA), sphingolipid release from the endoplasmic reticulum (ER), transcriptional defense gene reprogramming and programmed cell death. The *Arabidopsis* NB-LRRs RPMI, RPS2 and RPS5 associate with the plasma membrane and are in contact with FLS2 (Qi et al., 2011). *Arabidopsis* RPS4 localizes to endomembranes and nuclei and enters the nucleus through nuclear pore complexes.

As mentioned before, recent studies showed that under unchallenged conditions, plant NB-LRR transcripts can be regulated by 22 nt miRNAs through the production of secondary siRNAs or phased siRNAs (phasiRNAs) (Zhai et al., 2011, Li et al., 2012, Shivaprasad et al., 2012, Boccara et al., 2014-2015, Ouyang et al., 2014), that would deplete the immune receptor mRNAs in the absence of pathogens, to prevent an autoimmune response that could have negative consequences on the plant fitness. The process involves the cleavage of specific NB-LRR transcripts by 22 nt long miRNAs loaded in AGO1, resulting in 3' cleavage products that are subsequently converted into dsRNAs by RDR6 and further processed by DCL4 into 21 nt phasiRNAs (Halter and Navarro 2015). These can then act in *cis* or *trans* and target the transcripts from which they were produced, or other transcripts containing the complementary target sequence. Such is the example of the *Arabidopsis* miR472, which as the *Nicotiana* miR482, targets a specific nucleotide sequence present in the P-loop domain of NB-LRR proteins to produce phasi-RNAs. Additional studies in *Arabidosis* also showed that during the pattern triggered immunity response of the plant (PTI) upon flg22 treatment, miR472 was down regulated allowing the upregulation of several

transcripts including the important *Arabidopsis* plasma membrane RPS5 immune receptor, which resides in the same protein complex as the PTI receptor FLS2 (Boccara et al., 2014-2015, Fei et al., 2013, Qi et al., 2011). RPS5, together with the *Arabidopsis* RPMI and RPS2, associate with the plasma membrane, where they intercept effector activities to initiate effector-triggered immunity (ETI) (Axtell et al., 2003, Boyes et al., 1998, Mackey et al., 2003, Qi et al., 2012). Furthermore, as *mir472* and *rdr6 Arabidopsis* mutants were more resistant to Pto DC3000 expressing AvrPphB, the bacterial effector recognized by RPS5, they concluded that *miR472 and RDR6* together negatively regulate PTI and ETI. To sum up, upon pathogen MAMP detection, miR472 downregulation would be triggered, allowing the accumulation of NBB-LRR mRNAs to produce resistance proteins at an early stage of the elicitation (Boccara et al., 2014-2015). A list of target genes that accumulate more siRNAs in miR472 overexpressing transgenic *Arabidopsis* according to Boccara et al., (2014-2015), is shown in figure 5.4.

Figure 5.4. List of target genes in *Arabidopsis* that accumulate more siRNAs in transgenic miR472 overexpressing plants than in WT. (Boccara et al., 2014-2015).

AT1G12210	**RPS5-like 1**
AT1G12220	**Disease resistance protein (CC-NBS-LRR class) family (RPS5)**
AT1G12280	**LRR and NB-ARC domains-containing disease resistance protein**
AT1G12290	**Disease resistance protein (CC-NBS-LRR class) family**
AT1G15890	**Disease resistance protein (CC-NBS-LRR class) family**
AT1G51480	**Disease resistance protein (CC-NBS-LRR class) family**
AT1G53350	**Disease resistance protein (CC-NBS-LRR class) family**

It is important to mention that the conserved P-loop amino acid sequence (**GMGGVGKTTL**) that is recognized by *A.thaliana* miR472, and that is also present in the N gene of *Nicotiana*, occurs in diverse NB-LRR proteins that are targets of the superfamily of miRs miR472/482/2118 (Figure 5.5). Among the resistance proteins in *Arabidopsis* containing this sequence are ADR1-L1, RPS5 and RPP8, involved in resistance responses against the oomycete *Peronospora parasitica*, *Pseudomonas syringae* expressing the avrPphB effector and *Turnip crinkle virus* (TCV), respectively (Grant et al., 2003; Innes et al., 2005; Cooley et al., 2000).

miRNAs Target Conserved Sequences in Members of the NB-LRR Gene Families

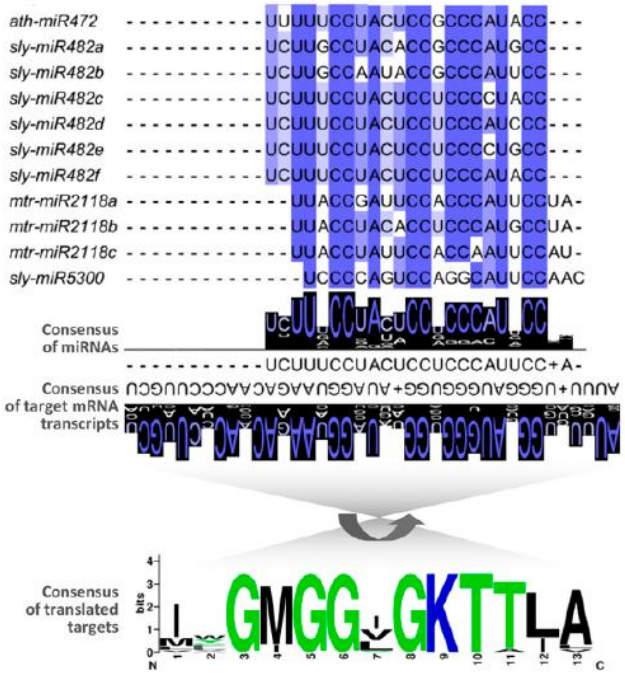

Fei et al., 2013

Figure 5.5. The miR472/482/2118 superfamily is a group of miRNAs that target nucleotides encoding the P-loop motif present in NB-LRR proteins. The consensus sequences present either in the miRNAs or their targets demonstrate a high degree of conservation. In the figure, miRNAs from *Arabidopsis* (ath), tomato (sly) and medicago (mtr) are shown in 5' to 3' orientation while the consensus mRNA target sequence is shown in 3' to 5' orientation. The conserved amino acid sequence of the P-loop is shown at the lower part of the figure.

It is noteworthy to mention that recent studies in *Arabidopsis* showed a gradual overaccumulation of some host miRNA target transcripts during viral infection with ORMV at days 7, 14 and 21 post inoculation (Hu et al., 2011). Interestingly, among them were transcripts belonging to resistance proteins (NBB-LRRs) regulated by miR472, and transcripts from AGO1, AGO2 and chromomethylase (CMT3), regulated by miR168, miR403 and miR823 respectively, and involved in RNA silencing (Figure 5.6).

miRNA reads	Targets AGI ID	log2/dpi 7	14	21
miR156/157 m 32488 inf 118565	AT1G27360	1.9	4.6	4.8
	AT1G27370	0.4	2.5	3.2
	AT1G53160	-0.6	-0.3	-1.9
	AT1G69170	1.5	1.9	2.1
	AT2G33810	1.2	1.0	-0.4
	AT2G42200	2.4	3.6	3.5
	AT3G15270	-0.1	0.2	-1.5
	AT3G57920	0.1	0.1	-0.1
	AT5G43270	0.2	-0.4	-0.9
	AT5G50570	-0.4	-0.6	-0.1
	AT5G50670	-0.4	-0.6	-0.1
miR159/319 m 43 inf 483	AT1G30210	0.1	-1.0	-1.1
	AT1G53230	0.2	1.1	0.9
	AT2G26950	0.0	-0.1	0.2
	AT2G31070	-0.9	-2.2	-1.9
	AT2G32460	0.1	0.5	0.1
	AT3G11440	-1.1	-0.1	-0.6
	AT4G26930	0.2	0.2	0.2
	AT5G06100	0.2	-0.1	0.3
	AT5G55020	0.0	0.2	0.1
miR161 m 963 inf 1833	AT1G06580	0.2	0.4	0.5
	AT1G62670	1.4	2.6	3.2
	AT1G62860	0.5	0.8	1.2
	AT1G62910	-0.1	0.0	0.1
	AT1G62930	0.2	0.3	0.4
	AT1G63070	0.1	0.0	0.0
	AT1G63080	0.2	0.3	0.4
	AT1G63130	0.7	1.4	2.1
	AT1G63150	0.1	0.4	0.8
	AT1G63230	0.2	-0.1	0.1
	AT1G63330	0.3	0.4	0.1
	AT1G63400	0.1	0.0	0.2
	AT1G64580	0.2	0.9	1.1
	AT2G41720	0.7	0.8	1.9
	AT3G16710	0.4	1.2	1.2
	AT4G26800	0.0	0.3	0.3
	AT5G16640	0.1	0.1	0.0
	AT5G41170	0.0	0.0	0.1
	AT5G65560	0.3	-0.6	0.6
miR163 m 43 inf 1833	AT1G66690	0.4	1.9	1.3
	AT3G44870	-2.2	-2.4	-2.9
	AT1G66700	0.4	1.9	1.3
	AT1G66720	0.1	0.2	0.2
	AT3G44860	-2.2	-2.4	-2.9
miR164 m 52 inf 409	AT5G07680	0.4	1.6	2.4
	AT5G39610	1.6	-1.5	-0.9
	AT1G56010	-0.4	-0.9	-1.2
	AT5G53950	0.0	0.1	0.0
	AT5G61430	-0.1	0.2	0.2
miR165/166 m 4213 inf 8546	AT1G30490	0.9	1.7	2.4
	AT1G52150	1.1	2.4	2.9
	AT2G34710	0.3	-0.5	0.1
	AT4G32880	0.3	-0.4	-0.5
	AT5G60690	-0.1	-0.2	0.2
miR169 m 37 inf 140	AT1G17590	-0.1	0.0	-0.9
	AT1G54160	0.0	-0.3	-1.7
	AT1G72830	0.0	0.0	-0.7
	AT3G05690	0.0	1.4	-1.2
	AT3G20910	0.9	1.0	0.6
	AT5G06510	0.0	0.6	-1.4
	AT5G12840	1.4	1.8	2.1

miRNA reads	Targets AGI ID	log2/dpi 7	14	21
miR170/171 m 0 inf 3	AT2G45160	-0.3	-1.7	-1.6
	AT3G60630	0.9	2.0	2.7
	AT4G00150	-0.5	0.1	0.2
miR172 m 401 inf 2041	AT2G28550	-0.7	-0.3	-1.2
	AT2G39250	-0.9	-1.1	-0.7
	AT3G54990	0.2	0.5	0.2
	AT4G36920	-0.2	0.4	-1.1
	AT5G60120	0.0	0.4	0.2
	AT5G67180	-0.4	-1.0	-2.9
miR393 m 0 inf 0	AT3G23690	0.2	-2.4	-1.9
	AT3G26810	1.1	1.5	1.9
	AT3G62980	0.9	0.2	1.3
	AT4G03190	0.5	-1.7	-0.9
miR395 m 0 inf 0	AT3G22890	-0.5	-0.2	-0.7
	AT4G14680	0.1	0.6	0.7
	AT5G10180	-0.5	-1.5	-1.5
	AT5G43780	0.6	0.3	-0.6
miR396 m 22 inf 148	AT2G22840	1.8	1.0	0.5
	AT2G36400	2.3	2.1	1.2
	AT4G37740	0.1	-1.4	-1.3
	AT5G53660	0.3	0.6	0.2
miR160 m 11 inf 8	AT1G77850	1.2	3.4	2.2
	AT2G28350	-0.3	-0.4	-0.7
	AT4G30080	1.2	2.5	2.4
miR397 m 0 inf 0	AT2G29130	-0.1	-0.1	0.1
	AT2G38080	0.0	-0.9	0.0
	AT5G60020	0.2	-1.0	0.2
miR400 m 5 inf 34	AT1G62670	1.4	2.6	3.2
	AT3G16710	0.4	1.2	1.2
	AT5G39710	0.0	-0.1	-0.3
	AT5G46680	-0.2	0.1	-0.2
NBB-LRRs → miR472 m 0 inf 0	AT1G12210	-0.1	-0.1	0.2
	AT1G12220	0.7	-0.8	0.0
	AT1G12280	1.7	2.0	2.0
	AT1G12290	0.2	0.5	1.7
	AT1G15890	1.2	2.7	3.5
	AT1G51480	0.0	0.1	0.0
	AT1G62630	0.5	-0.3	0.7
	AT1G63360	0.5	-0.3	0.7
	AT4G10780	0.1	0.0	0.3
	AT4G27190	0.1	0.1	0.1
	AT5G05400	0.1	0.0	0.0
	AT5G43730	0.1	-0.1	0.0
	AT5G43740	-0.7	-0.9	-0.3
	AT5G47260	-0.1	0.0	0.0
miR846 m 1 inf 6	At1G52050	0.1	0.1	0.3
	At1G52060	0.1	-0.1	0.3
	At1G52070	0.2	0.2	0.1
miR859 m 0 inf 0	At1G11810	0.1	0.0	-0.1
	At1G24793	0.2	-0.5	-1.0
	At3G13820	0.2	0.3	0.2
	At3G22710	-0.1	0.0	0.1
	At3G49520	0.1	0.2	0.1
	At4G33290	0.2	0.1	0.3

miRNA reads	Targets AGI ID	log2/dpi 7	14	21	
miR158 m 4390 inf 36875	AT3G03580	0.6	0.5	0.7	
mir162 m 0 inf 0	AT1G01040	0.9	-0.4	-0.3	
miR167 m 1521 inf 4721	AT1G30330	0.2	1.3	1.6	
	AT5G37020	0.1	-0.2	0.1	
miR168 m 780 inf 6810	AT1G48410	2.5	3.1	3.6	← AGO1
miR394 m 0 inf 0	AT1G27340	0.6	0.6	0.7	
miR398 m 0 inf 0	AT2G28190	2.5	1.7	-0.8	
	AT3G15640	0.8	1.1	0.5	
miR403 m 17 inf 89	AT1G31280	0.7	1.4	2.5	← AGO2
miR408 m 3 inf 24	AT2G02850	-0.1	0.8	0.2	
	AT2G30210	0.5	0.3	0.0	
miR773 m 0 inf 0	AT4G14140	-0.1	0.2	0.1	
miR775 m 50 inf 37	AT1G53290	-0.8	-1.0	-1.7	
miR774 m 0 inf 0	AT3G19890	-0.1	0.0	0.1	
miR776 m 0 inf 0	AT5G62310	-0.1	-0.2	0.1	
miR778 m 0 inf 0	AT2G22740	0.1	-0.3	0.2	
	AT2G35160	-0.2	0.0	-0.2	
miR780 m 0 inf 0	AT5G41610	0.3	0.4	1.2	
miR823 m 2 inf 6	At1G69770	1.1	2.2	3.0	← CMT3
miR824 m 35 inf 39	AT3G57230	0.0	-0.7	-0.3	
miR827 m 1 inf 8	AT1G02860	-0.1	-1.6	-1.7	
miR828 m 0 inf 0	At1G66370	0.0	0.9	-1.0	
miR842 m 0 inf 0	AT5G38550	0.3	-0.1	0.0	
miR844 m 0 inf 0	AT5G51270	0.1	-0.1	0.0	
miR857 m 1 inf 5	AT3G09220	0.0	0.4	0.9	
miR858 m 0 inf 0	AT2G47460	-0.1	0.3	0.3	
	AT3G08500	-0.1	0.2	-0.5	

Hu et al., 2011

Figure 5.6. Changes in the level of miRNA target transcripts upon ORMV infection at 7, 14, and 21 dpi. Heatmap shows log2-fold change values for the mRNA targets of specific miRNAs. The miRNA reads in mock-treated (m) and ORMV-infected (inf) plants is shown. Some miRNA targets show increased (red) and decreased (green) levels of expression upon infection.

Section VI. Aim of the present work

Considering that ORMV is a tobamovirus that can systemically infect *Arabidopsis thaliana* and *Nicotiana benthamiana* plants and, like other viruses that express RNA silencing suppressors, interfere with HEN1-mediated methylation of viral siRNAs and plant sRNAs (Akbergenov et al., 2006; Blevins et al., 2006), the aim of this work was to find out if a similar RNA silencing suppressor could be present in ORMV.

Even though previous work identified p126 as the silencing suppressor of TMV (Ding et al.,2004), the precise roles played by the two ORMV replicase components p125 and p182 during infection have not been determined yet. In the present work, using a wild type and a p125-deficient mutant ORMV virus to infect wild type Col-0 and siRNA biogenesis-deficient mutant lines of *A. thaliana* and wild type *N. benthamiana*, among other approaches, we dissect the function of both proteins, employing blot hybridization and deep sequencing of sRNAs to characterize their impact on the plant RNA silencing machinery, gaining insight on the function of DCLs and RDRs during viral infection, and the innate immunity response of the plant.

Section VII. Material and methods

7.1. Construction of the ORMV mutant clones

The plasmid pORMV containing the full-length cDNA of ORMV genomic RNA downstream of a T7 promoter and an ampicillin resistant gene was kindly provided by Dr. Fernando Ponz (Aguilar et al., 1996; accession NC_004422). Using pORMV (designated here as W) as template, a p125 stop codon mutant plasmid (designated as M) was constructed by PCR site directed mutagenesis by replacing the p125 amber stop codon TAG with a tyrosine codon TAC, in order to produce a mutant viral transcript able to express exclusively the viral replicase p182 but not the shorter protein p125 (Figure 7.1). First, using 1ng of pORMV DNA in a 50µl reaction in the presence of Vent® DNA Polymerase (NEB), two overlapping PCR products, 662 bp and 248 bp long, each containing the tyrosine codon TAC, were separately obtained employing the following pairs of primers (0.2 µM final concentration each): 5'- AGG TTG TTT ATC GAT GAG GGA TTA ATG CTG -3' (named **p180 Cla I_s)** and 5'-GTC GAT CTG TAA TTG **g**TA TTG GGT ACC CGA CTC TAC-3' (named **p126_stop_sup_as)** for the first product , and 5'-TCG GGT ACC CAA TA**c** CAA TTA CAG ATC GAC ACA GTG-3' (named **p126_stop_sup_s)** and 5'- GAA AAC CGG CCG TTC TTT CGG CAC TTG CAC -3' (named **p180 Xma III_as**) for the second product. The thermal cycling conditions were one cycle of 95°C for 2 min, 34 cycles of 95°C for 30 sec, 62°C for 40 sec, and 72°C for 1min, followed by a final cycle of 72°C for 10 min. Second, the two overlapping PCR products were used for "PCR ligation" to get a longer PCR product (881bp) containing the TAC mutation. 1ng of the 662 bp product and 0.37ng of the 248 bp product were put together in a 50 µl reaction in presence of Vent® DNA Polymerase (NEB) and the primers **p180 Cla I_s** and **p180 Xma III_as** (0.2 µM final concentration). The thermal cycling conditions were 95°C for 2 min, 34 cycles of 95°C (30 sec), 62°C (40 sec), and 72°C (1 min), followed by a final extension at 72°C (10 min).The resulting 881bp product was gel purified, trimmed with Cla I and Xma III restriction enzymes (NEB) at sites located in the flanking PCR primers, and cloned between ClaI and Xma III sites of pORMV in place of the wild type ORMV sequence. The resulting mutant clone M was selected following transformation of *E.coli DH5*α competent cells at 37°C in LB medium with Ampicillin 100mg/L and screening 12 colonies by plasmid isolation (Qiagen Miniprep kit) and restriction analysis with ClaI and XmaIII. The presence of the mutation TAC was confirmed for one of the clones by DNA sequencing (Fasteris SA) and this clone M was used for further experiments.

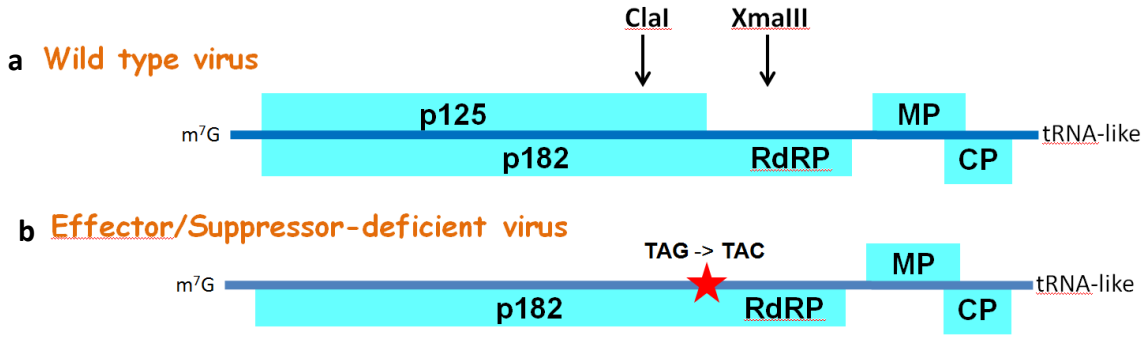

Figure 7.1. a) Wild type virus construct producing both p125 and p182 proteins. b) Mutant virus construct where the p125 amber stop codon TAG was replaced by the tyrosine codon TAC through site directed mutagenesis in order to exclusively produce p182.

As the available pORMV clone (W) did not display wild type disease symptoms, we sequenced sRNAs from Arabidopsis plants infected with wild type ORMV virions and reconstructed de novo the 6,303 nt wild-type ORMV genome sequence as a single sRNA contig from two independent sRNA libraries (Seguin et al., 2014a; Figure 7.2). The reconstructed genome differed from the original pORMV clone W at three positions of the ORMV sequence (G-to-A at position 12, A-to-T at position 231, and G-to-T at position 5612). To correct these errors, two synthetic DNA fragments and suitable restriction sites were used in order to obtain the reconstructed wild type ORMV genome clone, designated W41 (deposited in the Genbank as KF137561). Briefly, the original clone W was digested with EcoNI and NarI in order to replace a 418 bp fragment with the synthetic fragment containing an A at position 12 and a T at position 231 (Figure 7.3 and Supplementary Table S1). This partially repaired clone was named W4. W4 was then digested with NcoI and PstI to replace a second fragment with the 1Kb synthetic fragment containing a T at position 5612 and a NsiI site just downstream of the ORMV sequence and upstream of the PstI site, to yield clone W41. The fully repaired clone W41 was tested for infectivity in *N. benthamiana* plants and found to be completely biologically active, causing the disease symptoms indistinguishable from those of the wild type ORMV sap. In addition, a third partially repaired clone was obtained (clone W1) after digestion of the original clone (W) with NcoI and PstI to repair exclusively the 1Kb fragment as described before. The same procedure was followed in parallel to repair the p125 mutant clone M and get the constructs M4 and M41(Figure 7.3; Supplementary Table S1 and Figure 7.4).

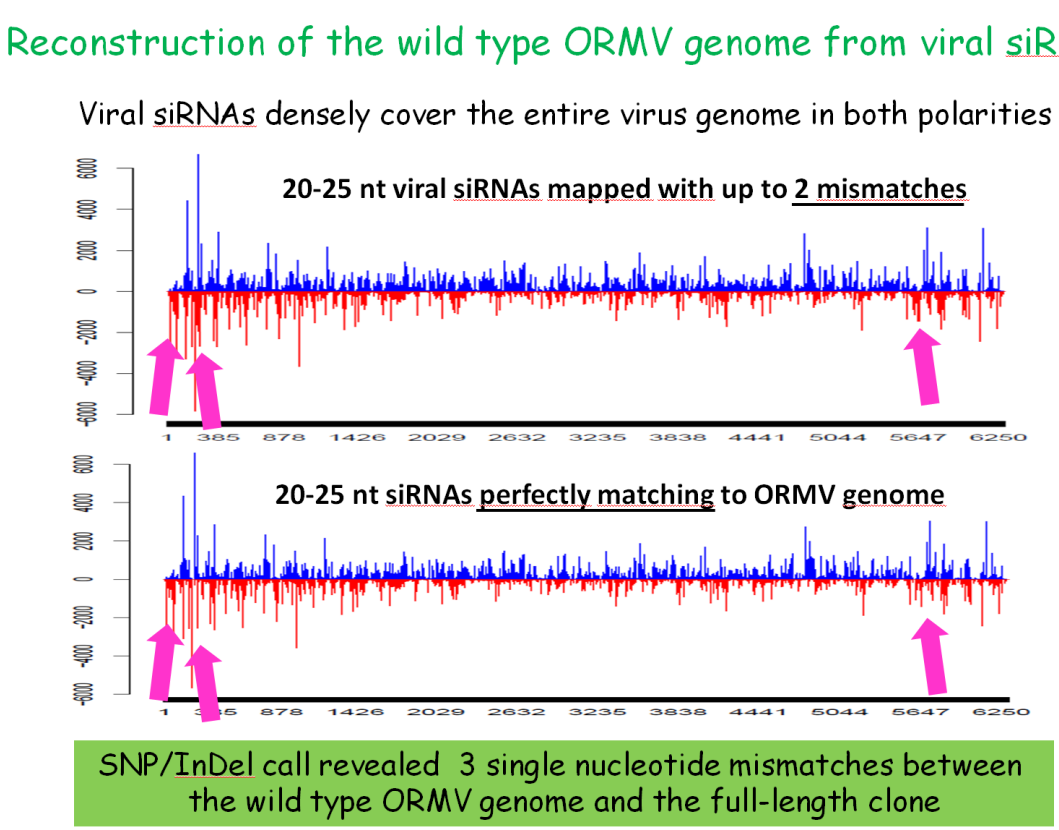

Figure 7.2. Maps of viral siRNAs from the original ORMV clone with two mismatches or perfect matching to the reference ORMV genome. The graphs plot the number of 20-25 nt viral siRNA reads (redundant and non redundant at each nucleotide position of the ORMV genome. Blue bars above the axis represent sense reads and red bars below the axis represent antisense reads. Mismatches between the original contig and the reference genome are indicated with pink arrows at three positions (G-to-A at position 12, A-to-T at position 231, and G-to-T at position 5612).

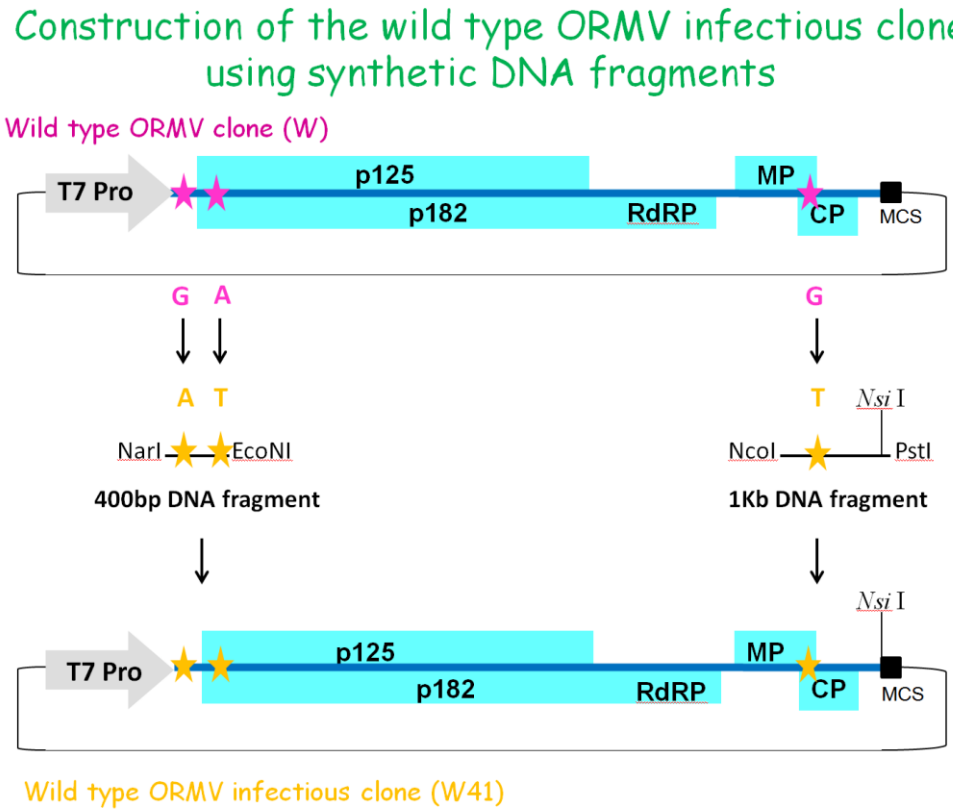

Figure 7.3. The plasmids containing the full-length ORMV genome sequence (W-original or W41-corrected) behind the T7 promoter are depicted schematically: the restriction sites Pst I or Nsi I, just downstream of the genome (located in multiple cloning site; MCS) were used for linearization of the plasmids respectively, followed by run-off transcription by T7 polymerase in the presence of a cap analog. The resulting in vitro transcripts (ORMV genomic RNA) were taken for mechanical inoculation of *Arabidopsis* or *N. benthamiana* plants.

In vitro transcription of ORMV constructs

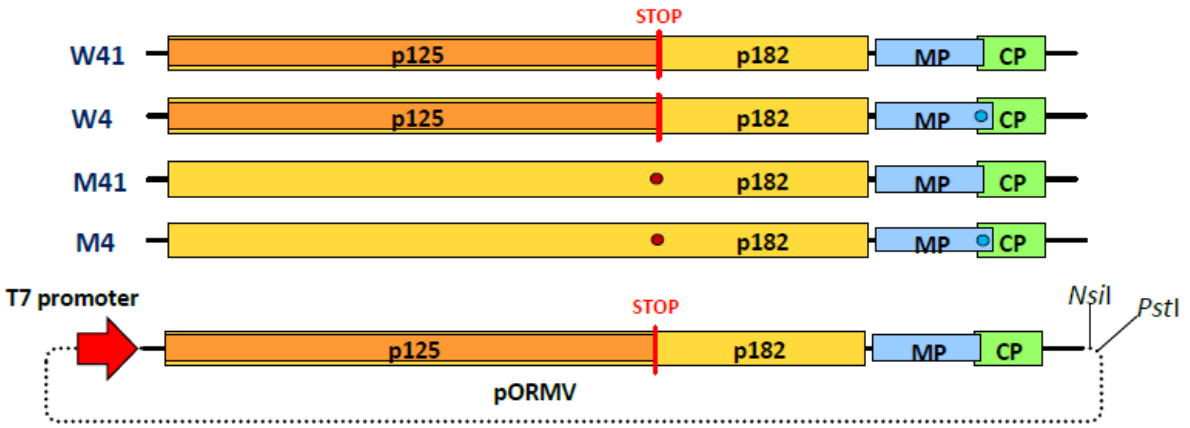

Fig. 7.4. Genome organization of ORMV with the expression of p125, p182, movement protein (MP) and coat protein (CP). The leaky STOP codon of p126 is shown as linear vertical line in red in the two wild-type constructs (W41 and W4) and the mutation of p126 STOP codon is shown as a red circle in the two mutant constructs (M41 and M4). The T-to-G substitution at position 5612 (mutating the MP stop codon and thereby elongating viral MP by an additional 19 amino acids) is shown as a blue circle in the constructs W4 and M4. Location of the T7 promoter and the restriction sites (*Nsi*I and *Pst*I) used to linearize the constructs before *in vitro* transcription are shown.

7.2. Gateway expression vectors for ORMV p125, p125/182 and p182 proteins

In order to express the ORMV proteins transiently in *Nicotiana benthamiana* 16c plants or stably in transgenic *Arabidopsis thaliana*, the Gateway technology was used to create the expression vectors using site directed recombination.

Using as a template the pORMV clone W, the coding sequences of p125 and p125/p182 were amplified as *att*B-PCR products (Gateway Technology) in the presence of Vent® DNA Polymerase (NEB) and the following pairs of primers: for p125, 5'-gggg aca agt ttg tac aaa aaa gca ggc tAC AcC ATG GCA CAA TTT CAA CAA ACA G-3'**(AttB1_Rep_s)** and 5'-gggg ac cac ttt gta caa gaa agc tgg gtC CTA TTG GGT ACC CGA CTC TAC CT-3' **(AttB2_p125_as)**, and for p125/p182, 5'-gggg aca agt ttg tac aaa aaa gca ggc tAC AcC ATG GCA CAA TTT CAA CAA ACA G-3' **(AttB1_Rep_s)** and 5'-gggg ac cac ttt gta caa gaa agc tgg gtc TCA AAC AAA AAA CAA ATC TTT AAA CAA CC-3' **(AttB2_p182_as)**. In order to amplify the coding sequence of p182 alone as an *att*B-PCR product, the mutant ORMV clone M was used as a template in the presence of Vent® DNA Polymerase (NEB) and the following primers **AttB1_Rep_s** 5'-gggg aca agt ttg tac aaa aaa gca ggc tAC AcC ATG GCA CAA TTT CAA CAA ACA G-3' and **AttB2_p182_as** 5'-gggg ac cac ttt gta caa gaa agc tgg gtc TCA AAC AAA AAA CAA ATC TTT AAA CAA CC-3'. All three *att*B-PCR products were separately cloned in a Gateway® pDONR™/Zeo Vector, and through a BP Clonase reaction (Gateway® BP Clonase® Enzyme Mix from Invitrogen™) three different entry clones were obtained. Through an LR reaction (Gateway® LR Clonase® Enzyme mix) and using three different destination vectors for each entry clone (pEarleygate binary constructs 100, 201, and 202 (Earley et al., 2006), the following expression vectors were obtained 100-p125 , 201-p125 , 202-p125,100-p182, 201-p182, 202-p182, 100-p125/p182, 201-p125/p182 and 202-p125/p182. All the expression vectors contained the T-DNA right and left borders, a

CaMV 35S promoter and an octopine synthase terminator, as well as kanamycin and phosphinotricine (or herbicide BASTA) resistance marker genes for bacterial and plant selection, respectively. The 100 vector contained the wild type ORMV protein sequences, while the 201 and 202 vectors contained an HA-tag and a FLAG-tag sequence at the N terminal end of the ORMV proteins, respectively. All final Gateway plasmids were amplified in *E.coli* DH5α bacteria in the presence of kanamycin (Figure 7.5).

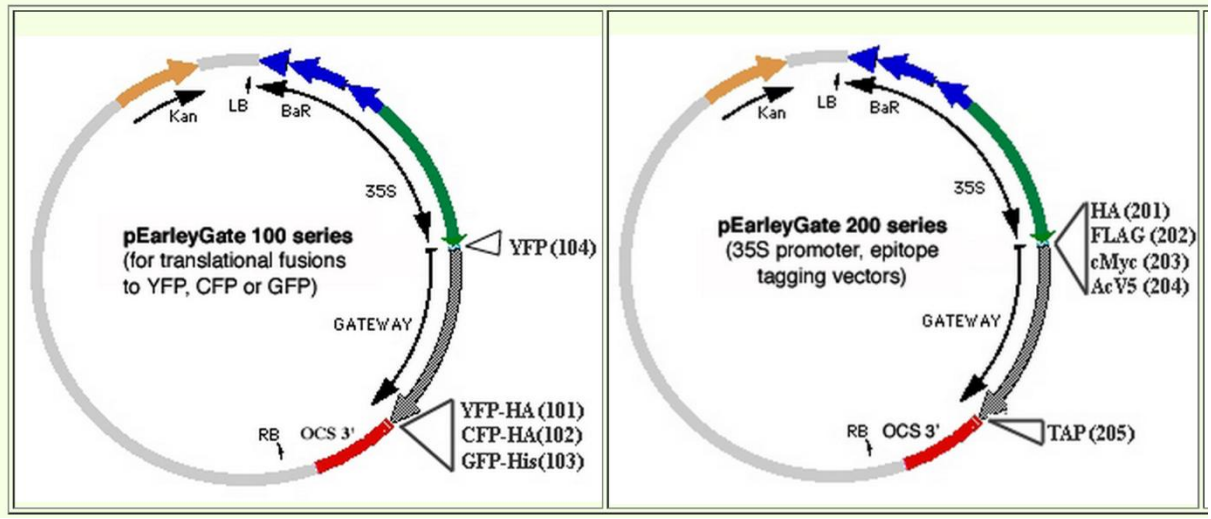

link: http://www.indiana.edu/~pikweb/Vectors%20homepage.html

Figure 7.5. pEarleyGate vectors used to express p125, p125/p182 and p182 in *Agrobacterium tumefaciens*.

7.3. *Agrobacterium* transformation

Agrobacterium tumefaciens strain GV3101 (rifampicin-resistant strain) was transformed by electroporation with the pEarleyGate constructs 100-p125, 201-p125, 202-p125,100-p182, 201-p182, 202-p182, 100-p125/p182, 201-p125/p182 and 202-p125/p182 (for expression of p125, p182, p125/182 and their HA- and FLAG-tagged versions). For each construct, 50µl of *Agrobacterium* competent cells were mixed with 200 ng of purified DNA in a pre-chilled 0.2 cm cuvette, and electroporated in a Bio-Rad GenePulser at 2.5 kV, 200 Ω, and 25 µF. After electroporation, 1ml of LB liquid medium was immediately added to the mix and the culture was kept at 28°C for 2 hours. 100 µl of the cell culture were then spread in LB agar medium with kanamycin (100 mg/L) and rifampicin (10 mg/L) and incubated at 28°C for 2-3 days until colonies could be seen. In order to screen for the colonies carrying the vectors with the correct ORMV protein sequences in the correct orientation, 2 colonies from each construct were chosen for colony PCR, using the following pair of specific primers: 5'-GTG GAT TGA TGT GAT ATC TCC ACT G-3' (**CaMV35Spro_#1**) and 5'-AGA TAC TCC AAC TCA AGA GTC CTT AGA CCA-3'(**Ormv323_as**). The *Agrobacterium* colonies containing the expected product size after electrophoresis were considered for further experiments.

7.4. Transgenic plants

Transgenic *Arabidopsis* plants were obtained by floral dipping transformation with *Agrobacterium tumefaciens* (Zhang et al., 2006). Two month old plants of *Arabidopsis thaliana* (genotype Col 0) at an early bolting stage, grown in soil at 20-25°C in the open greenhouse, were cleaned from flowers and left only with closed flower buds, and then were dipped in an *Agrobacterium tumefaciens* suspension for transformation (3 plants per construct). Briefly, a single *Agrobacterium* colony harboring the construct of interest in the binary vector, was inoculated in 2 ml of liquid LB medium containing kanamycin (100 mg/L) and rifampicin (10 mg/L) and incubated at 28°C for 1 day. This feeder culture was used to inoculate 200 ml of the same medium which was grown further at 28°C for 16 hours until OD_{600}=0.6. The cells were collected by centrifugation for 10 minutes at 4000g at room temperature, and gently resuspended in 200 ml of freshly made 5% sucrose solution. 0.02% of Silwet L-77 was added to the bacterial suspension which was placed in a plastic bag and immediately after, each plant was completely dipped in the suspension for 10 seconds. After removing the excess of liquid present on the plants by draining them on tissue paper, they were put on a tray and kept in the dark at 20°C overnight. Next day the plants were put back in the light chamber at 20°C until siliques with mature seeds were produced one month later. The harvested seeds were put on soil to germinate and the seedlings were sprayed with Basta (Bayer CropScience) solution in water (250 mg/L) two times per week. The Basta resistant seedlings (T1) were transferred to new pots and grown at 20°C until seeds were produced. As we were expecting segregation, these seeds were also put to germinate on soil and the seedlings were sprayed with the same Basta solution 2 times per week. The resistant seedlings (T2) were transferred to new pots, and the same procedure was repeated until Basta-resistant generations T3 and then T4 were obtained.

7.5. Genotyping by PCR

The transgenic *Arabidopsis* plants expressing the ORMV proteins 125 and 125/182 were identified by selecting the Basta resistant plants after 5 days and PCR genotyping using the following specific primers: 5'-GTG GAT TGA TGT GAT ATC TCC ACT G-3' (**CaMV35Spro_#1**) and 5'AGA TAC TCC AAC TCA AGA GTC CTT AGA CCA-3'(**Ormv323_as**), where the thermal cycling conditions were one cycle of 95°C for 2 min, 30 cycles of 95° for 30 sec, 58°C for 30 sec, and 72°C for 45 sec, followed by a final cycle of 72°C for 10 min. The transgenic plants expressing protein 182 were also identified by selecting the Basta resistant plants and using the following specific primers for PCR genotyping: 5'-GTG GAT TGA TGT GAT ATC TCC ACT G-3' (**CaMV35Spro_#1**) and 5' CGC GTC GAG ATG CTA AAT 3' (**Ormv141_as**) where the thermal cycling conditions were one cycle of 95°C for 2 min, 30 cycles of 95° for 30 sec, 55°C for 30 sec, and 72°C for 40 sec, followed by a final cycle of 72°C for 10 min. The transgenic lines expressing the wild type p125 protein from the 100-p125 transgene showed a strong phenotype which made easier their identification.

7.6. Agroinfiltration in *Nicotiana benthamiana*

Agrobacterium tumefaciens strains carrying a binary plasmid with the green fluorescent protein coding sequence (GFP) or the potyviral helper component proteinase coding sequence (HcPro), both under the control of CaMV 35S promoter, kindly donated by D. Baulcombe, and *Agrobacterium* strains harboring the ORMV coding sequences of interest also under the control of the CaMV 35S promoter (100-p125 , 201-p125 , 202-p125,100-p182, 201-p182, 202-p182, 100-p125/p182, 201-p125/p182 and 202-p125/p182), were initially grown on LB agar medium supplied with kanamycin (100 mg/L) and rifampicin (10 mg/L) at 28°C overnight and then in 20ml of liquid LB medium with kanamycin (100 mg/L) overnight at 28°C at 180rpm. After centrifugation of the cultures at 1100 g for 10 min, each bacterial pellet was resuspended in 40ml of MES (10 mM)-$MgCl_2$ (10 mM) buffer pH 5.6. The bacterial suspensions were induced with 150 µM acetosyringone for 3 hours at room temperature and adjusted at OD_{600} = 0.5 with MES-$MgCl_2$ pH 5.6 buffer before agroinfiltration.

Equal volumes of each cell suspension were infiltrated on the abaxial surface of the leaves of *Nicotiana benthamiana* 16C line with a 1 ml syringe (without needle) after first scratching slightly the tissue with a needle. Plants infiltrated exclusively with MES buffer (mock) or the *Agrobacterium* suspension carrying the 35S:GFP construct were used as controls. Mixed agroinfiltrations of the same *Agrobacterium* GFP suspension plus the *Agrobacterium* carrying the putative viral silencing suppressors (35S:GFP + 35S:HcPro or 35S:ORMV constructs) were made in a ratio 1:1 on the rest of the plants. Images of the agroinfiltrated leaves under UV light were taken at days 5 and 8 post infiltration in order to monitor the GFP transient expression in absence or presence of the putative viral silencing suppressors. *Nicotiana* plants were initially grown in soil in the open green house at 20-25°C and then kept under the same conditions after agroinfiltration.

7.7. Plant growth and virus inoculation conditions

Arabidopsis thaliana (ecotype Col-0) plants and its mutant/transgenic derivatives including the RNA silencing mutants (*rdr126* and *dcl234*) and transgenic plants p125, p182 and p125/182, were grown in soil at 20-25°C in the open greenhouse, or in Sanyo light chambers at 20°C under controlled light conditions (12 hours light/12 hours dark cycles). *Nicotiana benthamiana* wild type plants were grown in soil at 20-25°C in the open greenhouse or in Sanyo light chambers at 25°C also under 12 hours light/12 hours dark cycles. Upon ORMV inoculation, *Arabidopsis* and *Nicotiana* plants were kept at 25°C in the open greenhouse under 12 hours light/12 hours dark cycles or in Sanyo chambers at the same conditions.

7.8. Plant inoculation

Arabidopsis Col-0 plants and siRNA-deficient mutant lines *rdr126* and *dcl234* (3 plants of each), at a stage of about 5 weeks post germination, were mechanically inoculated using celite 545 (Merck) with the wild type ORMV virions contained in the sap of ORMV-infected *Nicotiana benthamiana* leaves or with *in vitro* RNA transcripts from the above described ORMV clones. The sap was prepared by grinding infected leaves in PBS buffer (10 mM Na_2HPO4, 2 mM KH_2PO4, 137 mM NaCl, 2.7 mM KCl, pH 7.4). Briefly, 20 µl of sap were

distributed on two leaves per plant (10 µl per leave) and mixed with a pinch of celite 545 (Merck). After rubbing softly with the finger the upper surface of the leaves with the mix, the plants were sprayed with water and put back in the light chamber at 25°C under controlled light conditions (12hours light/12 hours dark cycles). The *in vitro* transcripts were obtained from the plasmid DNA of pORMV (W) and its derivatives W41, W4, W1, M, M41, M4 and M1 linearized by NsiI or PstI digestion (or directly from non linearized plasmids) in a 4 hours reaction at 37°C using a T7 Megascript Kit (Ambion) and the cap analog m7G(5')ppp(5')G (Ambion) to cap the viral RNA, according to the manufacturer's instructions. Briefly, for a 20 µl reaction, 2 µl of each 75 mM nucleotide solution (ATP, CTP and UTP) were added to 1 µg of pORMV DNA resuspended in 4 µl of DEPC water. Further 2 µl of a 15 mM GTP solution and 3 µl of the 6 mM cap analogue solution were added to promote the capping of the transcripts, together with 2 µl of 10X T7 reaction buffer, 2 µl of T7 Enzyme Mix (T7 RNA polymerase from the kit) and 1 µl of RNase inhibitor (RNasin from Promega 40 units/µl). After 2 hours of incubation at 37°C, 1 µl of 75mM GTP was added to the mix and left at 37°C for 2 hours more. Before inoculation, the final volume of the reaction was diluted with DEPC-treated water in a 1:4 ratio from where 20 µl were used as an inoculum per plant mixed with celite and 20 µl were left for agarose gel analysis. The use of linearized (at the NsiI/PstI site) or non-linearized plasmids from each ORMV clone showed no difference on their relative infectivity on the plants, suggesting that when non linearized pORMV cDNA is used for transcription, different sizes of RNAs are produced and then cleaved, probably by host 3'-5' exonucleases, generating the genomic viral RNA (Figure 7.6).

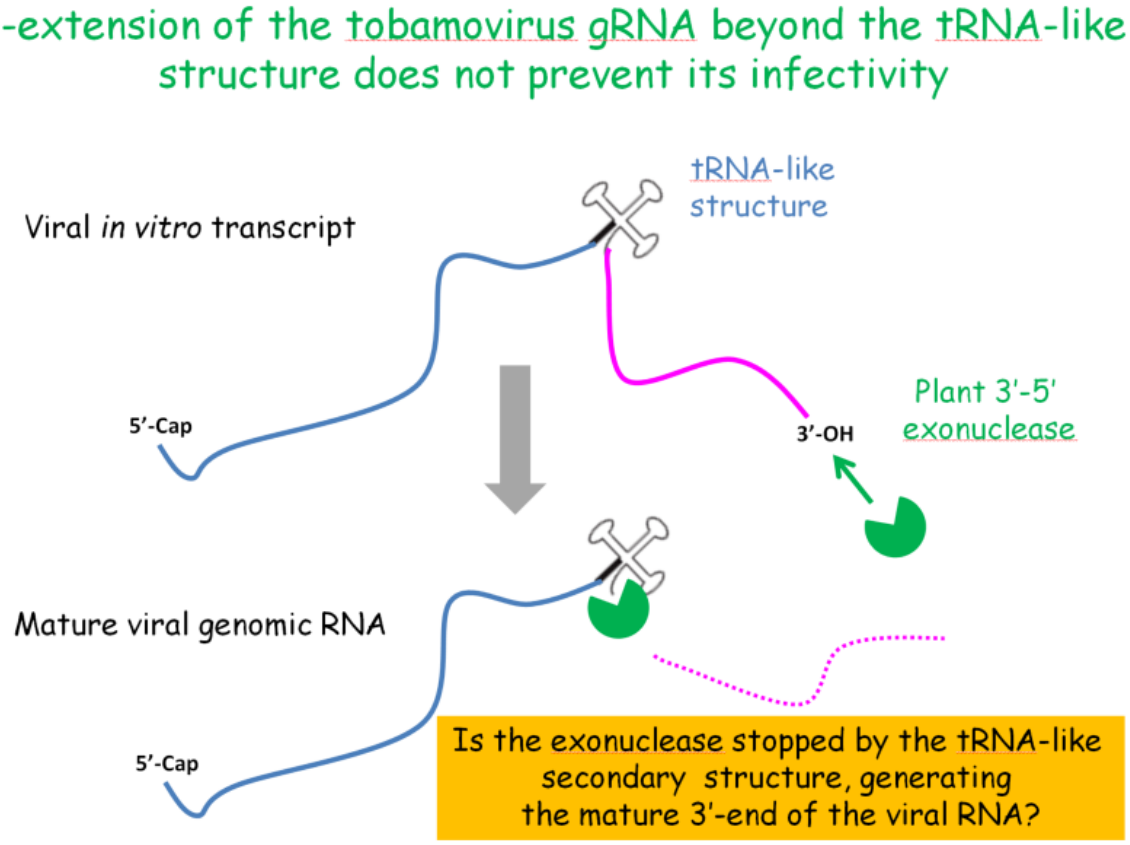

Figure 7.6 Diagram illustrating the mechanism by which ORMV genomic RNA containing a 3'-extension is probably obtained, by *in vitro* transcription using a non-linearized vector containg the viral cDNA sequence, and presumably processed in the host upon inoculation, by a plant 3'-5' exonuclease into its mature form.

7.9. Small RNA blot hybridization analysis in *Arabidopsis* and *Nicotiana benthamiana*

For both blot hybridization and Illumina deep-sequencing, the leaf tissue samples from ORMV sap-infected and mock-inoculated *Arabidopsis* plants (Col 0, *rdr126* and *dcl234*) were harvested at days 5, 14 and 22 post-inoculation respectively, and frozen in liquid nitrogen. Total RNA was isolated from 0.5 g of ground frozen tissue, obtained from a pool of three plants, using TRI Reagent (SIGMA) according to the manufacturer's protocol. 30 µg RNA were resuspended in 10 µl loading buffer (95% formamide, 20mM EDTA pH 8.0, 0.05% bromophenol blue, 0.05% xylene cyanol), heated at 95°C for 2 min and loaded in a 15% polyacrylamide-urea gel (with a 19:1 ratio of acrylamide to bis-acrylamide and 8 M urea). The gel was run using an SE 600 electrophoresis device (Hoefer, San Francisco, CA) at 300V for 4 hours and the RNA was then transferred to a Hybond N+ membrane (Amersham) by electroblotting (Bio-Rad Trans-Blot Electrophoretic Transfer Cell) in TBE buffer at 10 V overnight at 4°C. The RNA was crosslinked to the membrane twice with 1200 µ joules x100 UV light in a Stratalinker 1800 (Stratagene).Blot hybridization was made at 35°C overnight in UltraHyb-oligo buffer (Ambion) using as a probe, one or more short DNA oligonucleotides end labeled with P32 gamma ATP (Hartmann Analytic, Germany) by T4 polynucleotide kinase (Roche) and purified through MicroSpin G-25 columns (Amersham) according to the manufacturer's recommendations. The membrane was washed 3 times with 2X SCC, 0.5% SDS for 30 min at 35°C. The signal was detected by a phosphor screen after 1 to 6 days of exposure using a GE Typhoon 8600 imager (GE Healthcare Life Sciences). For repeated hybridizations the membrane was stripped with 0.5X SSC, 0.5% SDS for 30 min at 80°C and then with 0.1X SSC, 0.5% SDS for 30 min at 80°C. The DNA oligonucleotides were designed and ordered in Eurofins S.A.

Total RNA from ORMV infected *Nicotiana benthamiana* plants was extracted at day 5 and 26 post inoculation by taking 0.5 g of frozen ground tissue and adding 5 ml of GHCL extraction buffer (6.5 M guanidine hydrochloride; 100 mM Tris-HCL, pH 8; 100 mM sodium acetate, pH 5.5; 100 mM beta-mercaptoethanol). Once the mix was centrifuged at 10000g for 10 minutes at 4°C, the supernatant was treated according to the manufacturer's standard protocol with TRI Reagent (SIGMA). RNA was quantified with a ND-1000 UV-Vis Spectrophotometer (NanoDrop Technologies) and 10 to 30 µg total RNA were used for electrophoresis and blot hybridization as described before.

7.10. Long RNA blot hybridization analysis in *Arabidopsis* and *Nicotiana benthamiana*

Total RNA was isolated from 0.5 g of ground frozen tissue, obtained from leaves of individual plants or pools of plants, using TRI Reagent (SIGMA) according to the manufacturer's protocol. 20 µg RNA were resuspended in 6 µl of DEPC treated water (Diethylpyrocarbonate 0.1% v/v) and mixed with 6 µl RNA Gel Loading Dye (2X) (Thermo Scientific™), heated at 65°C for 3 minutes and loaded in a 1.2% denaturing agarose gel (1.2% agarose, 3% formaldehyde in MOPS buffer). A RiboRuler High Range RNA Ladder from 200 to 6000 bases (Thermoscientific) was also loaded into the agarose gel.The gel was run in Sub-Cell GT Cell (BioRad) nucleotide electrophoresis device at 100 V with MOPS buffer (0.02 M MOPS pH 7.0, 1mM EDTA, 5mM NaOAc) for 4 hours and then the RNA was transferred to a Hybond N+ membrane (Amersham) by capillary transfer in presence of transfer buffer (50mM NaH_2PO_4; 5mM EDTA pH 6.5 in DEPC water) for 24 hours. The RNA was crosslinked twice to the membrane with 1200 µ joules x100 UV light in a Stratalinker 1800

(Stratagene) and blot hybridization was made as described before for the small RNA blot hybridization.

7.11. β-elimination

For the β-elimination experiments, 20 µg of total RNA were dissolved in 17.5 µl borax buffer, pH 8.6 [4.375 mM borax (Fluka), 50 mM boric acid (Fluka)] and 2.5 µl of freshly prepared 0.2 M sodium periodate (Fluka) solution. As an internal control of the reaction, 250 pg of 22-nt non methylated GFP RNA (5'-uucaccuugaugccguucuucu-3', Dharmacon Inc.) were also included. The reaction mixture was incubated for 10 min at room temperature in the dark and, after addition of 2 µl glycerol, the incubation was repeated. The mixture was dried using SpeedVac, dissolved in 50 µl borax buffer, pH 9.5 (33.75 mM borax, 50 mM boric acid, pH adjusted by NaOH) and incubated for 90 min at 45°C. After the treatment, RNA samples were purified through Illustra MicroSpin G-25 Columns (GE Healthcare Life Sciences), dried and used for RNA blot hybridization as described before.

7.12. Deep sequencing and bioinformatic analysis of viral and plant small RNAs

Total RNA was isolated from pools of three plants, from *Arabidopsis* or *Nicotiana*, using the Trizol method as described above. Ten micrograms of total RNA for each sample from mock-inoculated and ORMV-infected wild-type or mutant plants were taken for preparation of sRNA libraries following Illumina's modified protocol for the sRNA library construction kit. The 19–30 nt RNA fraction from total RNA samples was purified on a 15% TBE–Urea acrylamide gel. A 5′-adenylated single-stranded adapter was first ligated to the 3′-end of the RNA using T4 RNA ligase without ATP followed by a second single-stranded adapter ligated at the 5′-end of the RNA using T4 RNA ligase in the presence of ATP. The resulting products were purified on a 10% TBE–Urea acrylamide gel before performing the cDNA synthesis and PCR amplification. The resulting libraries were sequenced on an Illumina Genome Analyzer HiSeq2000 following the manufacturer's protocol. After trimming the adaptor sequences, the datasets of all and unique reads were mapped to the reference genomes of *Arabidopsis thaliana* Col-0 (TAIR10), *Nicotiana benthamiana* (Niben.genome.v0.4.4) and ORMV (NC_004422.1), W41 (KF137561.1) or M41 and taken for further bioinformatics analysis. The results of bioinformatics analysis of the viral and host sRNA populations are summarized in (Supplementary Dataset S1). The mapping to the reference genomes was done using the bioinformatics tools Burrows-Wheeler Aligner (BWA) 0.5.9 and MISIS (www.fasteris.com/apps; Seguin et al., 2014[b]). For each reference genome and each sRNA size (20 to 25 nt), MISIS counted total number of reads, reads in forward and reverse orientation (Supplementary Dataset S2) and thus generated single-base resolution maps (Supplementary Dataset S3;) where for each position starting from the 5′ end of the reference genome, the number of matches starting at this position in forward (first base of the read) and reverse (last base of the read) orientation for each read length is given.

7.13. Western analysis

Leaves from *Arabidopsis thaliana* or *Nicotiana benthamiana* were collected and ground with liquid nitrogen. 30mg of ground frozen material were resuspended in 150 µl of 6X Laemmli SDS-PAGE Sample Loading Buffer (0.35 M Tris-HCl pH 6.8, 22.4% glycerol, 10% SDS, 0.6M DTT, bromophenol), vortexed briefly and heated for 3 minutes at 95°C. The samples were vortexed again briefly and centrifuged at 12 000g for 2 minutes to get a clear supernatant. SDS-PAGE was carried out in the discontinuous system described by Laemmli (Laemmli, 1970) employing a 9% SDS-PAGE gel and a 4% stacking gel in a Mini-PROTEAN Tetra Cell (BIO-RAD). 12µl aliquots from the supernatants were loaded in the gel together with 5µl of a pre-stained protein ladder (Thermo Scientific PageRuler Plus Prestained Protein Ladder) used as a reference of molecular weight. After 1 hour electrophoresis in Tris-glycine buffer pH 8.3 (25 mM Tris-Cl, 192 mM glycine, 0.1% SDS) at 100 V per gel, the proteins were transferred to an Amersham Hybond-P PVDF membrane 0.45 µm (GE Healthcare) for two hours in the presence of transfer buffer pH 8.3 (25 mM Tris-HCl, 192 mM glycine, 0.025% SDS, 20% (v/v) ethanol). The membrane was blocked at room temperature with 1% BSA (Sigma) in TBS-Tween buffer (25 mM Tris-HCl pH 7.4, 3 mM KCl, 140 mM NaCl, 0.1% Tween 20) for 1 hour. After 3 washes with TBS-Tween buffer, the following primary antibodies were used according to the different assays in TBS-Tween-1% BSA buffer at the indicated dilutions and incubated with the membrane at 4°C overnight: rabbit anti-125/182 replicase (1:4000) (raised against ORMV p125-specific synthetic peptide, see below), rabbit anti-AGO1 from *Arabidopsis* (1:8000) (Agrisera), rabbit anti-AGO2 from *Arabidopsis* (1:4000) (kindly provided by D. Baulcombe). After washing the membrane 3 times with TBS-Tween buffer, a secondary goat anti-rabbit antibody (1:10000) (Agrisera) was added in TBS-Tween-1% BSA at room temperature for 1 hour. After three additional washes with TBS-Tween buffer, the membrane was revealed by incubation at room temperature with the Amersham ECL Prime Western Blotting Detection Reagent (1ml of solution A + 1ml of solution B) for 3 minutes. Images were taken with an Azure c600 Imager.

In order to detect the ORMV p125 and p182, primary anti-peptide antibodies (Eurogentec sa) were raised in rabbits immunized with a synthetic peptide with the amino acid sequence GITRADKDNVRTVDS present in the ORMV p125 and p182 replicase. After being purified, the antibodies were used at the suggested dilution (1:4000) giving positive results for both proteins.

Section VIII. Results

8.1. p125 is a strong RNA silencing suppressor

As Blevins et al., (2006) demonstrated that ORMV infection interferes with HEN1-mediated methylation of plant and viral sRNAs, and Csorba et al., (2007) showed that p122 from TMV acts as a potent RNA silencing suppressor by binding siRNA and miRNA duplexes, interfering with their 3' terminal methylation, we hypothesized that the analogue protein encoded by ORMV, p125, could have a similar silencing suppression function. To test this hypothesis, we used the classical assay with transgenic *Nicotiana benthamiana* (16c line) plants expressing the green fluorescence protein (GFP), where p125, p182 and p125/p182 from ORMV were transiently expressed in the leaves by agroinfiltration, as described in Material and Methods, to test their potential to interfere with the local silencing of the GFP transgene (Fig 8.1 and 8.2.)

ORMV protein expression cassettes

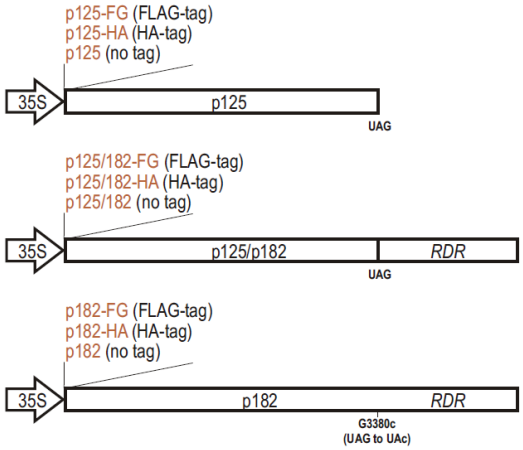

Figure 8.1. Schematic representation of ORMV protein expression constructs carrying ORMV p125, p125/182 or p182 protein coding sequences (with or without N-terminal HA- or FLAG-tags) under control of the CaMV 35S promoter, included in the binary vectors (pEarleyGate vectors) used to transform *Agrobacterium tumefaciens* by electroporation.

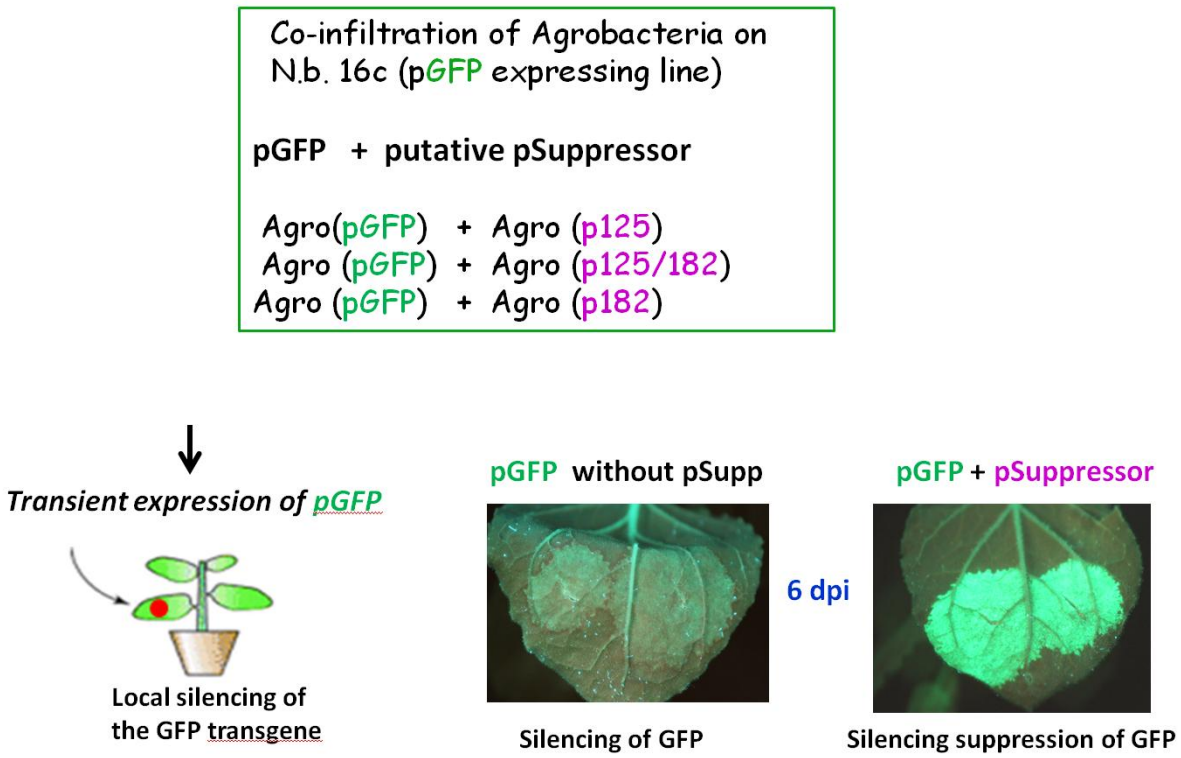

Figure 8.2. Transient protein expression in *N. benthamiana* with *Agrobacterium*. *Nicotiana benthamiana* 16c line leaves were infiltrated with 1:1 mixtures of *Agrobacterium tumefaciens* cells (adjusted to a final OD_{600}= 0.5) containing a binary plasmid expressing GFP and a binary plasmid expressing p125, p125/p182 or p182. Upon agroinfiltration, pGFP expression in the presence of the expressed viral proteins was evaluated under UV light at different time points, to identify the viral proteins that could be interfering with GFP RNA silencing.

The results revealed that p125 but not p182, is a strong suppressor of GFP silencing comparable to the viral suppressor HC-Pro (pHC-Pro), even in the presence of the hemagglutinin (HA) and flagellin (FLAG) N-terminal tags (Fig. 8.3). Indeed, suppression of the GFP transgene silencing could be confirmed by the permanence of the green fluorescent spot on the leaves of the plants where p125 was expressed, seen under UV light after 6 and 8 days post infiltration (dpi). A reduction of the silencing suppressor activity of p125 in the presence of p182 was also observed, indicated by the decreased fluorescence on the leaves in comparison to the strong fluorescence detected when p125 was only expressed (Fig. 8.3). We concluded that p125 is a strong GFP silencing suppressor.

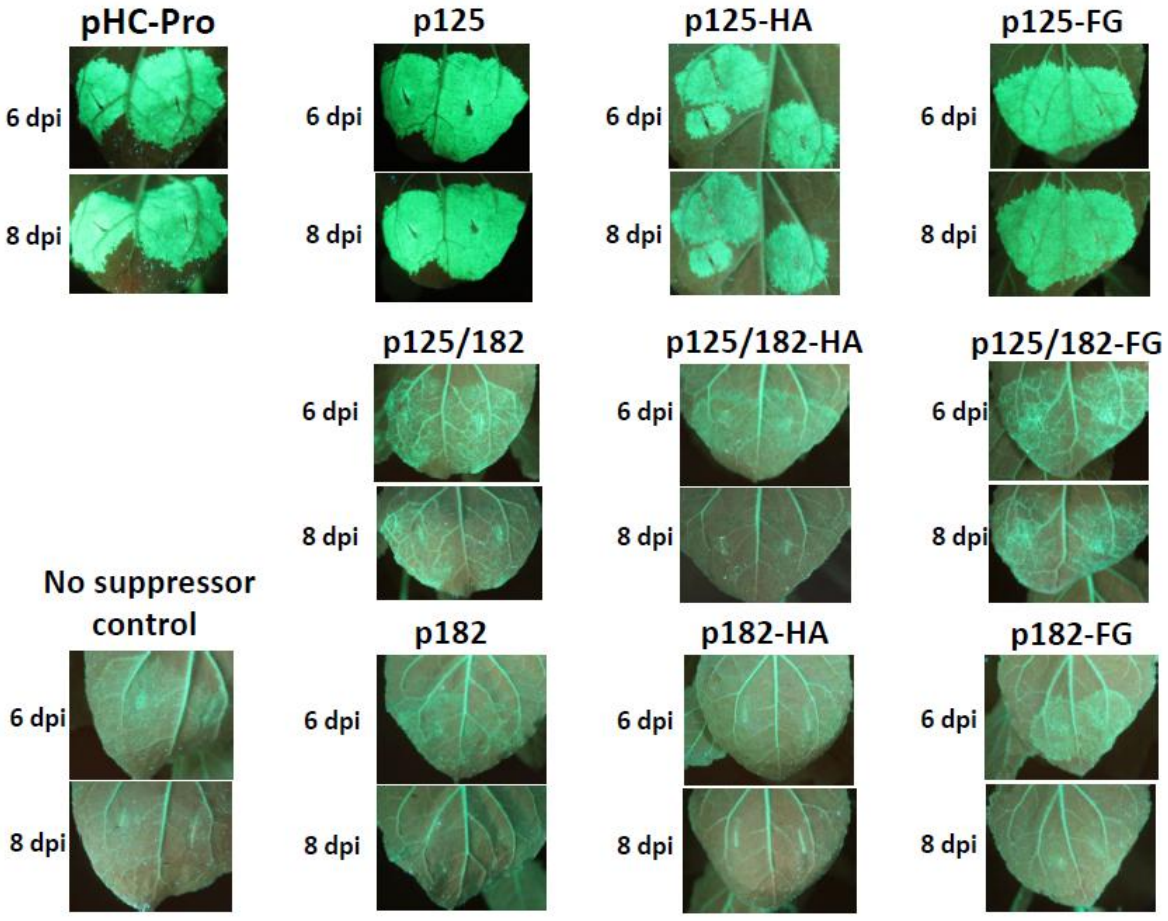

Figure 8.3 Effects of the transient expression of p125, p125/182 and p182 constructs on GFP transgene-induced silencing in *N. benthamiana* 16c leaves. In this experiment each construct was expressed on a separate leaf. GFP fluorescence images of the leaves under UV light were taken at 6 and 8 days dpi, following infiltration with an agro strain carrying a GFP expression cassette in combination with buffer (no suppressor control), an agro strain carrying the potyviral pHC-Pro (strong silencing suppressor control), or each ORMV protein expression cassette. The ORMV constructs without tag (p125, p125/182 and p182) contain the wild type ORMV protein sequences, while the constructs p125-HA, p125/182-HA and p182-HA have an HA-tag and the constructs p125-FG, p125/182-FG and p182-FG have a FLAG-tag fused to the N-terminus of the ORMV proteins.

Blot hybridization analysis revealed that the strong suppression of GFP silencing by p125 and pHC-Pro was not associated with a reduced accumulation of GFP transgene-derived siRNAs of sense or antisense polarities (Figure 8.4.), which is consistent with previous research implicating the duplex sRNA-binding activity of both HC-Pro (Garcia-Ruiz et al., 2015) and p125 homologs (Kurihara et al., 2007; Csorba et al.,2007) in silencing suppression. Further supporting this hypothesis, we found that transient expression of either p125 or pHC-Pro increased the accumulation of miR482*, which is normally degraded (Figure 8.4.). Note that the addition of an HA tag strongly compromised p125-mediated stabilization of miR482*, that neither p182 nor its HA- and FLAG-tagged derivatives were able to stabilize miR482*, and that p125 failed to stabilize miR482* when co-expressed with p182 (Figure 8.4.), demonstrating that the increased accumulation of miR482* is correlated with the strong GFP silencing suppression phenotypes exhibited by p125, p125-FG and pHC-Pro**.**

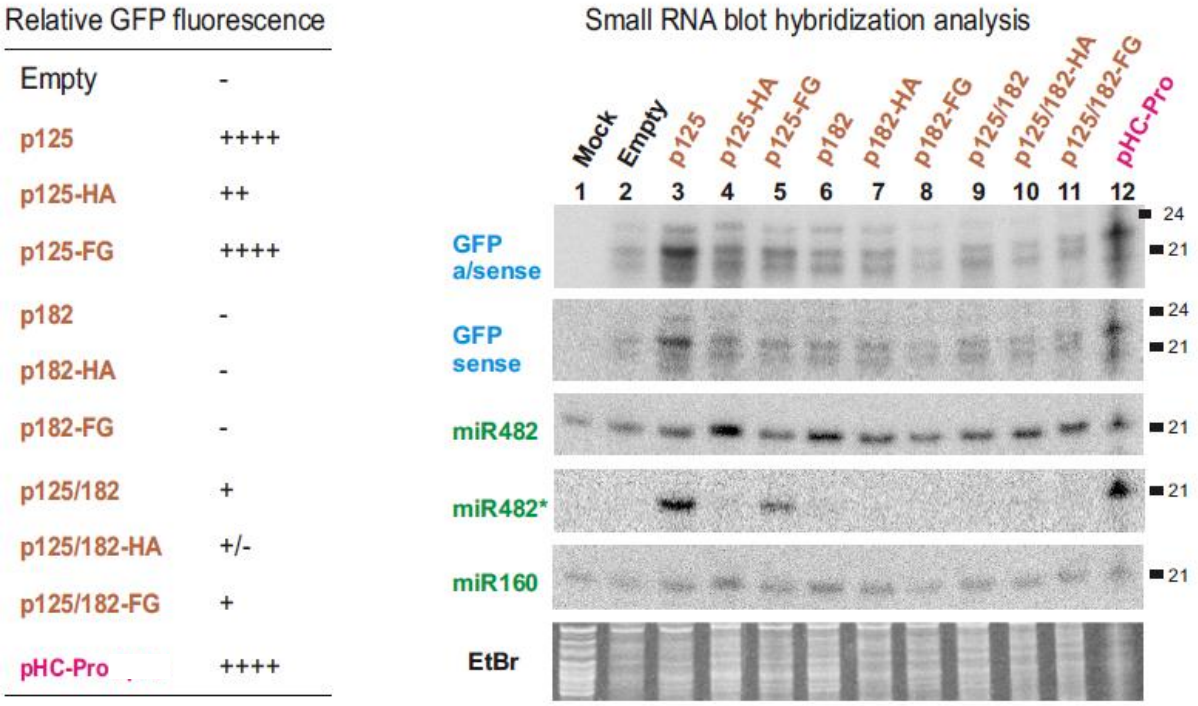

Figure 8.4. Effects of transient expression of the ORMV p125, p125/182 and p182 constructs on transgene-induced silencing (measured as relative GFP fluorescence; see Figure 8.3) and the accumulation of GFP siRNAs and plant miRNAs (examined by sRNA blot hybridization at 10 dpi) in *N. benthamiana* GFP transgenic 16c plants. The sRNA blot was successively hybridized with DNA oligonucleotide probes specific for GFP sense and antisense siRNAs and plant miR482, mi160 and miR482*. sRNA sizes are indicated. The EtBr-stained gel is shown as a loading control.

8.2. p125 transgene expression has an effect on miRNAs and tasiRNAs in *Arabidopsis*

In order to investigate the impact of p125, p182 and p125/182 on endogenous small RNAs, the same constructs were used to stably express these proteins in *Arabidopsis thaliana* as described in Material and Methods.

Phenotyping of *Arabidopsis* transgenic lines carrying each of the nine ORMV replicase constructs revealed that the expression of p125 without tags produced strong developmental abnormalities, resulting in adult plants exhibiting serration of the rosette leaf margins and curling of the stem. This is a phenotype remarkably similar to that produced by ORMV infection with the only difference that the latter produces chlorosis in older leaves (Fig. 8.5.)

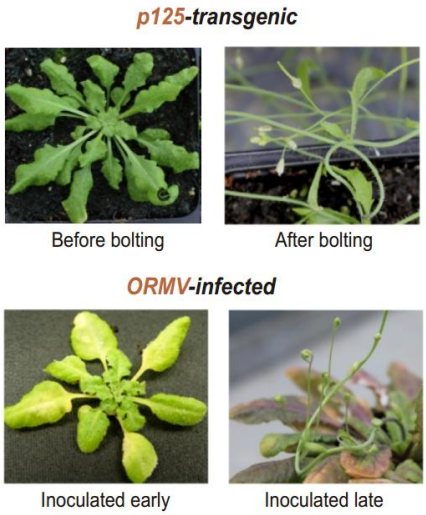

Figure 8.5. Representative phenotypes of the p125-transgenic plants (T2-plants of line 32) before and after bolting (see Fig. 8.8 for other lines and controls), compared to ORMV-infected A. thaliana Col-0 plants (the rosette leaves following early inoculation and the stem following late inoculation).

Phenotypes of *Arabidopsis* transgenic plants carrying the wild type p125

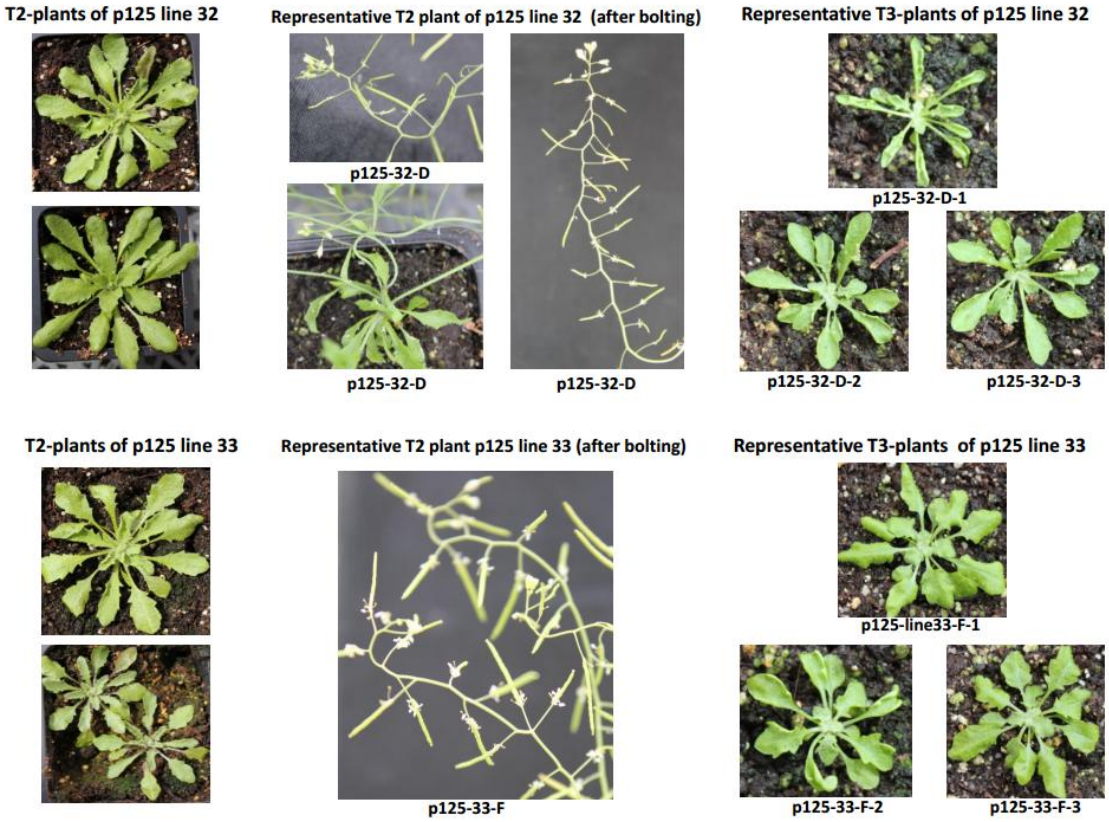

Figure 8.6. Phenotypes of Arabidopsis transgenic lines carrying the wild-type p125 expression construct. At maturity, seeds from each dipped T0 plant were collected and placed on soil to germinate. Transgenic seedlings were identified by their resistance to the herbicide BASTA (see Materials and Methods). The typical serrated morphology of the rosette leaves is shown for T2 and T3 plants obtained from 2 different T1 events (lines 32 and 33). A "zig-zag" stem curling phenotype can also be observed in T2 plants from both lines at the bolting stage.

The severity of the developmental defects exhibited by p125-transgenic lines correlated with the accumulation levels of some plant miRNAs (miR168 and miR472) and passenger strands of some miRNA (miR472*) and tasiRNA (siR255*) duplexes (Figure 8.7a. lanes 2,3,4,6,7,14,17,19,21).

Small RNA blot hybidization analysis of p125, p182 and p125/182 transgenic lines

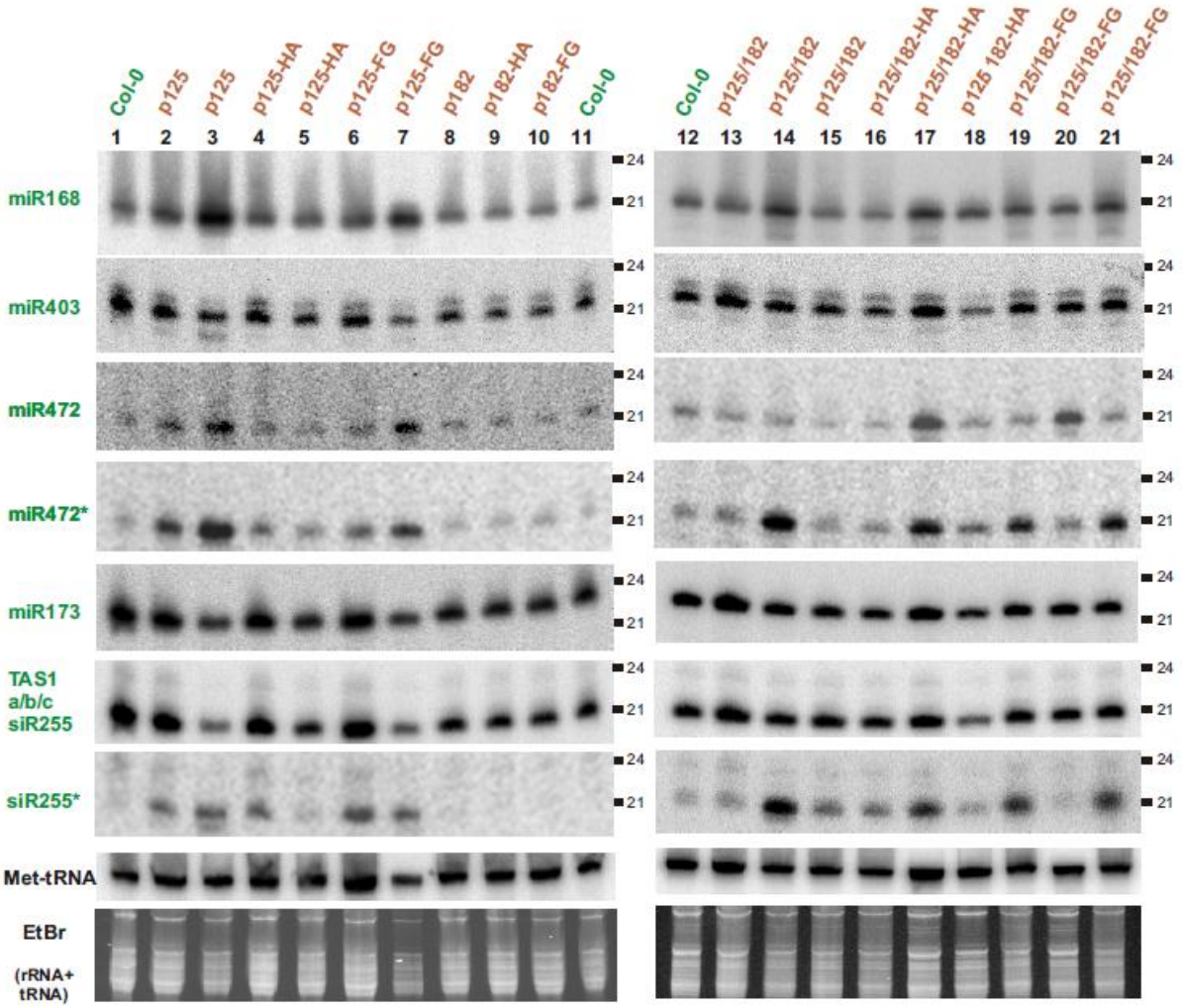

Figure 8.7a. sRNA blot hybridization analysis (15% PAGE) of total RNA samples from individual plants of Arabidopsis transgenic lines carrying p125 (T3-plants of line 32, lanes 2-3), p125-HA (T3-plants of line 40, lanes 4-5), p125-FG (T3-plants of line 49, lanes 6-7), p182 (T3-plant of line 1, lane 8), p182-HA (T3-plant of line 2, lane 9), p182-FG (T3-plant of line 1, lane 10), p125/182 (T2-plants of line 0, lanes 13-14; T2-plant of line 3, lane 15), p125/182-HA (T2-plants of line 0, lanes 13-14; T2-plant of line 3, lane 15), and p125/182-FG (T3-plants of line 1, lanes 16-18) expression constructs, or control wild-type plants (Col-0; lanes 1,11-12). The blot was successively hybridized with DNA oligonucleotide probes specific for plant miR168, miR403, miR173, miR472*, siR255 and siR255* and for Met-tRNA. sRNA sizes are indicated on each scan. The EtBr stained gel is shown as loading control.

The presence of HA- or FLAG-tag somewhat compromised the impact of p125 transgene expression on these siRNAs (Fig. 8.7a. lanes 4-7), which correlated with much weaker developmental abnormalities in p125-HA and p125-FG lines (Fig. 8.8). Likewise, weaker developmental abnormalities were observed in some of the transgenic lines carrying p125/p182 constructs (Fig. 8.9), in accordance with an intermediate impact on the endogenous plant sRNAs (Fig 8.7a, lanes 13,15,16,18,20). In contrast, transgenic lines carrying the p182 constructs, regardless of the flag status, did not exhibit any developmental abnormalities or aberrant accumulation of the examined plant siRNAs (Fig. 8.9. and Fig. 8.7a. lanes 8-10). Taken together, the relative activities of p125, p182 and p125/182 constructs stably integrated in *A. thaliana* transgenic plants correlate with the relative activities of the corresponding constructs transiently expressed in *N. benthamiana* leaves, indicating that p125 is a strong silencing suppressor that interferes with sRNA biogenesis and plant development. In contrast, transient or stable expression of p182 alone did not have any apparent effect, although we were not able to obtain transgenic lines where p182 expression was detectable by Western blotting (Figure 8.7b)

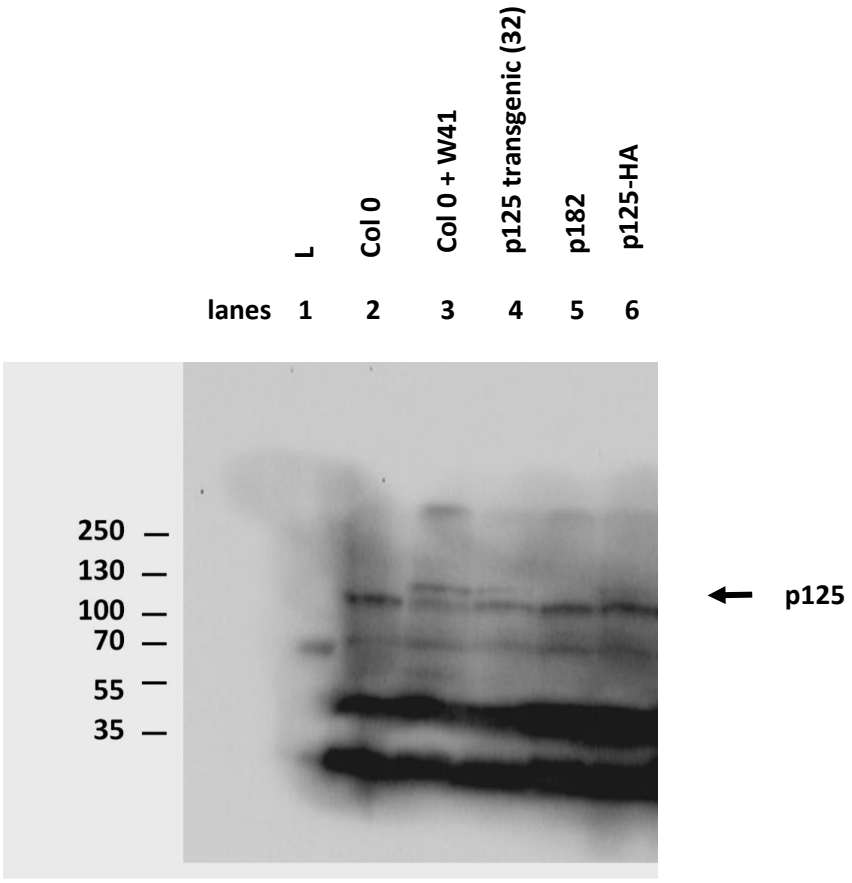

Figure 8.7.b. Western blot analysis using a p125/p182 specific antibody , showing the presence of p125 (although not p182) in *Arabidopsis* W41 infected plants (lane 3), and in *Arabidopsis* p125 transgenics (p125 line 32 and p125-HA line 45, lanes 4 and 6 respectively). No p182 can be detected in *Arabidopsis* p182 transgenic plants (lane 5).

Phenotypes of Arabidopsis transgenic lines carrying p125 with N-terminal HA or FLAG (FG) tags

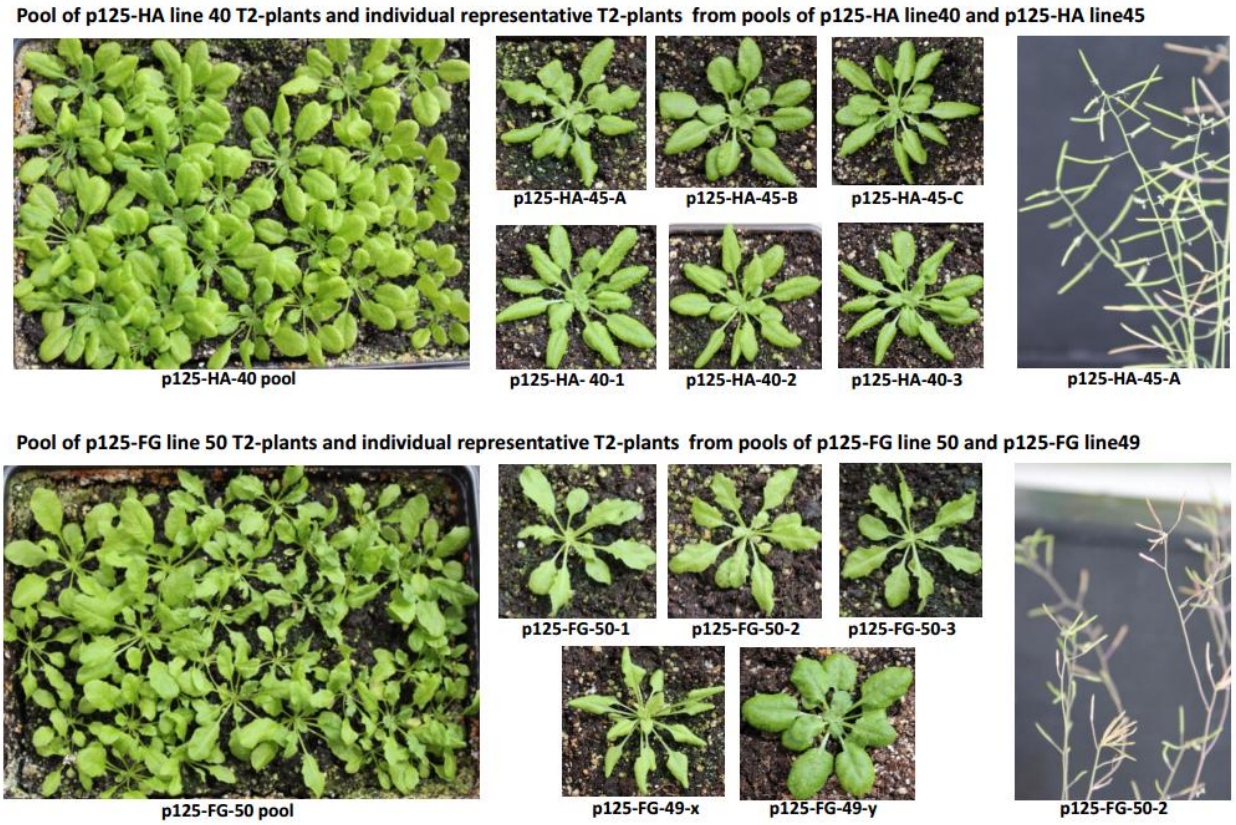

Figure 8.8. Phenotypes of Arabidopsis transgenic lines carrying p125 constructs with HA- or FLAG (FG)-tags. Images of the pools and of representative individuals of Basta-resistant T2-plants from two independent T1 transgenic events for p125-HA (lines 40 and 45) and p125-FG (lines 50 and 49). Note that p125-HA transgenic lines 40 and 45 exhibit almost no serration of the rosette leaves, and line 45 has a normal stem. p125-FG transgenic line 50 exhibits a strong serrated leaf phenotype and an aberrant silique arrangement at the bolting stage, while line 49 has two different rosette leaf phenotypes.

Phenotypes of *A. thaliana* transgenic lines carrying p182 and p125/182 constructs

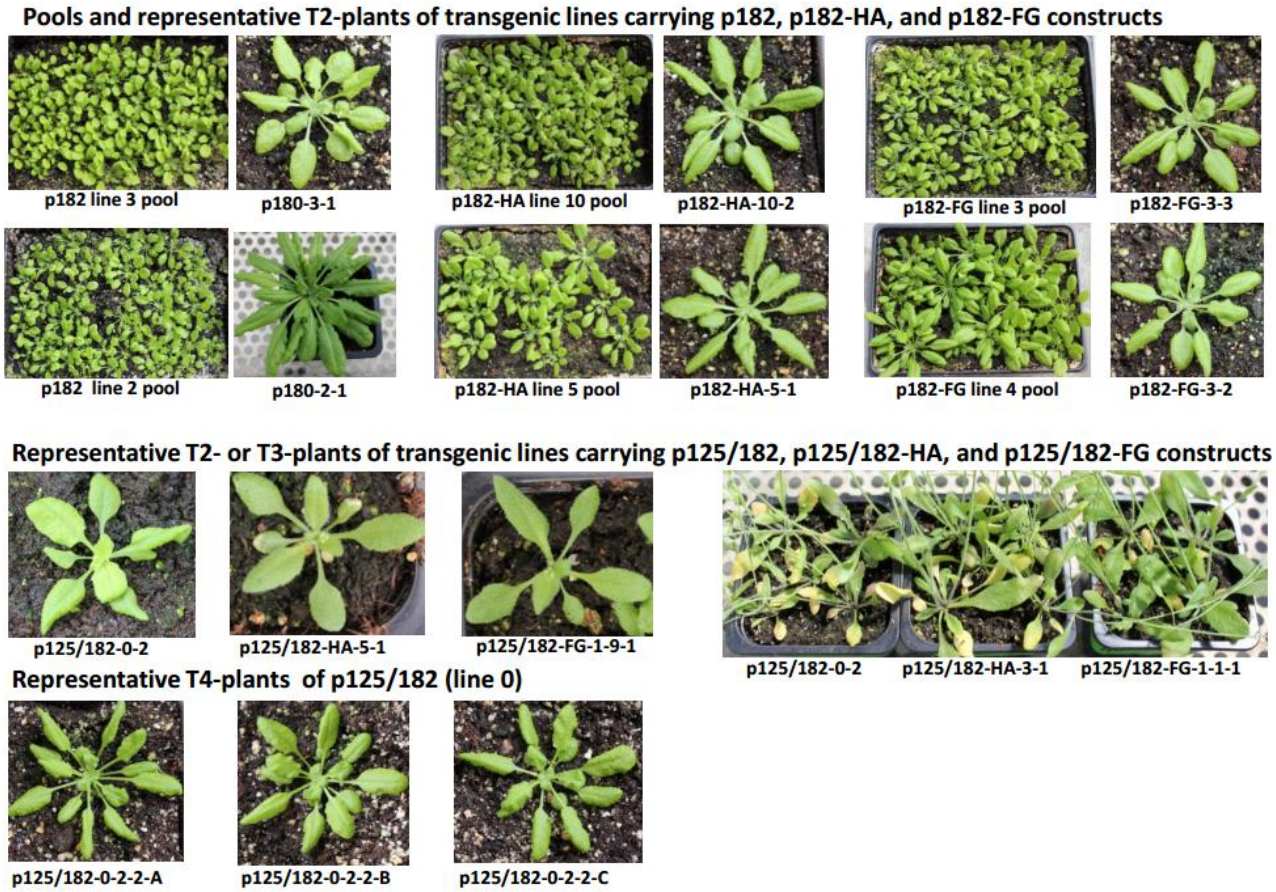

Figure 8.9. Phenotypes of A. thaliana transgenic lines carrying p182 or p125/182 transgenes without tag or with HA or FG tags. The top panels contain images of the pool and of representative individuals of Basta-resistant T2-plants from two T1 transgenic events for each construct: p182 (lines 3 and 2), p182-HA (lines 10 and 5) and p125-FG (lines 3and 4). Note that the transgenic T2 plants carrying the p182 constructs, regardless of tag status, exhibit normal rosette leaf phenotypes without serration. No stem curling or other inflorescence abnormalities were observed after bolting (not shown). The bottom panels show pictures of representative Basta-resistant T2-, T3- and T4-plants from independent T1 transgenic events for p125/182 constructs with and without tag: p125/182 (line 0), p125/182-HA (lines 5 and 3) and p125/182-FG (line 1). Note that some of the T2 plants exhibit slightly abnormal leaf phenotypes but no obvious serration or stem curling (not shown).

8.3. Infection of *Arabidopsis Col 0, rdr126, dcl234* with ORMV M41 or W41.

To better understand the induction and suppression of antiviral silencing during ORMV infection we performed an in-depth molecular characterization of wild-type *A. thaliana* (Col-0) and of the siRNA biogenesis-deficient triple mutant lines *dcl234* (*dcl2-5 dcl3-1 dcl4-2*) (Blevins et al., 2006) and *rdr126* (*rdr1-1 rdr2-1 rdr6-15*) (Blevins et al., 2011) at 5, 14 and 22 days post inoculation (dpi) with wild-type ORMV or a p125 stop codon mutant (UAG-to-UAC) derivative expressing p182 but not p125 (Figure 8.10e). The plants were inoculated either with ORMV sap or with *in vitro* transcripts of viral gRNA from wild-type and mutant virus clones, designated W41 and M41, respectively (see Materials and Methods Figure 7.4; Figure 8.10e). Viral RNAs and proteins were analyzed by Northern (Figures 8.10a and 8.10c) and Western (Figure 8.10f) blotting respectively, while viral and endogenous sRNAs were analyzed by blot hybridization (Figures 8.10b and 8.10d) and then by Illumina sequencing.

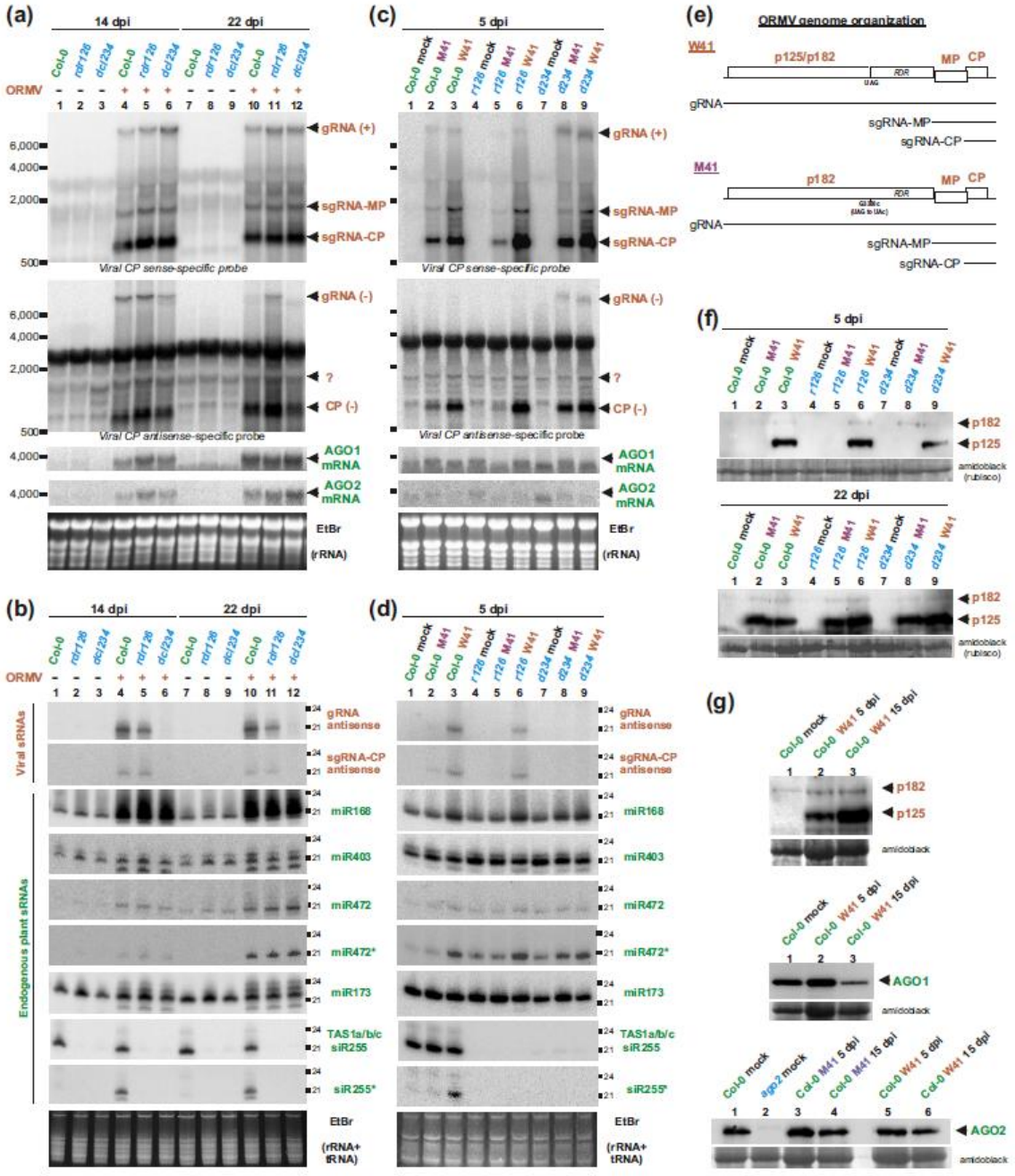

Figure 8.10. Blot hybridization analyses of viral and plant long RNAs, small RNAs and proteins in systemic (noninoculated) leaves of A. thaliana (Col-0, dcl234, or rdr126) and N. benthamiana (N.b.) plants infected with wild-type virus (ORMV, W41) or its p125 stop codon mutant (M41). Panels (A) and (C) show long RNA analysis (1% agarose denaturing gel) of ORMV positive-sense RNAs (gRNA, sgRNA-MP, sgRNA-CP) and negative-sense RNAs [gRNA(-) and CP(-)], and of A. thaliana AGO1 and AGO2 mRNAs in mock-inoculated (-) and virus-infected (+) Col-0, rdr126 and dcl234 plants at 14 and 22 days post-inoculation (dpi) with ORMV sap (A), and at 5 dpi with W41 and M41 in vitro transcripts (C). The cropped scans represent the blots successively hybridized with DNA oligonucleotide probes specific for the viral CP sense and antisense strands and the AGO1 and AGO2 coding strands (sequences for these and all other probes are given in Supplementary Table S1). The positions of RNA size markers are indicated on each scan. An abundant plant rRNA species cross-hybridized with the viral CP antisense-specific oligonucleotide probe is indicated by an asterisk. The question mark (?) indicates a presumptive viral MP(-) RNA species, the reliable detection of which is prevented by probe cross-hybridization to a co-migrating plant RNA species. EtBr-stained rRNA is shown as a loading control. Panels (B) and (D) show high-resolution sRNA analysis (15% PAGE) of the same total RNA samples from panels (A) and (C). The blots were successively hybridized with DNA oligonucleotide probes specific for viral antisense siRNAs derived from ORMV p125 and CP, as well as for plant miRNA (miR168, miR403, miR472, miR173), miRNA* (miR472*), siRNA (siR255) and siRNA* (siR255*) species. sRNA sizes are indicated. The EtBr-stained gel is shown as loading control. Panel (E) shows the genome organization of ORMV wild-type (W41) and mutant (M41) viruses. The ORFs are boxed and the encoded proteins (p125, p182, MP, and CP) are indicated above them. Positions of the p125 stop codon (UAG) in W41 and its mutation (UAG to UAc) in M41 are indicated. Viral genomic (gRNA) and subgenomic (sgRNA-CP and sgRNA-MP) RNAs are depicted by lines. Panels (F) and (G) show Western blots of ORMV p125 and p182 and A. thaliana AGO1 and AGO2 in Col-0, rdr126, dcl234 and ago2 plants infected with M41 or W41 at 5, 15 and 22 dpi. The membranes were incubated with anti-p125, anti-AGO1, or anti-AGO2 antibodies, and were stained with Amido Black afterwards to use the Rubisco bands as loading controls. The positions of p125 and p182 are indicated with arrows. Note that, in this particular experiment, the ORMV p125/p182-specific antibody cross-hybridized to a plant protein migrating just above p182 ("Col-0 mock" lane).

8.4. Double-stranded intermediates of viral replication are major substrates for DCLs

At all three time points, viral gRNA and sgRNAs accumulated to higher levels in dcl234 than in Col-0 plants (Figures 8.10a and 8.10c), coinciding with lower levels of viral siRNAs (Figures 8.10b and 8.10d). This finding is consistent with previous results implicating DCL4 along with DCL2 and DCL3 in ORMV siRNA biogenesis and antiviral defense (Blevins et al., 2006). In the rdr126 host, viral gRNA and sgRNAs also accumulated to higher levels than in Col-0 (Figures 8.10a and 8.10c). However, despite the absence of three RDRs known to generate siRNA precursors, viral siRNA production was not abolished in this background (Figures 8.10b and 8.10d). A. thaliana has three additional RDR genes of unknown function (RDR3a, RDR3b and RDR3c) (Wassenegger and Krczal, 2006) whose potential contribution to viral siRNA biogenesis in rdr126 plants cannot be formally ruled out. However, it would be plausible for DCLs to directly generate ORMV siRNAs from intermediate dsRNA forms arising during gRNA replication and sgRNA transcription; as a matter of fact, dsRNA species with sizes corresponding to viral gRNA and sgRNAs have previously been isolated from TMV-infected plants (Palukaitis et al.,1983).

In agreement with the latter possibility, a genome-sized long antisense RNA (designated gRNA(-)) likely functioning as a template for gRNA replication and sgRNA transcription, as well as a relatively more abundant short antisense RNA, comparable in size to sgRNA-CP and hence designated CP(-), were detected by means of strand-specific ORMV probes (Figures 8.10a and 8.10c). Since CP(-) RNA was produced in both Col-0 and rdr126 plants and accumulated to levels comparable to those of sgRNA-CP in every case (Figures 8.10a and 8.10c), this antisense viral RNA is likely synthesized by the viral replicase using sgRNA-CP as a template. In both wild-type and mutant plants, gRNA(-) accumulation peaked at 14 dpi and then decreased at 22 dpi (Figure 8.10a), indicating a decline in viral replication as gRNA(+) molecules (copied from gRNA(-) templates) are packaged into virions owing to the presence of increasing amounts of viral CP. At 5 dpi, gRNA(-) was detectable only in dcl234 (Figure 8.10c), suggesting that DCLs are targeting dsRNA viral replication intermediates since the earliest stages of viral infection.

8.5. Small RNA sequencing uncovers mechanisms of viral siRNA biogenesis

Illumina sequencing of the 19-30 nt fraction from total RNA samples of mock-inoculated and ORMV sap-infected *A. thaliana* Col-0, *rdr126* and *dcl234* plants at 14 and 22 dpi (used for Northern analysis in Figure 8.10a) yielded 12 libraries, each containing 3.1 to 7.8 million reads (Supplementary Dataset S1). The majority of these reads fell into a size range of 20 to 25 nts, known to be populated by endogenous plant miRNAs and siRNAs as well as viral siRNAs. This size range was selected for further bioinformatics analysis (see Materials and Methods).

Figure 8.11. Illumina sequencing counts of endogenous and viral sRNAs in mock-inoculated and ORMV-infected *A. thaliana* (Col-0, rdr126, or dcl234) at 14 and 22 dpi. (A) The graph shows the percentages of virus- and plant-derived sRNAs that mapped to ORMV or *Arabidopsis* genome reference sequences with zero mismatches in the pool of total 20-25 nt reads. (B) The graphs show the percentages of each size class for 20-25 nt virus- or *Arabidopsis*-derived sRNA reads that mapped to the corresponding reference sequence with zero mismatches.

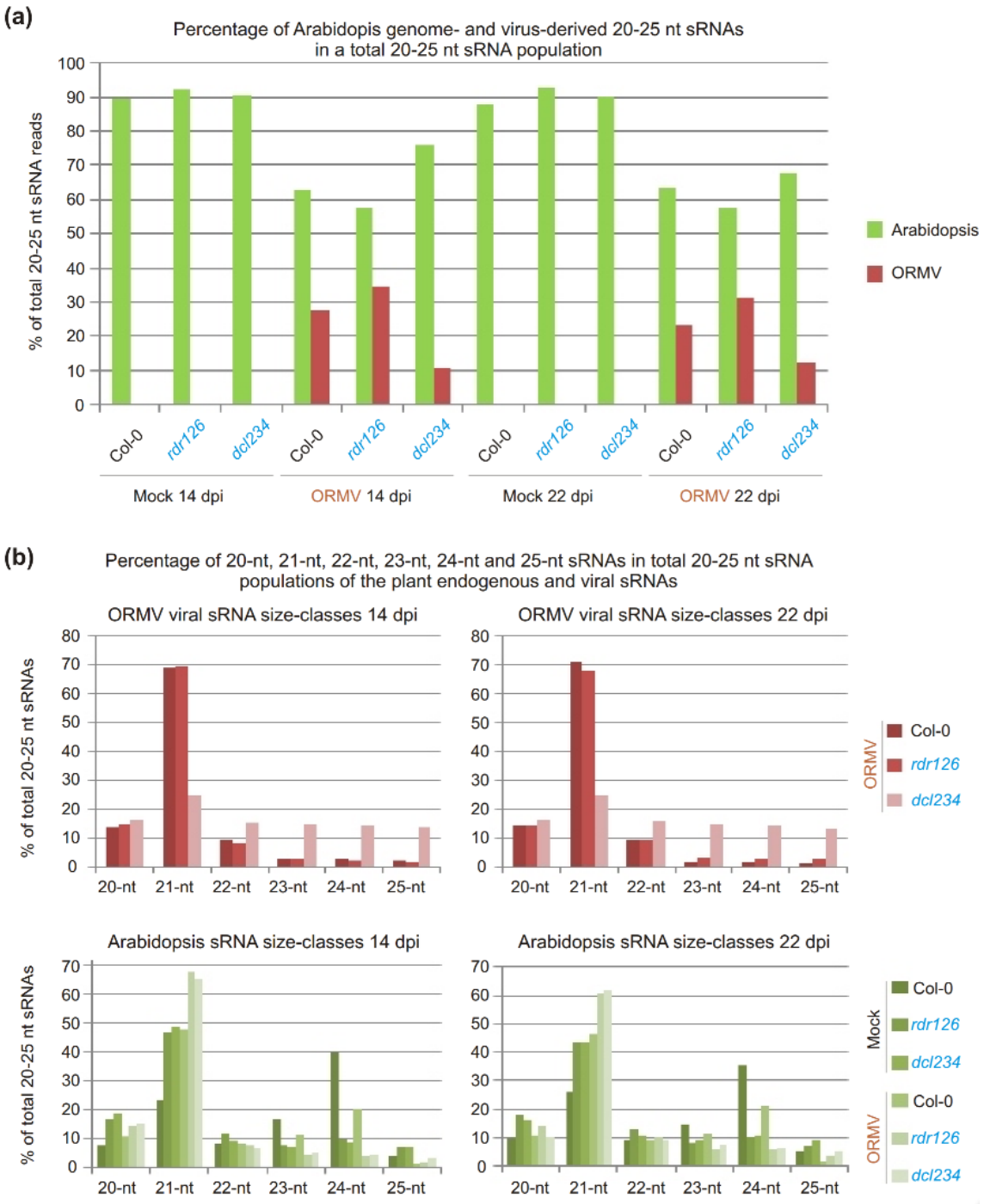

Zero-mismatch mapping of the sRNA reads to the 120 Mb *A. thaliana* TAIR10 reference genome and the 6.3 Kb ORMV genome revealed that viral sRNAs represented a large fraction (27% at 14 dpi and 23% at 22 dpi) of the 20-25 nt sRNA population in ORMV-infected Col-0 plants (Figure 8.11a; Supplementary Dataset S1). This proportion was even larger in ORMV-infected *rdr126* plants (35% at 14 dpi and 31% at 22 dpi) (Figure 8.11.a). However, since endogenous siRNA biogenesis is diminished in *rdr126*, thereby increasing the proportion of 21-nt reads (mostly representing miRNAs) within the 20-25 nt *Arabidopsis* reads (Figure 8.11b), we decided to normalize viral reads to the number of 21-nt endogenous *Arabidopsis* reads. The resulting figures were roughly equivalent between *rdr126* and Col-0 at 14 dpi (894,214 vs 908,107) and only slightly higher in *rdr126* at 22 dpi (898,249 vs 792,706) (Supplementary Dataset S1). Moreover, the size profiles of viral reads did not differ significantly between *rdr126* and Col-0; in both cases, 21-nt reads predominated (67-70% of 20-25 nt viral reads), followed by 20-nt (13-14%) and 22-nt (7-9%) reads (Figure 8.11b). Likewise, no substantial differences in the 5'-nucleotide profile (Supplementary Dataset S1) or viral genome distribution (Figure 8.12) of viral reads were observed between Col-0 and *rdr126* at any time point. Taken together, our findings indicate that RDR1, RDR2 and RDR6 are not essential for viral siRNA biogenesis.

The size profile of endogenous sRNAs changed significantly upon ORMV infection: at both 14 dpi and 22 dpi, 21-nt reads became the most abundant, surpassing the 24-nt reads that dominated in mock-inoculated Col-0 plants (Figure 8.11b), (Supplementary Dataset S1). A similar shift in sRNA size profiles was previously reported for ORMV-infected *A. thaliana* at 7 dpi, where it was found to correlate with the accumulation of many miRNAs as well as miRNA* and siRNA* passenger strands (Hu et al., 2012), and at 22 dpi in an earlier study (Blevins et al., 2006). We validated these findings for selected miRNAs and tasiRNAs by blot hybridization (Figures 8.10b and 8.10d). Notably, the accumulation of miRNAs and miRNA* species was generally more pronounced at the later time points (14 and 22 dpi rather than 5 dpi), and the levels of both miRNA and miRNA* were comparable between Col-0, dcl234 and rdr126 plants (Figures 8.10b and 8.10d). The latter finding indicates that endogenous RDRs are not involved in the upregulation of miRNA and miRNA* species triggered by ORMV infection, and validates the normalization procedure followed here for comparing viral siRNA levels between siRNA-deficient mutant lines and Col-0.

The number of viral sRNA reads was substantially lower in ORMV-infected dcl234 plants compared to Col-0 or rdr126 individuals. In this genetic background, viral reads represented only 11% and 12% of 20-25 nt reads at 14 and 22 dpi respectively which, when normalized per million Arabidopsis 21-nt reads, represents frequencies 4- and 3-fold lower than those of the corresponding time points in rdr126 or Col-0 plants (Figure 8.11b; (Supplementary Dataset S1). The size profile of viral reads in dcl234 plants was different as well at the two time points, with 21-nt reads constituting only 23% of 20-25 nt viral reads, i.e., 3 times lower than in rdr126 or Col-0 plants (Figure 8.11b). This is consistent with previous results implicating DCL4 in the biogenesis of 21-nt viral siRNAs in ORMV-infected Arabidopsis (Blevins et al., 2006). However, our finding that viral siRNA production was not abolished in dcl234 plants indicates that in this species the viral siRNA precursors can also be processed, although in a less efficient and precise manner, by DCL1 or some other RNase III-like endonuclease(s) that produces an sRNA population of broader and more evenly distributed size classes, exhibiting comparable numbers of 20-, 22-, 23-, 24- and 25-nt reads in addition to the slightly more abundant 21-nt reads (Figure 8.11b). Note that the Illumina protocol used

in our study only sequences RNA molecules bearing 5'-monophosphate and 3'-hydroxyl groups, which are typical of DCL and RNase III cleavage products.

An inspection of single-nucleotide resolution maps of ORMV-derived 20-25 nt reads revealed that viral siRNAs span the entire virus genome in both sense and antisense orientations without gaps in any strand (Supplementary Dataset S3; Figure 8.12). No strand bias was observed in Col-0 or rdr126 plants (Figure 8.12), supporting our hypothesis that siRNAs are processed from RDR-independent dsRNA precursors. In contrast, a strong bias towards gRNA(+) polarity was observed in dcl234 plants, where sense reads exceeded antisense reads ca. 9-fold at both 14 dpi (324,360 vs 34,565) and 22 dpi (420,344 vs 46,262). Interestingly, most antisense reads belonged to the 21-nt size class (Figure 8.12) or the less abundant 20-nt size class, while sense reads were more evenly distributed across other size classes (Supplementary Dataset S2). This finding implies that in dcl234, viral dsRNA replication intermediates are processed into 21-nt siRNA duplexes, presumably by DCL1, whereas viral single-stranded RNAs of sense polarity, i.e., gRNA(+) and sgRNAs, give rise to single-stranded sRNAs of all sizes, presumably through random cleavage by DCL1 or other RNase III-like endonuclease(s). In agreement with this hypothesis, in Col-0 and rdr126 plants (possessing all four DCLs) a substantial sense strand bias was only detected among the low abundance 23-nt, 24-nt and 25-nt reads (Supplementary Dataset S2; Figure 8.12).

Figure 8.12. Single-nucleotide resolution maps of 20-25 nt viral siRNAs from ORMV-infected A. thaliana (Col-0, rdr126, or dcl234) at 14 and 22 dpi. For each plant genotype and time point, the histograms plot the numbers of total 20-25-nt, 21-nt or 24-nt viral sRNA reads at each nucleotide position of the 6303 bp ORMV reference genome sequence (mapped with zero mismatches). The bars above the axis represent sense reads starting at each position and those below represent antisense reads ending at the respective position. A scaled ORMV genome diagram is shown above the histograms, with the ORFs boxed and their nucleotide positions indicated.

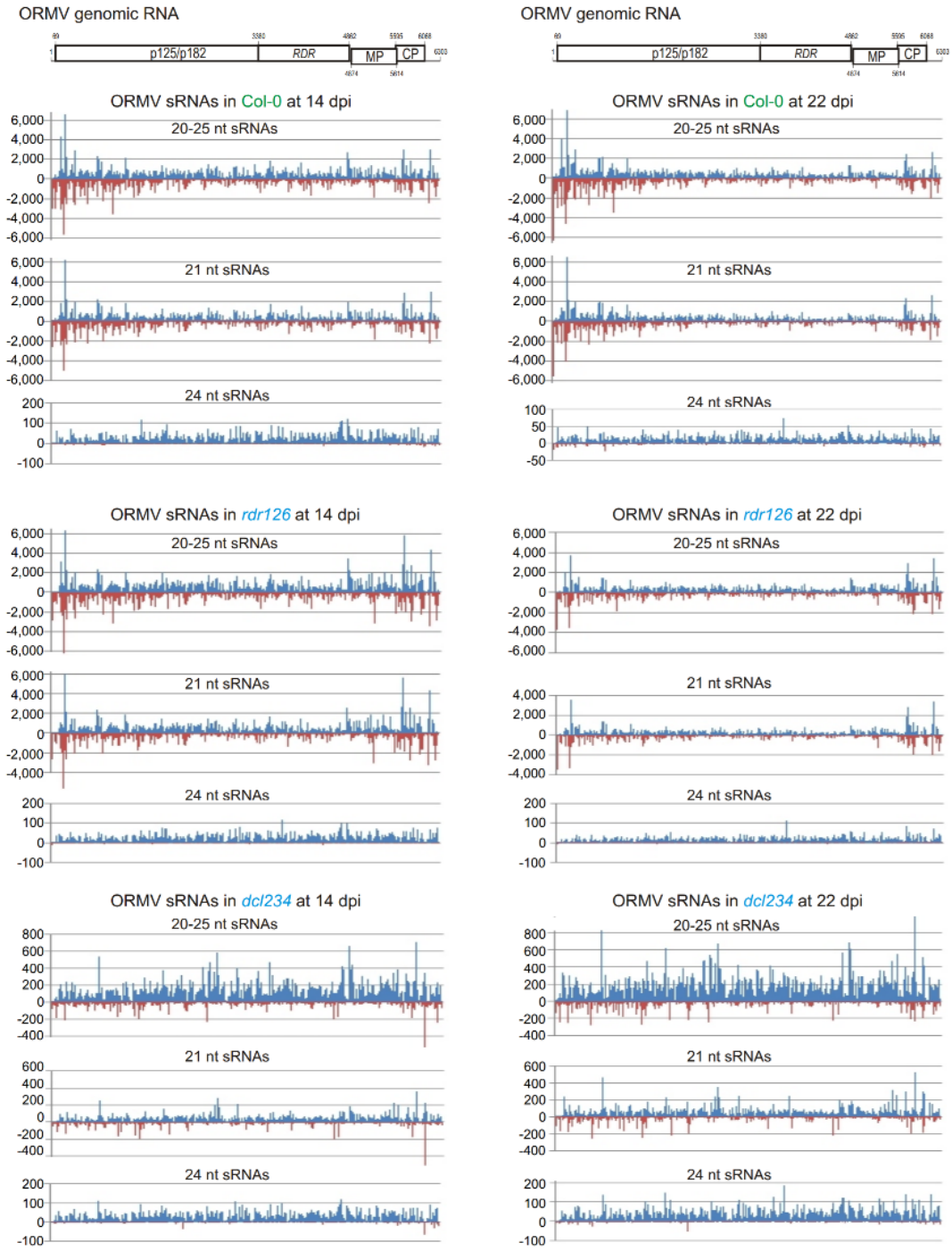

8.6. p125 is not essential for viral replication or movement but has a strong impact on silencing suppression and disease severity

Viral silencing suppressors can interfere with the antiviral activities of specific components of the RNA silencing machinery, which explains why the susceptibility of wild-type plants to certain viruses is often undistinguishable from that of mutant plants lacking the targered components. For instance, it was only by using suppressor-deficient mutants of *Cucumber mosaic virus* (CMV) and *Turnip mosaic virus* (TuMV) that the involvement of RDR6 and RDR1 in the biogenesis of secondary viral siRNAs and antiviral defense in *Arabidopsis* was demonstrated (Wang et al., 2010; Garcia-Ruiz et al., 2010; Wang et al., 2011).). Therefore, in an effort to dissect the involvement of the short and long (p125 and p182, respectively) components of the ORMV replicase complex in silencing suppression, we generated a mutant virus that can synthesize p182 but not p125 by changing the stop codon of the latter from TAG to TAC (which codes for tyrosine, the amino acid normally incorporated at this position via translational readthrough in other tobamoviruses) (Figure 8.10e). The mutation was introduced into ORMV infectious clone W41, where the 6303 nt consensus viral sequence (Seguin et al., 2014[a]) is placed under control of a T7 RNA polymerase promoter, as well as into its W4 derivative, which carries a T-to-G substitution at position 5612 (See Material and Methods Fig 7.4), obtaining the mutant clones M41 and M4. The parental clones W41 and W4 produce, upon delivery into *A. thaliana* Col-0 or *N. benthamiana* plants via inoculation of non linearized *in vitro* transcripts, a disease whose symptoms and severity are similar from those appearing after inoculation with wild-type ORMV virions (Figure 8.13 and Supplementary Figures S1a-S1C).

Col 0 virions 15dpi

Col 0 W41 15dpi

rdr126 W41 15dpi

rdr126 W4 15dpi

dcl234 W41 15dpi

dcl234 W4 15dpi

Nb virions 5dpi

Nb W41 5dpi

Nb W4 5dpi

Figure 8.13. *Arabidopsis* plants infected with virions or non linearized W41/W4 *in vitro* transcripts at 15dpi and *Nicotiana* plants infected with virions or non linearized W41/W4 *in vitro* transcripts at 5dpi. The disease symptoms are similar when virions or non linearized *in vitro* transcripts are used.

Following inoculation into *A. thaliana* Col-0, *rdr126* and *dcl234* plants, clones M41 and M4 exhibited lower virulence than their parental constructs, producing less severe symptoms by 22 dpi (Supplementary Figure S1C), which correlated with a reduced accumulation of viral gRNA(+) (Supplementary Figure S1G). RT-PCR/sequencing analysis revealed that in all the M41- and M4-infected Col-0, *rdr126* and *dcl234* plants of that time point, a p125 stop codon had reappeared in most viral gRNA molecules via an UAC-to-UAA reversion, and only a small fraction of viral RNA still carried the mutant UAC codon at this position (Supplementary Figures S1D-S1F). These results confirm earlier findings in TMV, where a similar UAG to UAU mutation at the stop codon was reverted *in vivo* to UAA (Ishikawa et al., 1986) (Figure 8.14).

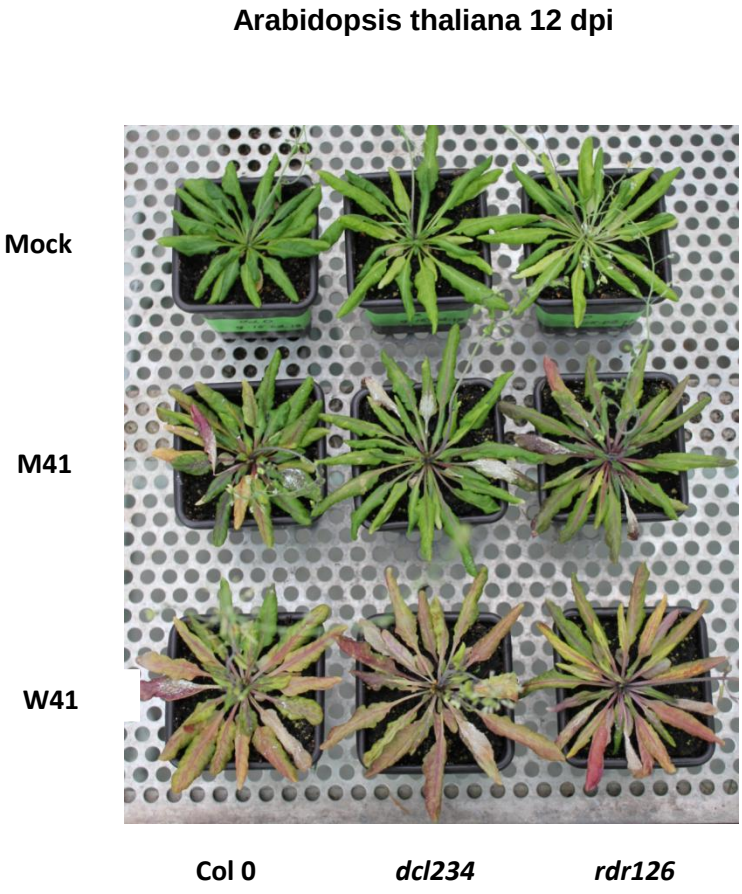

Figure 8.14. Arabidopsis plants Col-0, *dcl2/3/4* and *rdr1/2/6* infected with non linearized M41 and W41 *in vitro* transcripts showing disease symptoms at 12dpi. The original M41 virus had already reverted at this time point upon infection.

It is notable that even the impairment in siRNA biogenesis in *rdr126* and *dcl234* plants (see e.g. the tasiRNA siR225 and the repeat-associated siRNA siR1003 in Supplementary Figure S1H) did not compensate for the strong selective disadvantage suffered by p125-deficient viruses, as evidenced by their displacement by stop codon revertants along the course of the infection. However, it should be pointed out that the p125-deficient mutants could replicate and move systemically during the early stages of infection, because no p125 expression was detected in systemic leaves of M41-infected Col-0, *rdr126* or *dcl234* plants at 5 dpi (Figure 8.10f upper blot, lanes 2, 5, 8, figure 8.15a lanes 2 and 5). Accordingly, in both M41 and W41 infected plants, leaves with primary veins of purple color could be detected at 5 dpi, indicating the induction of anthocyanins probably due to systemic infection (Himeno et al., 2014) (Figure 8.15b).

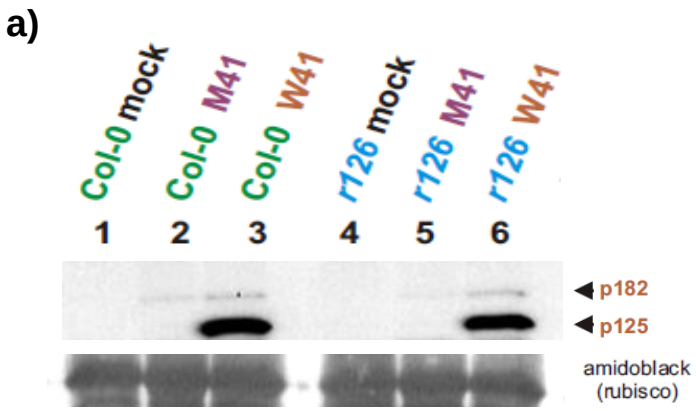

Figure 8.15a. Western blot analysis of p125 and p182 accumulation in *Arabidopsis* Col-0 and rdr1/2/6 plants infected with M41 or W41 at 5dpi, using a ORMV p125/p182 specific antibody. Amidoblack staining of rubisco is shown as loading control. The presence of ORMV p182 and p125 can de detected in W41 infected plants in a ratio of 1:10 as reported by Watanabe et al.,1999. Only p182 and not p125 can be detected in M41 infected plants, although in less amount than in W41 infected plants.

Figure 8.15b. Early signs of viral infection in leaves of *Arabidopsis* Col-0, *rdr1/2/6* and *dcl2/3/4* plants at 5dpi. Notice the purple color of the primary veins on some leaves of the plants infected with M41 or W41, compared to the Col-0 mock whose veins remain white and unaffected.

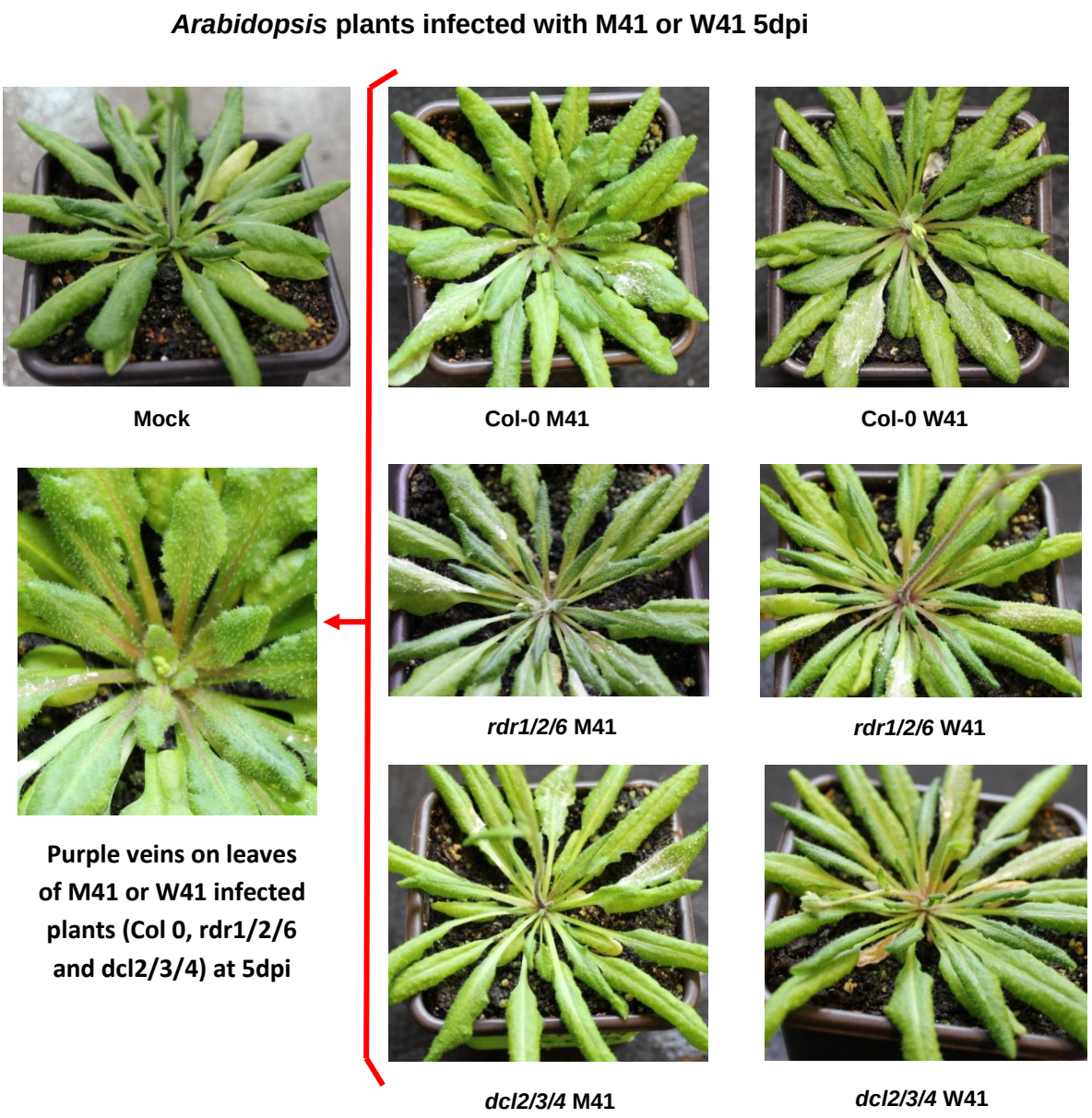

Consistently, no reversion of the stop codon was detected by deep sequencing and bioinformatic analysis M41 gRNA-derived small RNAs at 5 dpi. The gRNA and sgRNAs of M41 accumulated in all these plants, albeit at lower levels than in W41-infected plants (Figure 8.10c, compare lanes 2, 5, and 8 with lanes 3, 6, and 9). Notably, mutant virus RNAs accumulated to lower levels in *rdr126* than in Col-0, indicating that replication and/or systemic movement of the p125-deficient virus are not promoted, but restricted in the absence of RDR1, RDR2 and RDR6. On the other hand, they accumulated to higher levels in *dcl234* than in Col-0, indicating that the three DCLs substantially inhibit replication and/or systemic movement of the p125-deficient virus, presumably by processing viral dsRNA replication/transcription intermediates into siRNAs. Viral gRNA accumulated to comparable

levels in M41- and W41-infected *dcl234* plants (Figure 8.10c, lane 8 vs 9), as was the p182 protein (Figure 8.10f, upper blot, lane 8 vs 9), which, by contrast, could not be detected in M41-infected Col-0 and *rdr126* plants at 5 dpi (Figure 8.10f, upper blot, lanes 2 and 5), or was found in the same samples in less amount than in the W41-infected plants in a second Western (Figure 8.15 lanes 2 and 5). Hence, p125-deficient viruses could efficiently translate p182 and replicate gRNA only when DCL-mediated viral siRNA biogenesis was impaired.

To further examine whether p125 might affect viral siRNA biogenesis by inhibiting the activity of plant RDR1, RDR2 or RDR6, and whether p182 alone has any influence on the plant sRNA-generating machinery, we deep-sequenced sRNAs from Col-0 and *rdr126* plants systemically infected with M41 or W41 at 5 dpi. Bioinformatic analysis of viral sRNA reads revealed no stop codon reversion, confirming that the mutant virus population had not yet been overtaken by p125 stop codon revertants at this time point. W41-derived sRNAs comprised a large fraction of the 20-25 nt reads in both Col-0 and *rdr126*, even larger than that of endogenous *Arabidopsis* sRNAs reads (Figure 8.16a).

Figure 8.16. Illumina sequencing counts of endogenous and viral sRNAs in mock-inoculated and virus (W41, or M41)-infected A. thaliana (Col-0 or rdr126) at 5 dpi and N. benthamiana (N.b.) at 5 and 26 dpi. (A) Percentages of virus- and plant-derived sRNAs (mapped to ORMV and plant genome reference sequences with zero mismatches) in the pool of total 20-25 nt reads. (B) Size class percentages for 20-25 nt virus- and plant-derived sRNA reads (mapped with zero mismatches to the corresponding reference sequence).

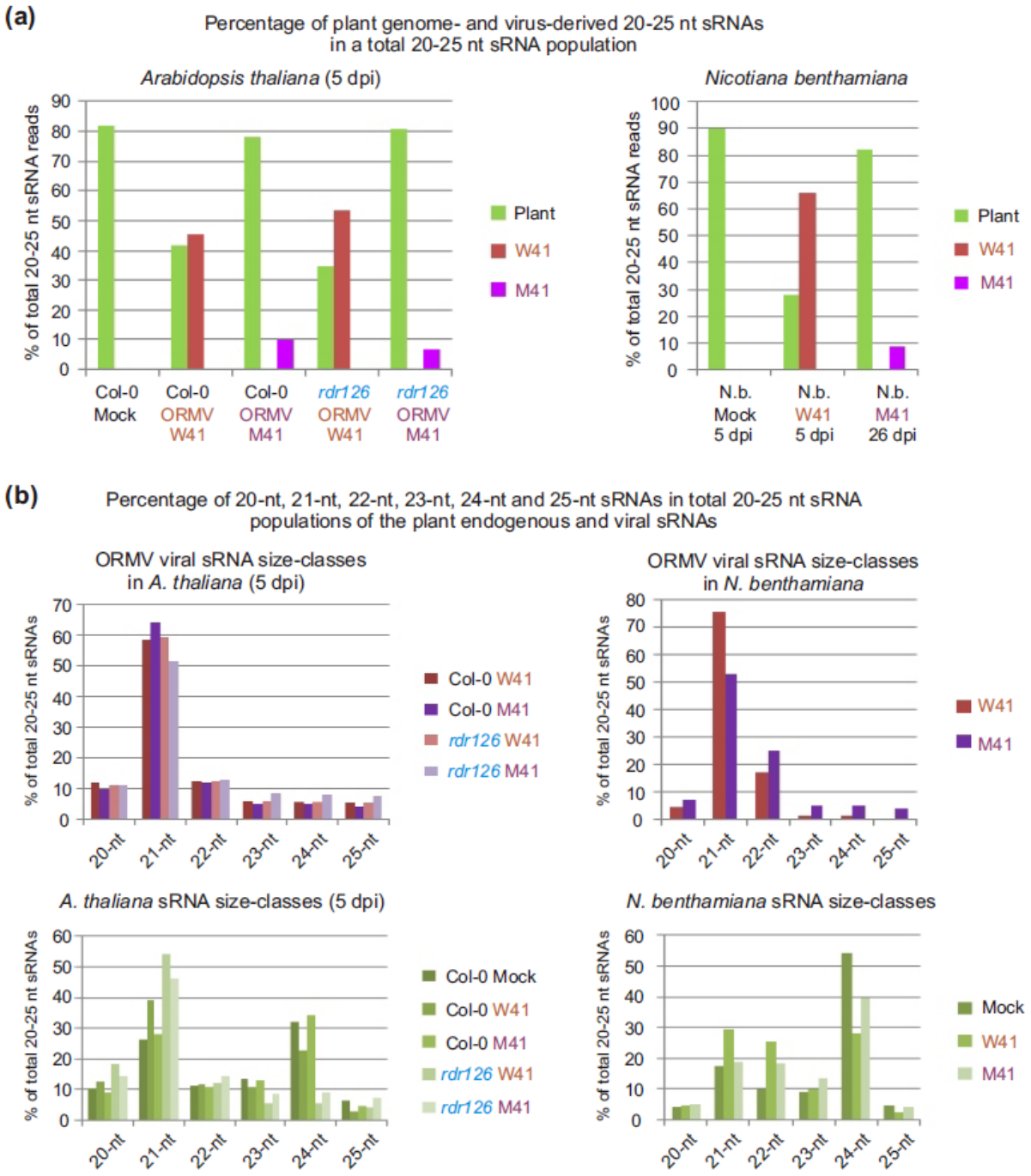

When normalized to 21-nt endogenous *Arabidopsis* reads, the accumulation of viral siRNAs was similar in Col-0 (2,800,511) and *rdr126* plants (2,852,744) (Supplementary Dataset S1). Moreover, an analysis of viral sRNA size classes (Figure 8.16b), single nucleotide resolution maps (Figure 8.17; Supplementary Dataset S3; and 5'-nucleotide profiles (Supplementary Dataset S1) did not find any significant difference between the ORMV-derived siRNAs of Col-0 and *rdr126* plants, indicating that RDR1, RDR2 and RDR6 do not play a significant role in the generation of siRNAs from wild-type virus at 5 dpi and thus extending the scope of our above-described findings for 14 and 22 dpi. Mutant (M41) virus-derived sRNAs accumulated to much lower levels than W41-derived sRNAs in both Col-0 and *rdr126* (Figures 8.16a and 8.10d), which correlated with the lower amount of viral long RNAs in the corresponding samples (Figure 8.10c). Although the normalized numbers of viral 20-25 nt reads for M41 in *rdr126* (181,155) were 2.5-fold lower than in Col-0 (442,742), which might be interpreted as a sign of RDR involvement in the production of secondary viral siRNAs in wild-type plants, as argued in earlier studies (Wang et al., 2010; Garcia-Ruiz et al., 2010; Wang et al., 2011), it should be pointed out that the amount of M41 long RNAs from which siRNAs are derived is also approximately 3-fold lower in *rdr126* than in Col-0 (Figure 8.10c, lane 5 vs 6). Furthermore, there are no significant differences between the size profiles (Figure 8.16b), single-nucleotide resolution maps (Figure 8.17) and 5'-teminal nucleotide identities (Supplementary Dataset S1) of mutant virus-derived sRNAs between Col-0 and *rdr126*. Taken together, our data indicate that at the early stages of infection, host RDR activity appears to promote the replication of the p125-deficient mutant virus in a manner independent of viral siRNA biogenesis, which operates mainly on a population of RDR-independent primary viral sRNAs. Also, viral p125 does not appear to inhibit the activities of any of the three host RDRs during wild-type virus infections, as no differences are apparent between the studied RDR-dependent endogenous siRNAs in wild-type or mutant virus infections (Figure 8.10d; Supplementary Figure S1H).

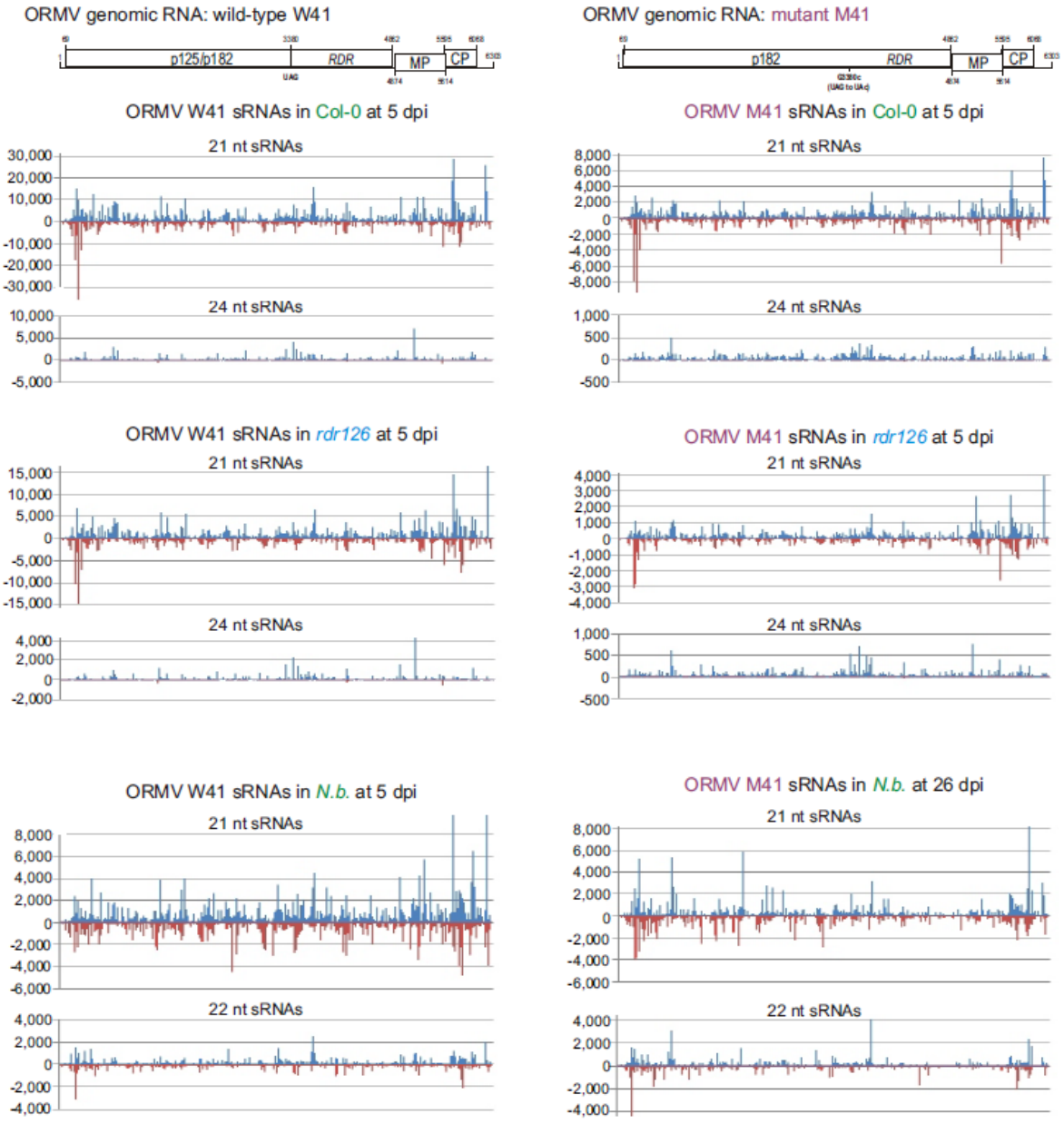

Figure 8.17 Single-nucleotide resolution maps of 20-25 nt viral siRNAs from virus (W41, or M41)-infected A. thaliana (Col-0 or rdr126) at 5 dpi and N. benthamiana (N.b.) at 5 and 26 dpi. For each plant genotype and time point, the histograms plot the numbers of total 20-25 nt, 21-nt and 24-nt viral sRNA reads at each nucleotide position of the 6303 bp W41 or M41 reference genome (mapped with zero mismatches); the bars above the axis represent sense reads starting at each respective position and those below represent antisense reads ending at the respective position. A scaled ORMV genome diagram is shown above the histograms, with the ORFs boxed and their nucleotide positions indicated.

In order to verify and extend the above findings to another host plant species, we tested if p125 deficiency also affects ORMV infection in the solanaceous plant *N. benthamiana*. Inoculation of *N. benthamiana* seedlings with wild-type ORMV virions or with *in vitro*-transcribed RNA from W41 or W4 resulted in severe disease symptoms, including stem necrosis and tilting at 5 dpi, followed by rapid plant death (Seguin et al., 2014[a]) (Supplementary Figure S1B). In contrast, inoculation with *in vitro*-transcribed RNA from p125-deficient viruses (M41 or M4) did not result in plant death, although disease symptoms were observed in upper (systemic) leaves of M41- and M4-infected plants at 26 dpi (Supplementary Figure S1B). The accumulation of viral gRNA and sgRNAs at 5 dpi for M41 and M4 was about 2-fold lower than for W41 and W4, and at 26 dpi the levels of mutant virus RNA were significantly lower than those of the wild-type, suggesting that plant defense mechanisms dampen virus replication in the absence of p125 (Supplementary Figure S1I).

Importantly, in systemic leaves of the mutant virus-infected plants no reversion of the mutated stop codon was observed at 5 dpi, and only a small fraction of viral RNA contained a reverted stop codon at 26 dpi (Figure 8.18 and Supplementary Figure S1E). Thus, the p125-deficient virus is able to replicate and spread systemically in *N. benthamiana* plants. Nonetheless, in one of the three repeated experiments there was detectable reversion of the stop codon and restoration of p125 expression in a single M41-inoculated plant (Supplementary Figure S1K), and when the sap of M41- or M4-infected plants was used to inoculate new individuals, p125 expression was quickly restored, leading to rapid death of the hosts. Thus, even though p125 is not essential for ORMV infection in *N. benthamiana*, p125-deficient viruses are eventually overtaken by stop codon revertants, although the process takes place at a much slower rate than in *A. thaliana.*

Figure 8.18 Infection of *N.benthamiana* with *in vitro* transcripts. The figure shows the disease symptoms caused by infection with *in vitro* transcripts from M41 or W41 ORMV constructs at 26 dpi, using a non-linearized pORMV vector in both cases. The plant infected with W41 wilted and presented stem necrosis already at 5 dpi while the M41 infected was even flowering at 26 dpi.

Mock

M41

W41

Deep sequencing of sRNAs revealed that at 5 dpi (before plant death), viral siRNAs are highly abundant in *N. benthamiana* plants inoculated with W41, since viral sequences comprise 65% of total 20-25 nt reads (Figure 8.16a). In contrast, p125-deficient virus-derived siRNAs accumulated to much lower levels at 26 dpi (9% and 20% of total 20-25 nt reads for M41 and M4, respectively) (Figure 8.16a; Supplementary Dataset S1), which correlates with lower levels of gRNA and sgRNAs. An analysis of single-base resolution maps of viral 20-25 nt reads revealed that the two most abundant viral siRNA size classes (21-nt and 22-nt) were equally distributed between both strands alongside the entire virus genome, and that siRNA hotspot patterns were similar between M41 and W41 (Figure 8.17; Supplementary Dataset S3;). Furthermore, 5'-terminal nucleotide frequency in viral reads was also comparable between M41 and W41 (Supplementary Dataset S1). Thus, despite substantial differences in overall accumulation levels, DCL-mediated processing of viral siRNAs from dsRNA precursors does not appear to be influenced by p125 in *N. benthamiana*, in agreement with our findings for *A. thaliana*.

8.7. p125 interferes with the methylation of viral and endogenous sRNAs during ORMV infection

It has been shown that ORMV interferes with HEN1-mediated methylation of viral siRNAs as well as of endogenous siRNAs and miRNAs in *A. thaliana* (Akbergenov et al., 2006; Blevins et al., 2006). To test whether p125 is responsible for this effect, we assessed the methylation status of sRNAs from W41- and M41-infected plants by a classical β-elimination method. If RNA is not modified at the 3'-terminal nucleotide, β-elimination removes it, leaving a truncated RNA with a 3'-phosphate whose mobility in denaturing 15% PAGE is shifted by two

nucleotides (Akbergenov et al., 2006) (see non-methylated 22-nt RNA (+) control, Figure 8.19). HEN1 methylates plant miRNAs and siRNAs at the 2'-hydroxyl of their 3'-terminal nucleotide, which blocks β-elimination. As can be observed (Figure 8.19), *A. thaliana* miR168 and miR173, *A. thaliana* siR255 and *N. benthamiana* miR168 and miR482 are methylated in non-infected plants and therefore fully resistant to β-elimination. In contrast, a significant fraction of viral siRNAs and endogenous sRNAs in wild-type virus (W41)-infected *A. thaliana* and *N. benthamiana* was sensitive to β-elimination (Figure 8.19, lanes 4 and 10), while both viral and endogenous (miR168 and miR482) siRNAs from *N. benthamiana* plants infected with the mutant virus (M41) were resistant to β-elimination (Figure 8.19, lane 6). This indicates that in the absence of p125, the virus is not able to block the methylation of viral siRNAs. Taken together, our data indicate that p182, when expressed in the absence of p125, does not interfere with HEN1-mediated methylation of viral and endogenous sRNAs.

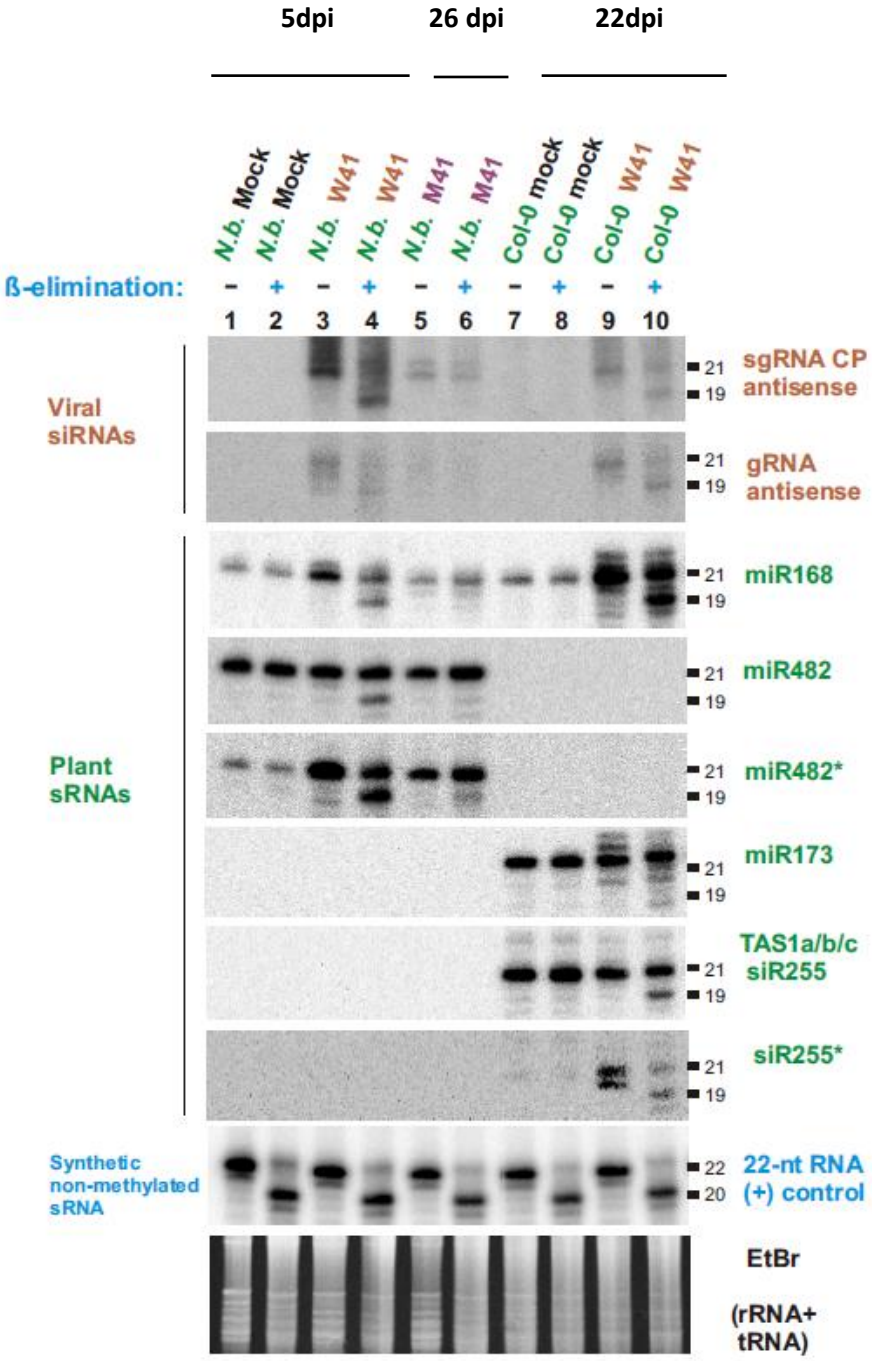

Figure 8.19. β-elimination analysis of viral and endogenous sRNAs in plants infected with wild-type (W41) or p125-deficient (M41) virus. Two aliquots were taken from each total RNA sample from N. benthamiana (N.b.) systemically infected with W41 (5 dpi) or M41 (26 dpi), or A. thaliana (Col-0) infected with W41 (22 dpi). One was treated with periodate (+) and the other with buffer (-) and both were analyzed by 15% PAGE and blotted. The blot was successively hybridized with DNA oligonucleotide probes specific for viral antisense siRNAs derived from ORMV p125 or CP genes, for plant miRNAs (miR168, miR482), miRNA* (miR482*), siRNA (siR255) and siRNA* (siR255*) species and for a synthetic non-methylated 22-nt RNA (spiked into each total RNA sample as an internal control). sRNA sizes are indicated on each scan. The EtBr-stained gel is shown as loading control.

Notably, although it has been shown that in *A. thaliana* HEN1 deficient mutant lines sRNA accumulation is impaired (Yu et al., 2005; Yang et al., 2006), such a phenomenon was not observed in ORMV-infected plants, where HEN1-mediated methylation is partially inhibited. On the contrary, viral siRNAs and many endogenous sRNAs accumulated to much higher levels in W41-infected plants compared to M41-infected plants, and plants infected with wild-type ORMV produced higher-than-normal levels of non-methylated passenger strands from endogenous miRNA and siRNA duplexes (Blevins et al., 2006) (Figure 8.19). It has been shown that p125 homologs from other tobamoviruses exhibit sRNA duplex-binding activity (Kurihara et al., 2007; Csorba et al., 2007), so a plausible explanation for this phenomenon would be that p125 is stabilizing non-methylated sRNA duplexes through such an interaction.

8.8. AGO1, AGO2 and RPS5 mRNAs overaccumulate in ORMV infected Arabidopsis plants.

In order to ascertain whether sRNA-mediated cleavage and degradation of target mRNAs is affected in ORMV-infected plants, we initially examined the relative accumulation of *AGO1* and *AGO2* mRNAs, known to be targeted by miR168 and miR403, respectively. Northern blot hybridization analysis revealed that the levels of these mRNAs were higher in 14 and 22 dpi ORMV-infected plants than in 5 dpi ORMV-infected plants or mock-inoculated controls, where these mRNAs could not be detected reproducibly (Figures 8.10a and 8.10c). However, a corresponding increase in the levels of the proteins encoded by these mRNAs was not detected by Western blot analysis; rather, the levels of AGO1 had decreased drastically by 15 dpi (Figure 8.10g). Hence, despite the apparent compromise of miRNA-directed mRNA cleavage, the translation of target mRNAs appears to be repressed by the overaccumulation of their miRNAs. Indeed, the degree of miR168 overaccumulation upon ORMV infection is much higher than that of miR403 (Figure 8.10b), fitting with the much more pronounced drop in the levels of AGO1, compared to AGO2 protein (Figure 8.10g). It is worth noting that ORMV-mediated up-regulation of miR168 depends on p125, as the p125-deficient virus did not up-regulate this miRNA in *A. thaliana* (Figure 8.10d) or *N. benthamiana* (Figure 8.19). Considering additional targets, the overaccumulation of RPS5 mRNA was also observed at 14 dpi and 22 dpi in infected plants (Figure 8.20b), correlating with the gradual increase of miR472 during infection (Figure 8.10b). It is noteworthy to mention that at day 22 post inoculation, most of the miR472 population is not methylated due to the presence of p125 (Figure 8.20c). Interestingly, RPS5 mRNA accumulation was also observed at 5dpi in ORMV infected *dlc2/3/4* plants (Figure 8.20a), suggesting that RPS5 is induced by M41 and W41 at an early stage of the viral infection. No overaccumulation of RPS4 mRNA was detected at the late time points of infection, in spite of the similarity between both RPS5 and RPS4 genes in the target site sequences for miR472 (Figure 8.20b and 8.21). Although the amount of RPS5 protein could not be evaluated in the infected plants at the different time points, the results put forward the idea that translation of RPS5 mRNA, as in the case of AGO1 and AGO2, is repressed in ORMV W41 infected plants through the increased levels of miR472.

Figure 8.20. Induction of RPS5 mRNA level is associated with increased miR472 accumulation in W41 infected *Arabidopsis* and accumulation of nonmethylated miR472 and miR472*. Systemically infected leaves of ORMV M41- or W41-inoculated *Arabidopsis thaliana* plants (Col 0, rdr1/2/6 and dcl2/3/4) were homogenized and used for RNA and protein extractions. The samples were used for: detection of relative virus accumulation at 5, 14 and 22 dpi visualized by Northern blot analysis using a viral CP sense-specific probe (a and b); detection of relative p125 and p182 accumulation in infected tissue at 5dpi by Western analysis using a ORMV p125/p182 specific antibody. Relative gel loadings are indicated by amidoblack staining of rubisco (a); detection of RPS5 mRNA expression visualized by Northern blot analysis using a DNA probe specific for a region downstream from the miR472 recognition site (RPS5 specific probe) and detection of RPS4 mRNA expression as negative control, using a DNA probe specific for RPS4 (a and b); sRNA Northern blot analysis using a DNA oligonucleotide probe specific for miR472 and miR472* before (-)and after (+) β elimination (c). Relative gel loadings are indicated by ethidium bromide staining of ribosomal RNAs (rRNA) (a,b) and rRNA+tRNA in case of the β elimination analysis (c).

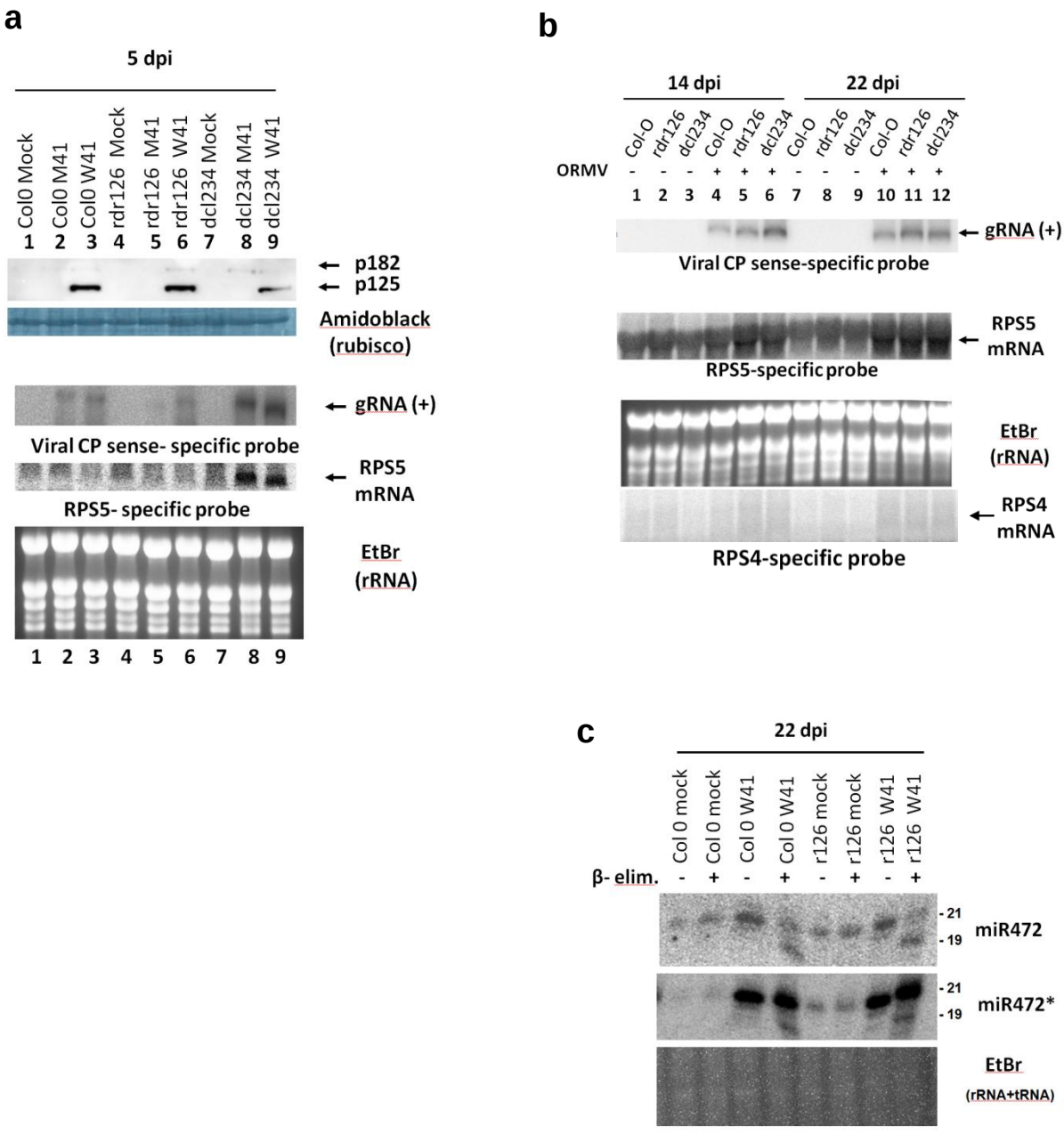

RPS5 is a target of miR472

	P LOOP	
Ath RPS4 AT5G45250	RII**G**VV**GM**P**G**I**GKTTLL**K	5'- GGGAUGCCCGGAAUUGGUAAAACCACA- 3' 3'-CC**A**UAC**CC**GCCU**C**A**U**CC**U**UUUU-5' **miR472**
Ath RPS5 AT1G12220	IL**G**LY**GM**G**G**V**GKTTLL**T	5'-GGUAUGGGGGGAGUAGGCAAAACGACA-3' 3'-CCAUACCC**G**CCUCAUCC**U**UUUU-5' **miR472**

Fig 8.21. In bold blue are shown the shared amino acids within the P-loop from RPS4 and RPS5. In light blue and underlined are shown the amino acids and corresponding codons within the P-loop between RPS4 and RPS5, which represent a potential target site for miR472. In bold red are shown the mismatches between miR472 and the P-loop nucleotide sequence present in RPS4 and RPS5, which show that RPS5 is a target of mir472 while RPS4 is not.

Section IX. General Discussion

In this work we investigated the roles of proteins p125 and p182 from the tobamovirus ORMV in viral gRNA replication, sgRNA transcription and suppression of sRNA-directed antiviral silencing during systemic infection in *A. thaliana* and *N. benthamiana*. With this purpose we constructed a mutant virus expressing exclusively p182 but not p125, by eliminating the stop codon preceding the RDR domain of the former, and tested it for infectivity in both, wild-type plants and silencing-mutant plants deficient in DCL- and RDR-dependent siRNA biogenesis. Furthermore, we examined the effects of both viral proteins, alone or in combination, on the plant sRNA-generating silencing machinery during their transient expression in *N. benthamiana* leaves and upon stable constitutive expression in *Arabidopsis* transgenic lines.

Functions of p125 and p182 in viral replication vs silencing suppression

Our analysis of the p125-deficient mutant virus in systemic leaf tissues of *A. thaliana* and *N. benthamiana* revealed that p125 is not essential for gRNA replication or sgRNA transcription. However, gRNA and sgRNAs of the p125-deficient mutant accumulated to levels lower than those of the wild type virus (Figure 8.10c, Supplementary Figure S1I), and stop codon revertants often accumulated and overtook the mutant population, restoring p125 expression (Figure 8.10f, Supplementary Figure S1K). These findings are consistent with previous observations in other tobamoviruses, where mutants expressing exclusively the readthrough replicase do replicate in tobacco protoplasts and plant tissues albeit with a reduced efficiency, and stop codon revertants restoring expression of the shorter protein appear at a high frequency (Ishikawa et al., 1986; Lewandowski and Dawson 2000; Knapp et al., 2001).

Theoretically, p125 can facilitate viral replication and/or transcription either indirectly through its silencing suppressor activity, or directly through the formation of a putative heterodimer with p182. In other tobamoviruses, the replicase and guanylyltransferase enzyme activities localize to membrane-bound heterodimers of the corresponding p125/p182 homologs (Osman and Buck 1996; Watanabe et al., 1999; Hagiwara et al., 2003; Komoda et al., 2007; Nishikiori et al., 2012), and leftover p125, which is present at molar excess, forms soluble oligomers in the cytoplasm (Watanabe et al., 1999), where it might assume additional roles unrelated to viral gRNA replication and sgRNA transcription. Indeed, non-membrane-bound heterodimers of the tobamoviral replication proteins have been implicated in silencing suppression via their sRNA binding activities (Hagiwara-Komoda et al., 2008). We demonstrate here that p125 is a strong silencing suppressor in the classical transient expression assay in *N. benthamiana* 16c plants (Figures 8.3 and 8.4) and that p125 is required for the inhibition of HEN1 activity that is observed during ORMV infection (Figure 8.19). We favor a scenario in which p125 facilitates viral replication and transcription through its antisilencing activity. Our data do not support an essential direct role of p125 in ORMV replication, as the p125-deficient virus was clearly able to infect systemically the entire plant without reverting the stop codon at 5 dpi in *A. thaliana* (Figure 8.10c and 8.10f) and up to 26 dpi in *N. benthamiana* (Supplementary Figures S1D and S1E). Hence, p125 is not essential for viral replication, cell-to-cell movement through plasmodesmata or systemic movement via vascular tissues.

Unlike p125, the readthrough replicase p182 does not appear to possess any silencing suppressor activity. Indeed, expression of p182 alone did not suppress GFP transgene-induced silencing in *N. benthamiana* 16c plants, and failed to affect sRNA biogenesis in transgenic *Arabidopsis* plants. The most compelling evidence for the inability of p182 to

suppress antiviral silencing comes from the molecular analysis of virus-derived sRNAs: the p125-deficient mutant virus was not able to interfere with HEN1-mediated methylation of viral siRNAs and plant sRNAs in systemically-infected plants (Figure 8.19).

Why is it that p182, containing the entire p125 polypeptide, is not able to suppress silencing? The C-terminal RDR domain of p182, which is missing in p125, may plausibly inhibit a potential anti-silencing activity residing elsewhere on the protein. On the one hand, p125-mediated suppression of antiviral silencing likely takes place in the cytoplasm, where free p125 may bind sRNA duplexes and interfere with the activity of HEN1, preventing RISC assembly. On the other hand, a fraction of p125 is likely sequestered into a membrane-bound replication/transcription complex through the formation of heterodimers with p182, whose RDR portion likely contains the membrane-targeting domain. This would explain the inhibitory effect of p182 co-expression on p125 suppressor activities in our transient and stable expression assays (Figures 8.3 and 8.9). During viral infection, p125 is produced in a ca. ten-to-one molar excess over p182 (Figure 8.10f; Supplementary Figure S1K), which would ensure that sufficient p125 is available in the cytoplasm to exert its antisilencing activity. Notably, p125 is the first viral protein to be translated from gRNA in a virus-infected cell, followed by p182 via p125 stop codon readthrough and then by replication of the gRNA from which both p125 and 182 were translated. It is tempting to speculate that the overexpression of p125 at the earliest stage of the viral replication cycle has the primary objective of ensuring that any primary viral siRNAs arising from the processing of gRNA replication and sgRNA transcription dsRNA intermediates by DCL activities are promptly bound and sequestered.

The biogenesis of viral siRNAs in ORMV-infected plants

Our data from deep sequencing of viral siRNAs (Figures 8.11,8.12,8.16,8.17) and blot hybridization (Figure 8.10) support the hypothesis that viral dsRNA replication and transcription intermediates, which span the entire ORMV genome, are already targeted by DCLs at the earliest stages of viral infection. First, both gRNA and gRNA(-) as well as sgRNA-CP and CP(-) accumulate to higher than wild-type levels at 5 dpi in *A. thaliana dcl234* (Figure 8.10c), where viral siRNA generation is impaired. Second, the population of virus-derived siRNAs in wild-type *A. thaliana* or *N. benthamiana* does not exhibit any site preference or strand bias throughout the ORMV genome, and this viral siRNA profile remains unaltered in *Arabidopsis rdr126* plants lacking functional RDR activities (Figures 8.11,8.12,8.16,8.17). Thus, DCLs appear to use directly dsRNA intermediates of viral gRNA replication (and possibly sgRNA transcription) for their processing into siRNAs. A similar mechanism whereby DCL directly process viral dsRNA replication intermediates has previously been proposed not only for other positive sense plant RNA viruses, such as the potyvirus TuMV (Garcia-Ruiz et al., 2010) and the cucumovirus CMV (Wang et al., 2010; Wang et al., 2011), but even for a positive-sense RNA virus in *Drosophila melanogaster*, where RDR genes do not exist (Flynt et al., 2009).

The analysis of the genetic requirements for viral siRNA biogenesis in ORMV-infected *A. thaliana* [(Blevins et al., 2006) and this study], coupled with viral sRNA profiling by deep sequencing in this study, confirms the notion that DCL4 is the primary antiviral dicer producing 21-nt viral siRNAs in this host, while DCL2 and DCL3 assume the role of secondary dicers producing 22-nt and 24-nt viral siRNAs respectively in the absence of DCL4 activity (Xie et al., 2004; Fusaro et al., 2006; Bouche et al., 2006; Blevins et al., 2006). Surprisingly, the comparative analysis performed here between ORMV-infected Col-0 and

dcl234 plants revealed that DCL1 or another RNase III-like enzyme might contribute to ORMV siRNA biogenesis in addition to DCL4, DCL2 and DCL3, although this contribution was rather minor in wild-type plants, becoming more pronounced only in a *dcl234* background. The processing of ORMV siRNA precursors in *dcl234* plants, whether by DCL1 or another RNase III-like activity, appears to be less efficient and precise, giving rise to sRNAs of a broader size range with a strong positive-strand bias, in addition to 21-nt siRNA duplexes (Figure 8.11b; Figure 8.12). DCL1 has previously been shown to be involved in viral siRNA biogenesis for the DNA viruses *Cabbage leaf curl geminivirus* (Blevins et al., 2006; Aregger et al., 2012) and *Cauliflower mosaic pararetrovirus* (Blevins et al., 2006; Blevins et al., 2011), using *A. thaliana* triple and quadruple *dcl* mutants. Notably, in the latter case, DCL1 produced a major fraction of 21-nt siRNAs from a viral dsRNA decoy (Blevins et al.,2011). A candidate RNase III-like activity that might also process ORMV siRNA precursors would be RTL1 and/or other members of the recently characterized *A. thaliana* RTL1 gene family (Shamandi et al., 2015; Elvira-Matelot et al., 2016).). Interestingly, RTL1 can be induced by viral infection and inactivated by viral silencing suppressors, and its transgenic overexpression in *A. thaliana* interferes with the activity of DCL2, DCL3 and DCL4 by targeting their endogenous dsRNA substrates (Shamandi et al., 2015).

A strong sense strand bias has been previously reported for viral siRNAs produced in wild-type plants infected with some positive sense RNA viruses, leading to the hypothesis that the main substrates for DCL4 and other DCLs are secondary structures formed by viral RNAs [see e.g., (Molnár et al., 2005)]. Our findings in ORMV-infected wild type plants do not support this hypothesis, although *dcl234* plants did exhibit a strong positive-strand bias. Perhaps the inactivation of the siRNA-generating DCLs by viral suppressors may unmask DCL1 or another RNase III-like enzyme that randomly cleaves abundant viral single-stranded RNAs of positive-sense polarity, although such bias might also arise from technical issues with certain sRNA cloning, sequencing and detection protocols (Smith et al., 2010; Harris et al., 2015).

Our analysis of wild-type and p125-deficient viruses in Col-0 and *rdr126* plants suggests that neither RDR1, RDR2 nor RDR6 are directly involved in the process whereby viral dsRNA gets processed into siRNAs, implying that most ORMV-derived siRNAs are primary, RDR-independent species. It should be noted, though, that despite the similar viral siRNA profiles of Col-0 and *rdr126* plants (Figures 8.11,8.12,8.16,8.17), the latter exhibited higher levels of wild-type ORMV gRNA by the late stages of infection (Figure 8.10a; Supplementary Figure S1G). Earlier studies of suppressor-deficient RNA viruses (Garcia-Ruiz et al., 2010; Wang et al., 2011) have suggested that in wild-type plants, RDR-dependent secondary viral siRNAs may play a role in restricting viral gRNA replication. In the present case, however, the lack of substantial differences between Col-0 and *rdr126* plants regarding global and local profiles of viral siRNA sizes, 5'-nucleotide identities and hot-spots along the ORMV genome indicates otherwise. Presumably the absence of RDR activities facilitates ORMV replication only indirectly, through the loss of endogenous plant siRNAs such as tasiRNAs and heterochromatic siRNAs that may normally downregulate the expression of gene products that facilitate viral replication. Still, it should be noted that replication of the p125-deficient virus was not facilitated in *rdr126* compared to Col-0 plants (Figure 8.10c).

Effect of p125 on the production, modification and activity of viral siRNAs and plant siRNAs and miRNAs

By comparing wild-type and p125-deficient mutant viruses, we demonstrated that p125 does not block the production of viral siRNAs; rather, viral siRNAs are produced at much higher levels in the presence of p125, concomitant with higher levels of viral gRNA replication, sgRNA transcription and increased disease severity. This suggests that virus-derived sRNAs are failing to restrict viral replication and transcription. We found that in the presence of p125, viral siRNAs become sensitive to β-elimination, although this does not lead to their destabilization, as expected based on the fact that endogenous siRNAs become unstable in *Arabidopsis* mutant lines lacking HEN1 (Yu et al., 2005; Yang et al., 2006). The observed stability of β-elimination-sensitive viral siRNA during infection with wild-type ORMV may arise from the binding of siRNA duplexes by p125, which would in turn prevent HEN1-mediated methylation, prevent the formation of RISCs and thus interfere with siRNA-directed cleavage and/or translational repression of viral RNAs, as has been proposed for p122, a p125 homolog from crucifer-infecting TMV (Csorba et al., 2007 and figure 7.21). Still, we do not have any direct evidence supporting this hypothesis. On the contrary, what indirect evidence we do have, based on the analysis of *AGO1* and *AGO2* gene expression in ORMV-infected plants, indicates that an increased accumulation of miR168 and miR403 actually leads to translational repression of their target mRNAs (*AGO1* and *AGO2*, respectively) despite higher-than-normal levels of the latter (Figures 8.10a and 8.10g). If the absence of the 3'-methyl group in these miRNAs plays additionally an important role to carry out this function, needs to be determined, considering that miRNAs without a 3'- methyl group could be exposed to trimming and/or addition of nucleotides (Ren et al., 2014; Wang et al., 2015). Concomitant increases in the levels of miR168 and *AGO1* mRNA accompanied by a drop in the levels of AGO1 protein have previously been observed during infections of *A. thaliana* with different RNA viruses, including the cruciferous strain of TMV (Várallyay et al., 2010; Várallyay and Havelda 2013), so our data extend these findings to ORMV and demonstrate that p125 is responsible for the perturbation of miR168 and AGO1 expression during ORMV infection. Our results differ however from those obtained by other groups, that report the increase of protein AGO2 upon translational repression of AGO1 in plants infected with TCV and CMV (Harvey et al., 2011). Despite AGO2 mRNA overaccumulation during ORMV infection, AGO2 protein does not increase. The induction of miR168 and miR403 mediated by p125 can be part of a viral counter-defense strategy to repress AGO1 and AGO2 translation and thus prevent the formation of viral siRNA-AGO1 and viral siRNA-AGO2 complexes, whose involvement in antiviral defense is well documented (Wang et al., 2011; Carbonell et al., 2012; Garcia-Ruiz et al., 2015) (Figure 8.21). The increased accumulation of *AGO1* and *AGO2* mRNAs observed at later stages of ORMV-infection (Figure 8.10a) is likely part of a plant counter-counter-defense strategy involving a feedback regulation loop to restore and maintain normal levels of AGO1 and AGO2 proteins.

The analysis of p125-transgenic lines and plants infected with either wild-type or p125-deficient viruses indicates that in addition to the abovementioned miR168 and miR403, other miRNA and miRNA* species are induced in a p125-dependent manner. One particularly important example is miR472 (Figures 8.10b and 8.10d) which has been shown to regulate plant innate immunity against non-viral pathogens (Boccara et al., 2014-2015). Because pattern-triggered immunity (PTI) has been implicated in antiviral defense (Korner et al., 2013; Niehl et al., 2016; Nicaise and Candresse., 2016) and a viral silencing suppressor protein has been shown to suppress PTI and other immune responses in virus-infected *A. thaliana*

(Zvereva et al., 2016), it is conceivable that p125 may also suppress immune responses. The induction of miR472 mediated by p125 could be part of a viral counter-defense strategy to repress a broad group of resistance genes, among them RPS5, which has been involved in PTI and ETI responses typically aimed at non viral pathogens (Boccara et al., 2014-2015; Ade et al., 2007). p125-mediated induction of miR472 would thus downregulate PTI and ETI-related genes like SUMM2 and RPS5 for example, to contribute to suppress the antiviral response (Figure 9.1). The induction of miR472 however, would seem to have an impact only on the translation of specific resistance proteins since no overaccumulation of RPS4 mRNA could be detected, in spite of containing a P-loop-encoding-RNA-sequence similar to the one in RPS5 (Figures 9.2 and 8.21). Whether p125-mediated HEN1 suppression and p125-triggered perturbations of the plant sRNA-directed silencing pathways (including those that regulate immune responses) stem from a significant contribution of PTI or ETI to plant defenses against ORMV, and whether p125 is directly involved in PTI or ETI suppression, constitute therefore valuable avenues of research.

Target prediction for *Arabidopsis* miR472

miRNA Acc.	Target Acc.	Expect	UPE	Alignment	Target Description	Inhibition	Multiplicity
uuuuuccuacucogcccauacc	AT1G51480.1	1.0	N/A	miRNA 22 CCAUACCCGCCUCAUCCUUUUU 1 Target 799 GGUAUGGGGGGAGUAGGAAAAA 820	| Symbols: | Disease resistance protein (CC-NBS-LRR class) family | chr1:19090847-19094306 REVERSE LENGTH=2826	Cleavage	1
uuuuuccuacucogcccauacc	AT5G43740.1	1.0	N/A	miRNA 22 CCAUACCCGCCUCAUCCUUUUU 1 Target 605 GGUAUGGGGGGAGUAGGAAAAA 626	| Symbols: | Disease resistance protein (CC-NBS-LRR class) family | chr5:17564738-17568802 FORWARD LENGTH=2866	Cleavage	1
uuuuuccuacucogcccauacc	AT5G43740.2	1.0	N/A	miRNA 22 CCAUACCCGCCUCAUCCUUUUU 1 Target 631 GGUAUGGGGGGAGUAGGAAAAA 652	| Symbols: | Disease resistance protein (CC-NBS-LRR class) family | chr5:17564739-17568802 FORWARD LENGTH=2892	Cleavage	1
uuuuuccuacucogcccauacc	AT1G12290.1	1.0	N/A	miRNA 22 CCAUACCCGCCUCAUCCUUUUU 1 Target 544 GGCAUGGGUGGAGUAGGAAAAA 565	| Symbols: | Disease resistance protein (CC-NBS-LRR class) family | chr1:4178359-4181247 REVERSE LENGTH=2889	Cleavage	1
uuuuuccuacucogcccauacc	AT1G12290.2	1.0	N/A	miRNA 22 CCAUACCCGCCUCAUCCUUUUU 1 Target 1116 GGCAUGGGUGGAGUAGGAAAAA 1137	| Symbols: | Disease resistance protein (CC-NBS-LRR class) family | chr1:4178359-4182593 REVERSE LENGTH=3461	Cleavage	1
uuuuuccuacucogcccauacc	AT1G12210.1	2.5	N/A	miRNA 22 CCAUACCCGCCUCAUCCUUUUU 1 Target 547 GGUAUGGGUGGAGUAGGCAAAA 568	| Symbols: RFL1 | RPS5-like 1 | chr1:4140948-4143605 FORWARD LENGTH=2658 **RPS5-like 1**	Cleavage	1
uuuuuccuacucogcccauacc	AT5G63020.1	2.5	N/A	miRNA 22 CCAUACCCGCCUCAUCCUUUUU 1 Target 541 GGUAUGGGUGGAGUAGGUAAAA 562	| Symbols: | Disease resistance protein (CC-NBS-LRR class) family | chr5:25283063-25286002 REVERSE LENGTH=2856	Cleavage	1
uuuuuccuacucogcccauacc	AT4G14610.1	2.5	N/A	miRNA 22 CCAUACCCGCCUCAUCCUUUUU 1 Target 547 GGAAUGGGUGGAGUGGGAAAAA 568	| Symbols: | pseudogene, disease resistance protein (CC-NBS-LRR class), putative, domain signature CC-NBS-LRR exists, suggestive of a disease resistance protein.; blastp match of 45% identity and 2.2e-162 P-value to GPI|24461866|gb|AAN62353.1|AF506028_20|AF506028 NBS-LRR type disease resistance protein {Poncirus trifoliata} | chr4:8380848-8383496 REVERSE LENGTH=2649	Cleavage	1
uuuuuccuacucogcccauacc	AT4G10780.1	2.5	N/A	miRNA 22 CCAUACCCGCCUCAUCCUUUUU 1 Target 538 GGUAUGGGGGGAGUAGGCAAAA 559	| Symbols: | LRR and NB-ARC domains-containing disease resistance protein | chr4:6634779-6637467 REVERSE LENGTH=2679	Cleavage	1
uuuuuccuacucogcccauacc	AT5G43730.1	2.5	N/A	miRNA 22 CCAUACCCGCCUCAUCCUUUUU 1 Target 623 GGUAUGGGGGGAAUAGGAAAAA 644	| Symbols: | Disease resistance protein (CC-NBS-LRR class) family | chr5:17560179-17562929 FORWARD LENGTH=2751	Translation	1
uuuuuccuacucogcccauacc	AT1G12220.1	2.5	N/A	miRNA 22 CCAUACCCGCCUCAUCCUUUUU 1 Target 623 GGUAUGGGGGGAGUAGGCAAAA 644	| Symbols: RPS5 | Disease resistance protein (CC-NBS-LRR class) family | chr1:4144935-4147817 FORWARD LENGTH=2883 **RPS5**	Cleavage	1
uuuuuccuacucogcccauacc	AT1G15890.1	2.5	N/A	miRNA 22 CCAUACCCGCCUCAUCCUUUUU 1 Target 630 GGUAUGGGGGGAGUAGGUAAAA 651	| Symbols: | Disease resistance protein (CC-NBS-LRR class) family | chr1:5461317-5464223 FORWARD LENGTH=2907	Cleavage	1
uuuuuccuacucogcccauacc	AT1G12220.2	2.5	N/A	miRNA 22 CCAUACCCGCCUCAUCCUUUUU 1 Target 611 GGUAUGGGGGGAGUAGGCAAAA 632	| Symbols: RPS5 | Disease resistance protein (CC-NBS-LRR class) family | chr1:4144572-4147911 FORWARD LENGTH=2965	Cleavage	1
uuuuuccuacucogcccauacc	AT1G12280.1	2.5	N/A	miRNA 22 CCAUACCCGCCUCAUCCUUUUU 1 Target 547 GGCAUGGGUGGAGUAGGCAAAA 568	| Symbols: | LRR and NB-ARC domains-containing disease resistance protein | chr1:4174875-4177559 REVERSE LENGTH=2685 **SUMM2**	Cleavage	1
uuuuuccuacucogcccauacc	AT4G27190.1	2.5	N/A	miRNA 22 CCAUACCCGCCUCAUCCUUUUU 1 Target 511 GGCAUGGGAGGAGUAGGUAAAA 532	| Symbols: | NB-ARC domain-containing disease resistance protein | chr4:13620977-13623934 REVERSE LENGTH=2958	Cleavage	1

Figure 9.1. miR472 predicted targets in *Arabidopsis thaliana*. Notice that RPS5-like1, RPS5 and SUMM2 (Suppressor of MKK1 MKK2 2) miR472 targets are also present in figure 5.4.

Figure 9.2. Sequences producing significant alignments with the GMGGVGKTTL amino acid sequence present in the P-loop from *Arabidopsis* resistance protein RPS5 and the resistance protein "N" from *Nicotiana*.

Sequences producing significant alignments:		Score (bits)	E Value
AT5G43740.2	Symbols: | Disease resistance protein (CC-NB...	25	3.9
AT5G43740.1	Symbols: | Disease resistance protein (CC-NB...	25	3.9
AT5G05400.1	Symbols: | LRR and NB-ARC domains-containing...	25	3.9
AT5G63020.1	Symbols: | Disease resistance protein (CC-NB...	25	3.9
AT5G47250.1	Symbols: | LRR and NB-ARC domains-containing...	25	3.9
AT4G33300.2	Symbols: ADR1-L1 | ADR1-like 1 | chr4:1605116...	25	3.9
AT4G33300.1	Symbols: ADR1-L1 | ADR1-like 1 | chr4:1605116...	25	3.9
AT4G10780.1	Symbols: | LRR and NB-ARC domains-containing...	25	3.9
AT4G27190.1	Symbols: | NB-ARC domain-containing disease ...	25	3.9
AT4G27220.1	Symbols: | NB-ARC domain-containing disease ...	25	3.9
AT1G12220.2	Symbols: RPS5 | Disease resistance protein (C...	25	3.9
AT1G12290.2	Symbols: | Disease resistance protein (CC-NB...	25	3.9
AT1G61180.2	Symbols: | LRR and NB-ARC domains-containing...	25	3.9
AT1G62630.1	Symbols: | Disease resistance protein (CC-NB...	25	3.9
AT1G12290.1	Symbols: | Disease resistance protein (CC-NB...	25	3.9
AT1G12220.1	Symbols: RPS5 | Disease resistance protein (C...	25	3.9
AT1G12210.1	Symbols: RFL1 | RPS5-like 1 | chr1:4140948-41...	25	3.9
AT1G12280.1	Symbols: | LRR and NB-ARC domains-containing...	25	3.9
AT1G15890.1	Symbols: | Disease resistance protein (CC-NB...	25	3.9
AT1G51480.1	Symbols: | Disease resistance protein (CC-NB...	25	3.9
AT1G61310.1	Symbols: | LRR and NB-ARC domains-containing...	25	3.9
AT1G61300.1	Symbols: | LRR and NB-ARC domains-containing...	25	3.9
AT1G61190.1	Symbols: | LRR and NB-ARC domains-containing...	25	3.9
AT1G61180.1	Symbols: | LRR and NB-ARC domains-containing...	25	3.9
AT1G63360.1	Symbols: | Disease resistance protein (CC-NB...	25	3.9
AT1G63350.1	Symbols: | Disease resistance protein (CC-NB...	25	3.9
AT5G36930.2	Symbols: | Disease resistance protein (TIR-N...	25	5.6
AT5G43470.2	Symbols: RPP8, HRT, RCY1 | Disease resistance...	25	5.6
AT5G36930.1	Symbols: | Disease resistance protein (TIR-N...	25	5.6
AT5G43730.1	Symbols: | Disease resistance protein (CC-NB...	25	5.6
AT5G48620.1	Symbols: | Disease resistance protein (CC-NB...	25	5.6
AT5G43470.1	Symbols: RPP8, HRT, RCY1 | Disease resistance...	25	5.6
AT5G35450.1	Symbols: | Disease resistance protein (CC-NB...	25	5.6
AT1G27170.2	Symbols: | transmembrane receptors;ATP bindi...	25	5.6
AT1G10920.2	Symbols: LOV1 | NB-ARC domain-containing dise...	25	5.6
AT1G27180.1	Symbols: | disease resistance protein (TIR-N...	25	5.6
AT1G27170.1	Symbols: | transmembrane receptors;ATP bindi...	25	5.6
AT1G53350.1	Symbols: | Disease resistance protein (CC-NB...	25	5.6
AT1G59620.1	Symbols: CW9 | Disease resistance protein (CC...	25	5.6
AT1G10920.1	Symbols: LOV1 | NB-ARC domain-containing dise...	25	5.6
AT5G17680.1	Symbols: | disease resistance protein (TIR-N...	24	7.7

Transcriptome profiling of ORMV-infected Col-0 plants at 7, 14 and 21 dpi during a previous study revealed a general up-regulation of cellular mRNAs targeted by miRNAs and/or tasiRNAs, concomitant with an increased accumulation of their respective miRNAs and tasiRNAs (Figure 5.8, Hu et al., 2011). Since in our experiments we also see the accumulation of RPS5 mRNA during infection, it is tempting to suggest that AGO1, AGO2, RPS5, SUMM2 as well as CHROMOMETHYLASE3 (CMT3) among others, are genes that are translationally repressed during infection. This major perturbation of the host miRNA and siRNA pathways, triggered by p125 as we established here, may constitute a contributing factor for the development of the severe disease symptoms that characterize the later stages of ORMV infection. Indeed, our analysis of *Arabidopsis* transgenic lines carrying p125, p182 or p125/182 constructs revealed that p125 expression partially recapitulates viral disease symptoms, such as serration of the rosette leaves and curling of the stem (Figures 8.5 and 8.6). This is consistent with previous studies demonstrating that the transgenic expression of viral suppressors from different viruses causes developmental abnormalities in *Arabidopsis*, accompanied by major perturbations of its miRNA and siRNA pathways [e.g., (Chapman et al., 2004; Shivaprasad et al., 2008)].

It is worth pointing out that even in *dcl234* and *rdr126* plants, where major components of the RNA silencing machinery are missing, stop codon revertants where p125 expression is restored are quickly selected during infections with p125-deficient ORMV mutants, indicating the presence of a selective pressure for this effector imposed by other defense pathways such as those of plant innate immunity. In either case, RNA silencing and innate immunity work in concert to restrict viral replication and systemic movement (Zvereva and Pooggin., 2012), so that relieving the selection pressure for p125 expression may require suppressing the activities of both, immune responses and the siRNA silencing pathways (Figure 9.3).

Figure 9.3. Effect of p125 on the production, modification and activity of viral siRNAs and plant siRNAs and miRNAs. a) Transient formation of double-stranded replication intermediates by the viral replicase p182, mainly processed by the host DCL4 and DCL2 into viral siRNAs; p125 sequesters viral siRNAs duplexes avoiding them to be loaded in AGO proteins and to be 3'-methylated by HEN1, thus preventing siRNA-mediating targeting of the viral RNAs. b) p125 induces miR168, miR403 and miR472 expression which repress the translation of their respective targets mRNAs AGO1, AGO2 and RPS5 (NBB-LRR), causing a simultaneous impact on the RNA silencing machinery and immune responses of the plant.

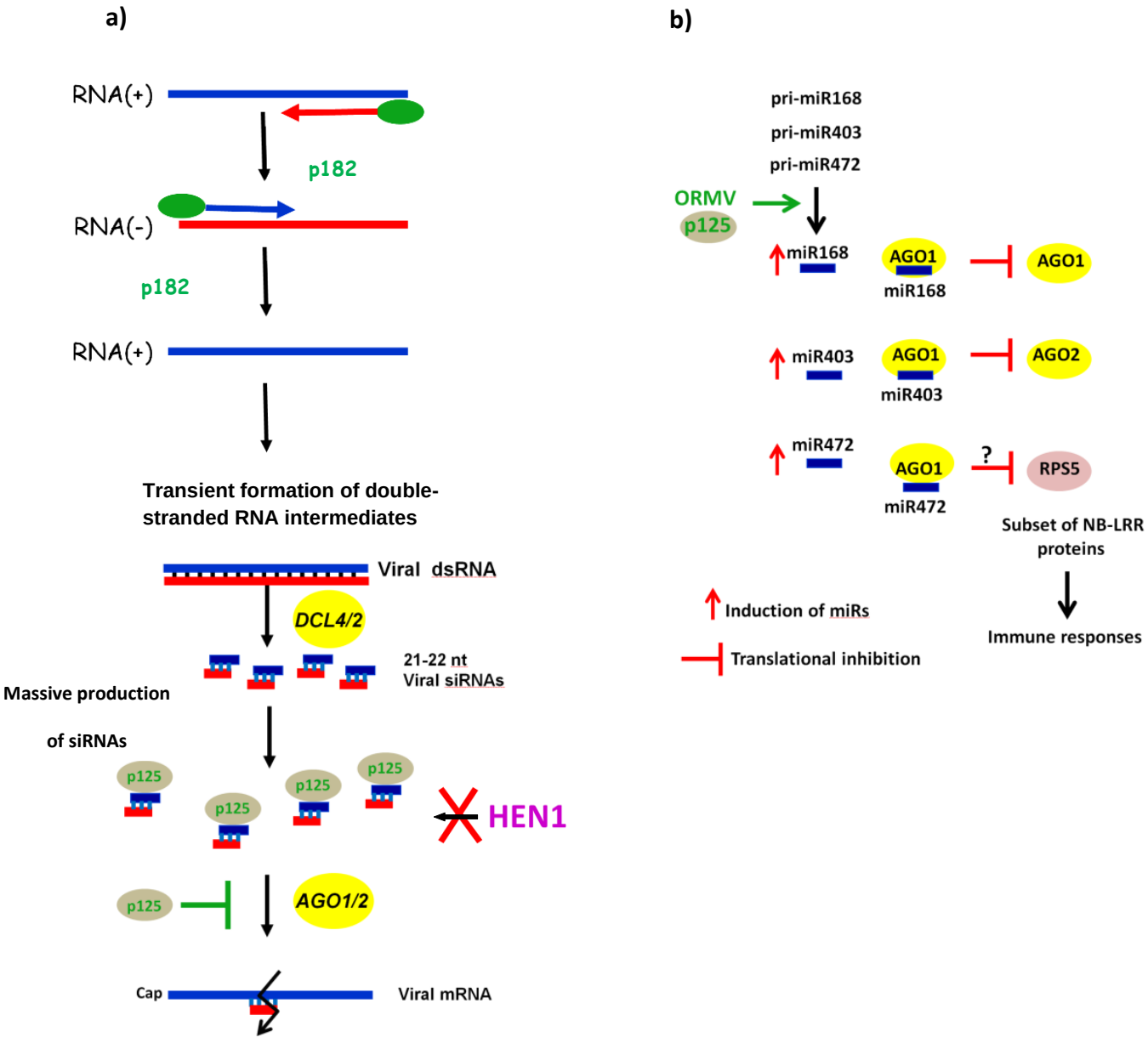

Section X. References

Abbink TEM, Tjernberg PA, Bol JF and Linthorst HJM (1998). Tobacco Mosaic Virus Helicase Domain Induces Necrosis in N-Gene-Carrying Tobacco in the Absence of Virus Replication. MPMI 11: 1242-1246

Ade J, DeYoung BJ, Golstein C, Innes RW. (2007). Indirect activation of a plant nucleotide binding site-leucine-rich repeat protein by a bacterial protease. PNAS 104:2531–36

Aguilar I, Sánchez F, Martin Martin A, Martínez Herrera D and Ponz F (1996). Nucleotide sequence of Chinese rape mosaic virus (oilseed rape mosaic virus), a crucifer tobamovirus infectious on Arabidopsis thaliana. Plant. Mol. Biol. 30:191-197

Ahola T1, Lampio A, Auvinen P, Kääriäinen L. (1999). Semliki Forest virus mRNA capping enzyme requires association with anionic membrane phospholipids for activity. EMBO J. 18:3164-72.

Akbergenov R, Si-Ammour A, Blevins T, Amin I, Kutter C, Vanderschuren H, Zhang P, Gruissem W, Meins F Jr, Hohn T, Pooggin MM (2006). Molecular characterization of geminivirus-derived small RNAs in different plant species. Nucleic Acids Res 34: 462-471

Allen E, Xie Z, Gustafson AM, Carrington JC. (2005). MicroRNA-directed phasing during trans-acting siRNA biogenesis in plants. Cell 121:207–21

Almeida R and Allshire RC (2005). RNA silencing and genome regulation. Trends in Cell Biology 15:251-258

Alquist P. (2002). RNA-dependent RNA polymerases, viruses, and RNA silencing. Science 296:1270-3. Review.

Ameres SL and Zamore PD (2013). Diversifying microRNA sequence and function. Nat Rev. Mol. Cell Biol. 14: 475-488

Aoki S and Takebe I (1975). Replication of Tobacco Mosaic Virus RNA in Tobacco Mesophyll Protoplasts Inoculated in Vitro. Virology 65: 343-354

Aregger M, Borah BK, Seguin J, Rajeswaran R, Gubaeva EG, Zvereva AS, Windels D, Vazquez F, Blevins T, Farinelli L, Pooggin MM. (2012). Primary and secondary siRNAs in geminivirus-induced gene silencing. PLoS Pathog. doi:10.1371/journal.ppat.1002941.

Aukerman MJ, Sakai H. (2003). Regulation of flowering time and flower organ identity by a MicroRNA and its *APETALA2*-like target genes. *Plant Cell* 15: 2730-2741

Axtell MJ (2013). Classification and Comparison of Small RNAs from Plants. Annual Review of Plant Biology 64:137-159

Axtell MJ, Staskawicz BJ. (2003). Initiation of RPS2-specified disease resistance in Arabidopsis is coupled to the AvrRpt2-directed elimination of RIN4. Cell 112:369–77

Axtell, M.J., Jan, C., Rajagopalan, R., and Bartel, D.P. (2006). A two-hit trigger for siRNA biogenesis in plants. Cell 127, 565–577.

Azevedo J, García D, Pontier D, Ohnesorge S, Yu A, García S, Braun L, Bergdoll M, Hakimi MA, Lagrange T, Voinnet O. (2010) Argonaute quenching and global changes in dicer homeostasis caused by a pathogen-encoded GW repeat protein. *Genes Dev.* 24:904-915

Baker B, Zambryski P, Staskawicz B, Dinesh-Kumar SP (1997). Signaling in Plant-Microbe Interactions. Science 276: 726-733

Bartel DP. (2004). MicroRNAs: genomics, biogenesis, mechanism, and function. *Cell* 116:281–297

Bartel DP (2009). MicroRNAs: target recognition and regulatory functions. Cell.136:215-33. doi: 10.1016/j.cell.2009.01.002. Review.

Baumberger, N., and Baulcombe, D.C. (2005). Arabidopsis ARGONAUTE1 is an RNA Slicer that selectively recruits microRNAs and short interfering RNAs. Proceedings of the National Academy of Sciences of the United States of America 102, 11928-11933..

Baumberger N, Tsai CH, Lie M, Havecker E, Baulcombe DC.(2007). The Polerovirus silencing suppressor P0 targets ARGONAUTE proteins for degradation.Curr Biol.17:1609-14.

Baulcombe D. (2004). RNA silencing in plants. *Nature* 431:356–363

Behm-Ansmant I et al., (2006). mRNA degradation by miRNAs and GW 182 requires both CCR4:NOT deadenylase and DCP1: DCP2 decapping complexes. Genes Dev. 20, 1885-1898.

Bernstein E, Caudy AA, Hammond SM, Hannon GJ (2001). Role for a bidentate ribonuclease in the initiation step of RNA interference. Nature 409: 363-366

Bhargava A, Mansfield SD, Hall HC, Douglas CJ, Ellis BE. (2010). MYB75 functions in regulation of secondary cell wall formation in the Arabidopsis inflorescence stem. Plant Physiol 154:1428–1438

Blevins T., Rajeswaran R., Aregger M., Borah B.K., Schepetilnikov M., Baerlocher L., Farinelli L., Meins F.Jr., Hohn T., and Pooggin M.M. (2011). Massive production of small RNAs from a non-coding region of *Cauliflower mosaic virus* in plant defense and viral counterdefense. *Nucleic Acid Res.* 39:5003-5014.

Blevins T, Rajeswaran R, Shivaprasad PV, Beknazariants D, Si-Ammour A, Park HS, Vazquez F, Robertson D, Meins Jr F, Hohn T and Pooggin M.M. (2006). Four plant Dicers mediate viral small RNA biogenesis and DNA virus induced silencing. Nucleic Acids Research 34:6233-6246.

Boccara, M., Sarazin, A., Thiébeauld, O., Jay, F., Voinnet, O., Navarro, L., and Colot, V. (2014 and correction in 2015). The Arabidopsis miR472-RDR6 silencing pathway modulates PAMP- and effector-triggered immunity through the post-transcriptional control of disease resistance genes. PLoS Pathog. 10:e1003883

Bohmert K, Camus I, Bellini C, Bouchez D, Caboche M, Benning C.(1998). AGO1 defines a novel locus of Arabidopsis controlling leaf development. EMBO J. 17:170-80.

Boller T, Felix G: A renaissance of elicitors: perception of microbe-associated molecular patterns and danger signals by pattern-recognition receptors. Annu Rev Plant Biol (2009), 60:379-406.

Bollman KM, Aukerman MJ, Park MY, Hunter C, Berardini TZ, Poethig RS.(2003). HASTY, the Arabidopsis ortholog of exportin 5/MSN5, regulates phase change and morphogenesis. Development 130:1493-504.

Borevitz JO1, Xia Y, Blount J, Dixon RA, Lamb C(2000). Activation tagging identifies a conserved MYB regulator of phenylpropanoid biosynthesis. Plant Cell 12(12):2383-239

Borsani O, Zhu J, Verslues PE, Sunkar R, Zhu J-K. (2005). Endogenous siRNAs derived from a pair of natural cis-antisense transcripts regulate salt tolerance in Arabidopsis. Cell 123:1279–91

Bortolamiol, D., Pazhouhandeh, M., Marrocco, K., Genschik, P., Ziegler-Graff, V.,(2007). The Polerovirus F box protein P0 targets ARGONAUTE1 to suppress RNA silencing. *Curr. Biol.* 17:1615–1621.

Bouche N, Lauressergues D, Gasciolli V, Vaucheret H.(2006) An antagonistic function for Arabidopsis DCL2 in development and a new function for DCL4 in generating viral siRNAs. EMBO J. 25:3347–3356.

Boyes DC, Nam J, Dangl JL. (1998). The Arabidopsis thaliana RPM1 disease resistance gene product is a peripheral plasma membrane protein that is degraded coincident with the hypersensitive response. PNAS 95:15849–54

Braun JE, Huntzinger E and Izaurralde E (2012). A molecular link between miRISCs and deadenylases provides new insight into the mechanism of gene silencing by microRNAs. Cold Spring Harb. Perspect. Biol.4.

Brodersen P and Voinnet O. (2006). The diversity of RNA silencing pathways in plants. *Trends Genet* 22:268-280

Brodersen P, Sakvarelidze-Achard L, Brunn-Rasmussen Marianne, Dunoyer Patrice, Yamamoto YY, Sieburth L, Voinnet O. (2008). Widespread Translational Inhibition by Plant miRNAs and siRNAs. Science 320: 1185 -1190

Brosseau, C., and Moffett, P. (2015). Functional and Genetic Analysis Identify a Role for Arabidopsis ARGONAUTE5 in Antiviral RNA Silencing. The Plant cell 27, 1742-1754.

Buchmann, R.C., Asad, S., Wolf, J.N., Mohannath, G., Bisaro, D.M., (2009). Geminivirus AL2 and L2 proteins suppress transcriptional gene silencing and cause genome-wide reductions in cytosine methylation. J. Virol. 83: 5005–5013

Buck KW. (1996). Comparison of the replication of positive-stranded RNA viruses of plants and animals. Adv. Virus Res 47:159-251

Buck KW. (1999). Replication of tobacco mosaic virus RNA. Phil. Trans. R. Soc. Lond. B. 354:613-627

Buhtz, A., Springer, F., Chappell, L., Baulcombe, D. C. & Kehr, J. (2008). Identification and characterization of small RNAs from the phloem of Brassica napus. Plant J. 53, 739–749

Burgyán J. (2008). Role of silencing suppressor proteins. Methods Mol Biol 451: 69–79

Cai X, Hagedorn CH, Cullen BR. (2004). Human microRNAs are processed from capped, polyadenylated transcripts that can also function as mRNAs. *RNA (New York, NY)* **10**: 1957–1966.

Carbonell, A., Fahlgren, N., Garcia-Ruiz, H., Gilbert, K.B., Montgomery, T.A., Nguyen, T., Cuperus, J.T., Carrington, J.C., (2012). Functional analysis of three Arabidopsis ARGONAUTES using slicer-defective mutants*. Plant Cell* 24, 3613–3629.

Carbonell A and Carrington JC (2015). Antiviral roles of plant ARGONAUTES. Current Opinion in Plant Biology: 27:111-117

Carmell MA, Xuan Z, Zhang MQ, Hannon GJ. (2002). The Argonaute family: tentacles that reach into RNAi, developmental control, stem cell maintenance, and tumorigenesis. Genes Dev.16:2733-42

Chapman EJ, Carrington JC (2007). Specialization and evolution of endogenous small RNA pathways. *Nat Rev Genet* 8:884-896

Chapman, E.J., Prokhnevsky, A.I., Gopinath, Dolja, V.V., Carrington, J.C., (2004). Viral RNA silencing suppressors inhibit the microRNA pathway at an intermediate step*. Genes Dev*. 18, 1179–1186.

Chellappan P, Masona MV, Vanitharani R, Taylor NJ, Fauquet CM. (2004). Broad spectrum resistance to ssDNA viruses associated with transgene-induced gene silencing in cassava. Plant Mol Biol. 56:601-11.

Chen HM, Chen LT, Patel K, Li YH, Baulcombe DC and Wu SH (2010). 22- nucleotide RNAs trigger secondary siRNA biogenesis in plants. PNAS 107: 15269-15274

Chiu, M.H., Chen, I.H., Baulcombe, D.C., Tsai, C.H., (2010). The silencing suppressor P25 of Potato virus X interacts with Argonaute1 and mediates its degradation through the proteasome pathway. Mol. Plant Pathol. 11, 641–649.

Chujo T, Ishibashi K, Miyashita S, Ishikawa M. (2015). Functions of the 5'- and 3'-untranslated regions of tobamovirus RNA. Virus Research (in press)

Cole AB, Király L, Lane LC, Wiggins BE, Ross K, and Schoelz JE. (2004). Temporal Expression of PR-1 and Enhanced Mature Plant resistance to Virus Infection is Controlled by a Single Dominant Gene in a New *Nicotiana* Hybrid. Molecular Plant-Microbe Interactions 17: 976-985.

Cooley MB, Pathirana S, Wu HJ, Kachroo P, Klessig DF. (2000). Members of the Arabidopsis HRT/RPP8 family of resistance genes confer resistance to both viral and oomycete pathogens. Plant Cell, 12 (5) (2000), pp. 663–676

Creamer, K.M., Partridge,J.F., (2011). RITS-connecting transcription, RNA interference, and heterochromatin assembly in fission yeast. Wiley interdisciplinary reviews. RNA 2,632–646.

Csorba, T., Bovi, A., Dalmay, T., Burgyán, J., (2007). The p122 subunit of Tobacco Mosaic Virus replicase is a potent silencing suppressor and compromises both small interfering RNA- and microRNA-mediated pathways. J. Virol. 81,11768–11780.

Csorba T, Kontra L, Burgyán J., (2015) viral silencing suppressors: Tools forged to fine-tune host pathogen coexistence. *Virology* 479-480: 85-103. http://10.1016/j.virol.2015.02.028

Csorba T, Pantaleo V, Burgyán J (2009) RNA silencing: an antiviral mechanism. *Adv Virus Res* 75:35–71

Cui H, Tsuda K, Parker JE (2015). Effector-Triggered Immunity: From Pathogen Perception to Robust Defense. Annu. Rev. Plant Biol. 66:487-511

Cuperus JT et al., (2010). Unique functionality of 22-nt miRNAs in triggering RDR6-dependent siRNA biogenesis from target transcripts in *Arabidopsis*. *Nat. Struct. Mol. Biol.* 17: 997-1003

Curaba J and Chen X (2008). Biochemical Activities of *Arabidopsis* RNA-dependent RNA Polymerase 6. The Journal of Biological Chemistry 283: 3050-3066

Dangl J.L. and Jones J.D.G.(2001). Plant pathogens and integrated defence responses to infection. Nature 411: 826-833

Deleris A, Gallego-Bartolomé J, Bao J, Kasschau KD, Carrington JC, Voinnet O (2006). Hierarchical action and inhibition of plant Dicer-like proteins in antiviral defense. *Science* 313:68-71

den Boon JA, Díaz A, and Ahlquist P (2010) Cytoplasmic Viral Replication Complexes. *Cell Host and Microbe* 8: 77-85

Denli AM, Tops BBJ, Plasterk RHA, Ketting RF, Hannon GJ. (2004). Processing of primary microRNAs by the Microprocessor complex. Nature 432: 231–235.

Deslandes L, Rivas S: Catch me if you can: bacterial effectors and plant targets. Trends Plant Sci 2012, 17:644-655.

Devert A, Fabre N, Floris M, Canard B, Robaglia C, Crété P (2015). Primer-Dependent and Primer Independent Initiation of Double Stranded RNA Synthesis by Purified Arabidopsis RNA-Dependent RNA-Polymerases RDR2 and RDR6. *PLOS ONE* 10:1-17

Diaz-Pendon, J.A., Li, F., Li, W.X., Ding, S.W., (20079. Suppression of antiviral silencing by cucumber mosaic virus 2b protein in Arabidopsis is associated with drastically reduced accumulation of three classes of viral small interfering RNAs. Plant Cell 19, 2053–2063.

Dinesh-Kumar SP, Tham WH, and Baker B. (2000) Structure-function analysis of the tobacco mosaic virus resistance gene N. Proc Natl Acad Sci 97:14789-14794

Ding SW (2010) RNA-based antiviral immunity. *Nat Rev Immunol* 10:632–644

Ding SW, Voinnet O (2007) Antiviral immunity directed by small RNAs. *Cell* 130:413–426

Ding, X. S., J. Liu, N. H. Cheng, A. Folimonov, Y. M. Hou, Y. Bao, C. Katagi, S. A. Carter, and R. S. Nelson. (2004). The Tobacco mosaic virus 126-kDa protein associated with virus replication and movement suppresses RNA silencing. Mol. Plant-Microbe Interact. 17:583–592.

Dixon, R. A., Harrison, M. J. & Lamb, C. J. (1994). Early events in the activation of plant defense responses. A. Rev. Phytopathol. 32, 479-501.

Donaire L et al., (2008) Structural and genetic requirements for biogenesis of tobacco rattle virus-derived small interfering RNAs reveals effective and widespread targeting of viral genomes. *Virology* 392: 203-214.

Du, Z., Xiao, D., Wu, J., Jia, D., Yuan, Z., Liu, Y., Hu, L., Han, Z., Wei, T., Lin, Q., Wu, Z., Xie, L., (2011). p2 of rice stripe virus (RSV) interacts with OsSGS3 and is a silencing suppressor. Mol. Plant Pathol. 12, 808–814.

Duan, C.G., Fang, Y.Y., Zhou, B.J., Zhao, J.H., Hou, W.N., Zhu, H., Ding, S.W., Guo, H.S., (20129. Suppression of Arabidopsis ARGONAUTE1-mediated slicing, transgene- induced RNA silencing, and DNA methylation by distinct domains of the cucumber mosaic virus 2b protein. Plant Cell 24, 259–274. doi: 10.15252/embj.201489453.

Duan CG, Zhang H, Tang K, Zhu X, Qian W, Hou YJ, Wang B, Lang Z, Zhao Y, Wang X, Wang P, Zhou J, Liang G, Liu N, Wang C, Zhu JK. (2015). Specific but interdependent functions for Arabidopsis AGO4 and AGO6 in RNA-directed DNA methylation. EMBO 34: 581-592.

Dunoyer P., Himber C., Voinnet O. (2005). DICER-LIKE 4 is required for RNA interference and produces the 21-nucleotide small interfering RNA component of the plant cell-to-cell silencing signal. Nature Genet. 37:1356–1360.

Dzianott A, Sztuba-Solińska J, Bujarski JJ. (2012). Mutations in the antiviral RNAi defense pathway modify Brome mosaic virus RNA recombinant profiles. Mol Plant Microbe Interact. 2012 Jan;25(1):97-106. doi: 10.1094/MPMI-05-11-0137

Earley KW, Haag JR, Pontes O, Opper K, Juehne T, Song K and Pikaard CS. (2006). Gateway-compatible vectors for plant functional genomics and proteomics. The Plant Journal 45:616-629

Elvira-Matelot, E., Hachet, M., Shamandi, N., Comella, P., Sáez-Vásquez, J., Zytnicki, M., and Vaucheret, H. (2016). Arabidopsis RNASE THREE LIKE2 Modulates the Expression of Protein-Coding Genes via 24-Nucleotide Small Interfering RNA-Directed DNA Methylation. Plant Cell 28:406-425.

Endres, M.W., Gregory, B.D., Gao, Z., Foreman, A.W., Mlotshwa, S., Ge, X., Pruss, G.J., Ecker, J.R., Bowman, L.H., Vance, V., (2010). Two plant viral suppressors of silencing require the ethylene-inducible host transcription factor RAV2 to block RNA silencing. PLoS Pathog. 6, e1000729.

Erickson FL, Holzberg S, Calderon-Urrea A, Handley V, Axtell M, Corr C, Baker B. (1999). The helicase domain of the TMV replicase proteins induces the N-mediated defence response in tobacco. Plant J.18:67-75

Eun C, Lorkovic ZJ, Naumann U, Long Q, Havecker ER, Simon SA, Meyers BC, Matzke AJ, Matzke M. (2011). AGO6 functions in RNA-mediated transcriptional gene silencing in shoot and root meristems in Arabidopsis thaliana. PLoS One. 6:e25730. doi: 10.1371/journal.pone.0025730.

Fahlgren N, Montgomery TA, Howell MD, Allen E, Dvorak SK, Alexander AL, Carrington JC. (2006). Regulation of AUXIN RESPONSE FACTOR3 by TAS3 ta-siRNA affects developmental timing and patterning in Arabidopsis. Curr Biol. 16: 939-44

Fátyol K, Ludman M and Burgyán J. (2016). Functional dissection of a plant Argonaute. Nucleic Acids Research 44: 1384-1397. doi: 10.1093/nar/gkv1371

Fei Q, Xia R, Meyers BC (2013). Phased, secondary, small interfering RNAs in posttranscriptional regulatory networks. Plant Cell 25:2400-2415.

Feng F, Zhou JM (2012). Plant–bacterial pathogen interactions mediated by type III effectors. Curr Opin Plant Biol 15:469-476.

Flynt A, Liu N, Martin R, Lai EC (2009). Dicing of viral replication intermediates during silencing of latent *Drosophila* viruses. Proc. Natl. Acad. Sci. USA 106: 5270-5275

Frank, F., Sonenberg, N., and Nagar, B. (2010). Structural basis for 5'-nucleotide base-specific recognition of guide RNA by human AGO2. Nature 465, 818-822.

Frank, F., Hauver, J., Sonenberg, N., and Nagar, B. (2012). Arabidopsis Argonaute MID domains use their nucleotide specificity loop to sort small RNAs. The EMBO journal 31, 3588-3595.

Fukudome A and Fukuhara T (2016). Plant dicer-like proteins: double-stranded RNA-cleaving enzymes for small RNA biogenesis. J Plant Res. DOI 10.1007/s10265-016-0877-1

Fusaro AF et al., (2006). RNA interference- inducing hairpin RNAs in plants act through the viral defence pathway. *EMBORep* 7:1168-1175

Fusaro AF, Correa RL, Nakasugi K, Jackson C, Kawchuk L, Vaslin MFS, Waterhouse PM (2012) The Enamovirus P0 protein is a silencing suppressor which inhibits local and systemic RNA silencing through AGO1 degradation. *Virology* 426: 178-187

Galliet DR and Walbot V. (1992). Identification of the motifs within the tobacco mosaic virus 5'-leader responsible for enhancing translation. Nucleic Acids Research 20:4631- 4638

Gandikota M, Birkenbihl RP, Höhmann S, Cardon, GH, Saedler H and Huijser P (2007). The miRNA 156/157 recognition element in the 3' UTR of the Arabidopsis SBP box gene *SPL3* prevents early flowering by translational inhibition in seedlings. The Plant Journal 49:683-693

García-Ruíz, H et al., (2010) *Arabidopsis* RNA-dependent RNA polymerases and dicer-like proteins in antiviral defense and small interfering RNA biogenesis during Turnip Mosaic Virus infection. *Plant Cell* 22:481-496

García-Ruíz H, Carbonell A, Hoyer JS, Fahlgren N, Gilbert KB, Takeda A, Giampetruzzi A, García-Ruíz MT, McGinn MG, Lowery N, Martínez Baladejo MT, Carrington JC. (2015). Roles and Programming of Arabidopsis ARGONAUTE Proteins during *Turnip Mosaic Virus* Infection. PLOS Pathogens 11(3): e1004755. doi:10.1371/journal. ppat.1004755

Giner, A., Lakatos,L., Garcia-Chapa, M.,Lopez-Moya, J.J.,Burgyan,J., (2010). Viral protein inhibits RISC activity by argonaute binding through conserved WG/GW motifs. PLoSPathog.6,e1000996.

Glick, E., Zrachya, A., Levy, Y., Mett, A., Gidoni, D., Belausov, E., Citovsky, V., Gafni, Y., (2008). Interaction with host SGS3 is required for suppression of RNA silencing by tomato yellow leaf curl virus V2 protein. Proc. Natl. Acad. Sci. USA 105, 157–161.

Gomez-Gomez, L. and Boller,T., (2000). FLS2: an LRR receptorlike kinase involved in the perception of the bacterial elicitor flagellin in Arabidopsis. Mol. Cell 5, 1003–1011

Goto, K., Kobori, T., Kosaka, Y., Natsuaki, T., Masuta, C., (2007). Characterization of silencing suppressor 2b of cucumber mosaic virus based on examination of its small RNA-binding abilities. Plant Cell Physiol. 48, 1050–1060.

Grant JJ1, Chini A, Basu D, Loake GJ. (2003). Targeted activation tagging of the Arabidopsis NBS-LRR gene, ADR1, conveys resistance to virulent pathogens. Mol Plant Microbe Interact. 16 669-680

Grdzelishvili VZ, Chapman SN, Dawson WO, and Lewandowski DJ. (2000). Mapping of the Tobacco Mosaic Virus Movement Protein and Coat Protein Subgenomic RNA Promoters in Vivo. Virology 275, 177–192

Gregory RI, Yan KP, Amuthan G, Chendrimada T, Doratotaj B, Cooch N, Shiekhattar R. (2004). The Microprocessor complex mediates the genesis of microRNAs. *Nature* **432**: 235–240.

Gu, S., Jin, L., Huang, Y., Zhang, F., and Kay, M.A. (2012). Slicing-independent RISC activation requires the argonaute PAZ domain. Current biology : CB 22, 1536-1542.

Guo, H., Song, X., Xie, C., Huo, Y., Zhang, F., Chen, X., Geng, Y., Fang, R., (2013). Rice yellow stunt rhabdovirus protein 6 suppresses systemic RNA silencing by blocking RDR6-mediated secondary siRNA synthesis Mol. Plant - Microbe Interact. 26, 927–936.

Haag JR, Pikaard CS. (2011). Multisubunit RNA polymerases IV and V: purveyors of non-coding RNA for plant gene silencing. Nat Rev Mol Cell Biol.12:483-92. doi: 10.1038/nrm3152. Review.

Haas, G., Azevedo, J., Moissiard, G., Geldreich, A., Himber, C., Bureau, M., Fukuhara, T., Keller, M., Voinnet, O., (2008). Nuclear import of CaMV P6 is required for infection and suppression of the RNA silencing factor DRB4. EMBO J. 27, 2102–2112.

Hagiwara-Komoda, Y., Hirai, K., Mochizuki, A., Nishiguchi, M., Meshi, T., and Ishikawa, M. (2008). Overexpression of a host factor TOM1 inhibits tomato mosaic virus propagation and suppression of RNA silencing. Virology 376:132-139.

Hagiwara, Y., Komoda, K., Yamanaka, T., Tamai, A., Meshi, T., Funada, R., Tsuchiyab, T., Naito, S., and Ishikawa, M. (2003). Subcellular localization of host and viral proteins associated with tobamovirus RNA replication. EMBO J. 22:344-353.

Halter T and Navarro L. (2015). Multilayer and interconnected post transcriptional and co-transcriptional control of plant NLRs. Current Opinion in Plant Biology 26:127-134

Han J, Lee Y, Yeom KH, Nam JW, Heo I at al (2006). Molecular basis for the recognition of primary microRNAs by the Drosha-DGCR8 complex. Cell 125 (5): 887-901

Han YH, Xiang HY, Wang Q, Li YY, Wu WQ, Han CG, Li DW, Yu HI (2010). Ring structure amino acids affect the suppressor activity of melon aphid-borne yellows virus P0 protein. *Virology* 406: 21-27

Harries, P.A., Palanichelvam,K., Bhat, S., Nelson,R.S., (2008). Tobacco mosaic virus 126-kDa protein increases the susceptibilityof Nicotiana tabacum to other viruses and its dosage affects virus-induced gene silencing. Mol.Plant Microbe Interact. 21,1539–1548.

Harris, C. J., Molnar, A., Müller, S. Y., and Baulcombe, D. C. (2015). FDF-PAGE: a powerful technique revealing previously undetected small RNAs sequestered by complementary transcripts. Nucleic Acids Res. 43:7590-7599

Harvey JJ, Lewsey MG, Patel K, Westwood J, Heimstädt S, Carr JP, and Baulcombe DC (2011). An antiviral defense role of AGO2 in plants. PLoS ONE 6: e14639

Havecker ER, Wallbridge LM, Hardcastle TJ, Bush MS, Kelly KA, Dunn RM, Schwach F, Doonan JH, Baulcombe DC. (2010). The Arabidopsis RNA-directed DNA methylation argonautes functionally diverge based on their expression and interaction with target loci. Plant Cell 22:321–334.

Havelda Z, Várallyay E, Válóczi A, Burgyán J.(2008). Plant virus infection-induced persistent host gene downregulation in systemically infected leaves Plant J. 55: 278-88. doi: 10.1111/j.1365-313X.2008.03501.x

Hemmes, H., Lakatos, L., Goldbach, R., Burgyán, J., Prins, M., (2007). The NS3 protein of rice hoja blanca tenuivirus suppresses RNA silencing in plant and insect hosts by efficiently binding both siRNAs and miRNAs. RNA 13, 1079–1089.

Henderson IR, Zhang XY, Lu C, Johnson L, Meyers BC, Green PJ, Jacobsen SE (2006) Dissecting Arabidopsis thaliana DICER function in small RNA processing, gene silencing and DNA methylation patterning. Nat Genet 38:721–725. doi:10.1038/ng1804

Himeno M, Kitazawa Y, Yoshida T, Maejima K, Yamaji Y, Oshima K & Namba S (2014). Purple top symptoms are associated with reduction of leaf cell death in phytoplasma-infected plants. Scientific Reports | 4 : 4111 | DOI: 10.1038/srep04111

Hirashima K and Watanabe Y (2003). RNA Helicase Domain of Tobamovirus Replicase Executes Cell-to-Cell Movement Possibly through Collaboration with its Nonconserved Region. J.Virol 22:12357-12362

Ho CK and Shuman S. (2002). Bacteriophage T4 RNA ligase 2 (gp24.1) exemplifies a family of RNA ligases found in all phylogenetic domains. PNAS 99:12709-12714

Höck J and Meister G. (2008). The Argonaute protein family. Genome Biology 9:210 doi:10.1186/gb-2008-9-2-210.

Hu, Q., Hollunder, J., Niehl, A., Korner, C.J., Gereige, D., Windels, D., Arnold, A., Kuiper, M., Vazquez, F., Pooggin, M., Heinlein, M., (2011). Specific impact of tobamovirus infection on the Arabidopsis small RNA profile. PloS One 6, e19549.

Innes R and Ade J. (2005). Indirect activation of the Arabidopsis disease resistance protein RPS5 by the Pseudomonas effector AvrPphB. 16TH INTERNATIONAL CONFERENCE ON ARABIDOPSIS RESEARCH, Duke University, Durham, NC. USA.

Ishibashi K, Miyashita S, Katoh E and Ishikawa M (2012) Host membrane proteins involved in the replication of tomabovirus RNA. *Current Opinion in Virology* 2:699-704

Ishikawa M, Meshi T, Motoyoshi F, Takamatsu N and Okada Y. (1986). *In vitro* mutagenesis of the putative replicase genes of tobacco mosaic virus. Nucleic Acids Research 14: 8291-8305

Ishikawa M, Meshi T, Ohno T, Okada Y. (1991). Specific cessation of minus-strand RNA accumulation at an early stage of tobacco mosaic virus infection. J. Virol. 65:861-868

Iwakawa H and Tomari Y (2013). Molecular Insights into microRNA- Mediated Translational Repression in Plants. Molecular Cell 52: 591-601

Iwakawa H and Tomari Y (2015). The Functions of MicroRNAs: mRNA Decay and Translational Repression. Trends Cell Biol. 25:651-65. doi: 10.1016/j.tcb.2015.07.011. Review.

Jaubert, M., Bhattacharjee, S., Mello, A.F., Perry, K.L., Moffett, P., (2011). ARGONAUTE2 mediates RNA-silencing antiviral defenses against potato virus X in Arabidop- sis. Plant Physiol. 156, 1556–1564.

Ji L and Chen X (2012) Regulation of small RNA stability: Methylation and beyond. *Cell Res* 22: 624-636

Ji, L., Liu, X., Yan, J., Wang, W., Yumul, R.E., Kim, Y.J., Dinh, T.T., Liu, J., Cui, X., Zheng, B., Agarwal, M., Liu, C., Cao, X., Tang, G., and Chen, X. (2011). ARGONAUTE10 and ARGONAUTE1 regulate the termination of floral stem cells through two microRNAs in Arabidopsis. PLoS genetics 7, e1001358.

Jones JD, Dangl JL (2006). The plant immune system. Nature 444:323-329.

Jones-Rhoades MW, Bartel DP, Bartel B (2006). MicroRNAs and their regulatory roles in plants. Annual Review of Plant Biology 57:19-53

Kasschau KD, Fahlgren N, Chapman EJ, Sullivan CM, Cumbie JS, Givan SA, Carrington JC. (2007). Genome-wide profiling and analysis of Arabidopsis siRNAs. PLoS Biol.5:e57

Kidner CA and Martienssen (2005). The developmental role of microRNA in plants . Current Opinion in Plant Biology 8:38-44

Kim YK, Heo I, Kim VN (2010) Modifications of small RNAs and their associated proteins. *Cell* 143: 703-709

Kim Y.J., Maizel A., Chen X., (2014). Traffic into silence: endomembranes and post-transcriptional RNA silencing. EMBOJ.33,968–980.

Knapp, E., Dawson, W. O., and Lewandowski, D. J. 2001. Conundrum of the lack of defective RNAs (dRNAs) associated with tobamovirus infections: dRNAs that can move are

not replicated by the wild-type virus; dRNAs that are replicated by the wild-type virus do not move. J. Virol. 75:5518-5525.

Komoda, K., Mawatari, N., Hagiwara-Komoda, Y., Naito, S., and Ishikawa, M. 2007. Identification of a ribonucleoprotein intermediate of tomato mosaic virus RNA replication complex formation. J. Virol, 81:2584-2591.

Kontra L, Csorba T, Tavazza M, Lucioli A, Tavazza R, Moxon S, Tisza V, Medzihradsky A, Turina M, Burgyán J. (2016). Distinct Effects of p19 RNA Silencing Suppressor on Small RNA Mediated Pathways in Plants. Plos Pathogens. DOI:10.1371/journal.ppat.1005935

Kørner, C. J., Klauser, D., Niehl, A., Domínguez-Ferreras, A., Chinchilla, D., Boller, T., Heinlein, M., and Hann, D. R. 2013. The immunity regulator BAK1 contributes to resistance against diverse RNA viruses. Mol. Plant Microbe Interact. 26:1271-1280.

Koukiekolo R, Jakubek ZJ, Cheng J, Sagan SM, Pezacki JP.(2009). Studies of a viral suppressor of RNA silencing p19-CFP fusion protein: a FRET-based probe for sensing double-stranded fluorophore tagged small RNAs. Biophys Chem.143:166-9. doi: 10.1016/j.bpc.2009.05.001. Erratum in: Biophys Chem. 2009

Kozlowska-Makulska A, Guilley H, Szyndel MS, Beuve M, Lemaire O, Herrbach E, Bouzoubaa S (2010) PO proteins of European beet-infecting poleroviruses display variable RNA silencing suppression activity. *J. Gen. Virol*. 91:1082-1091

Kurihara, Y., Inaba, N., Kutsuna, N., Takeda, A., Tagami, Y., and Watanabe, Y. (2007). Binding of tobamovirus replication protein with small RNA duplexes. J. Gen. Virol. 88: 2347-2352

Kurihara Y, Takashi Y, Watanabe Y. (2006). The interaction between DCL1 and HYL1 is important for efficient and precise processing of pri-miRNA in plant microRNA biogenesis. RNA 12: 206-212

Laakkonen P, Ahola T, Kääriäinen L. (1996). The effects of palmitoylation on membrane association of Semliki forest virus RNA capping enzyme. J Biol Chem. 271:28567-71.

Laemmli UK (1970). Cleavage of structural proteins during the assembly of the head of bacteriophage T4: Nature 227:680

Lakatos, L., Csorba, T., Pantaleo, V., Chapman, E.J., Carrington, J.C., Liu, Y.P., Dolja, V.V., Calvino, L.F., Lopez-Moya, J.J., Burgyán, J., (2006). Small RNA binding is a common strategy to suppress RNA silencing by several viral suppressors. EMBO J. 25, 2768–2780.

Landthaler M, Yalcin A, Tuschl T. (2004). The human DiGeorge syndrome critical region gene 8 and its D-melanogaster homolog are required for miRNA biogenesis. Curr Biol 14: 2162–2167.

Lanet E, Delannoy E, Sormani R, Floris M, Brodersen P, Crété Patrice, Voinnet Olivier and Robaglia Christophe (2009) Biochemical Evidence for Translational Repression by Arabidopsis MicroRNAs. *The Plant Cell* 21: 1762-1768

Law, J. A. & Jacobsen, S. E. Establishing, maintaining and modifying DNA methylation patterns in plants and animals. Nature Rev. Genet. 11, 204–220 (2010).

Lee Y, Kim M, Han JJ, Yeom KH, Lee S, Baek SH, Kim VN. (2004). MicroRNA genes are transcribed by RNA polymerase II. EMBO J 23: 4051–4060.

Levine, A., Pennell, R.I., Alvarez, M.E., Palmer, R. and Lamb, C. (1996) Calcium-mediated apoptosis in a plant hypersensitive disease resistance response. Curr. Biol. 6, 427–437.

Lewandowski, D. J., and Dawson, W. O. (2000). Functions of the 126- and 183-kDa proteins of tobacco mosaic virus. Virology 271:90-98.

Lewsey, M., Robertson, F.C., Canto, T., Palukaitis, P., Carr, J.P., (2007). Selective targeting of miRNA-regulated plant development by a viral counter-silencing protein. Plant J. Cell Mol. Biol. 50, 240–252.

Lewsey, M.G., Murphy, A.M., Maclean, D., Dalchau, N., Westwood, J.H., Macaulay, K., Bennett, M.H., Moulin, M., Hanke, D.E., Powell, G., Smith, A.G., Carr, J.P., (2010). Disruption of two defensive signaling pathways by a viral RNA silencing suppressor. Mol. Plant - Microbe Interact. 23, 835–845.

Li F, Pignatta D, Bendix C, Brunkard JO, Cohn MM, et al., (2012). MicroRNA regulation of plant innate immune receptors. Proc. Natl. Acad. Sci. USA 109:1790–95

Li J, Yang Z, Yu B, Liu J and Chen X (2005) Methylation Protects miRNAs and siRNAs from a 3’ -End Uridylation Activity in Arabidopsis. *Current Biology* 15: 1501- 1507

Lingel A, Simon B, Izaurralde E, Sattler M. (2004). Nucleic acid 3'-end recognition by the Argonaute2 PAZ domain. Nat Struct Mol Biol 11: 576-577

Lingel A, Simon B, Izaurralde E, Sattler M. (2003). Structure and nucleic-acid binding of the drosophila

Liu J, Carmell MA, Rivas FV, Marsden CG, Thomson JM, Song JJ, Hammond SM, Joshua-Tor L, Hannon GJ (2004) Argonaute2 is the catalytic engine of mammalian RNAi. *Science* 305:1437–1441

Liu Y, Zhai H, Zhao K, Wu B, Wang X (2012) Two suppressors of RNA silencing encoded by cereal-infecting members of the family *Luteoviridae*. *J.Gen. Virol.* 93:1825-1830

Love, A.J., Laird, J., Holt, J., Hamilton, A.J., Sadanandom, A., Milner, J.J., (2007). Cauliflower mosaic virus protein P6 is a suppressor of RNA silencing. *J. Gen.Virol*. 88, 3439–3444.

Lozsa, R., Csorba, T., Lakatos, L., Burgyán, J., (2008). Inhibition of 3' modification of smallRNAs in virus-infected plants require spatial and temporal co-expression of small RNAs and viral silencing-suppressor proteins. *Nucleic Acids Res*. 36, 4099–4107.

Lu S, Sun Y and Chiang VL (2009). Adenylation of plant miRNAs. *Nucleic Acids Res.* 37:1878-1885

Lund E, Dahlberg JE (2006). Substrate selectivity of exportin 5 and Dicer in the biogenesis of microRNAs. Cold Spring Harb. Symp. Quant. Biol. 71:59-66

Lynn K, Fernandez A, Aida M, Sedbrook J, Tasaka M, Masson P, Barton MK. (1999). The PINHEAD/ZWILLE gene acts pleiotropically in Arabidopsis development and has overlapping functions with the ARGONAUTE1 gene. Development. 1999 Feb;126(3):469-81

Ma, J.B., Ye, K., and Patel, D.J. (2004). Structural basis for overhang-specific small interfering RNA recognition by the PAZ domain. Nature 429, 318-322.

Ma X, Cao X, Mo B, and Chen X (2013). Trip to ER. MicroRNA-mediated translational reppression in plants. *RNA Biology* 10: 1586-1592

Mackey D, Belkhadir Y, Alonso JM, Ecker JR, Dangl JL. (2003). Arabidopsis RIN4 is a target of the type III virulence effector AvrRpt2 and modulates RPS2-mediated resistance. Cell 112:379–89

Maillard PV, Ciaudo C, Marchais A, Li Y, Jay F, Ding SW, Voinnet O. (2013). Antiviral RNA interference in mammalian cells. Science 342: 235-238.

Mallory AC and Vaucheret H (2006). Functions of microRNAs and related small RNAs in plants. Nat Genet 38: S31-S36

Malpica-López N, Rajeswaran R, Beknazariants D, Seguin, J, Golyaev V, Farinelli L and Pooggin MM. Revisiting the roles of tobamovirus replicase complex proteins in viral replication and silencing suppression. Mol Plant Microbe Interact. doi:10.1094/ MPMI-07-17-0164-R.

Manavella PA, Koenig D, Weigel D. (2012). Plant secondary siRNA production determined by microRNA-duplex structure. PNAS 109:2461-2466

Mangwende T, Wang ML, Borth W, Hu J, Moore PH, Mirkov TE, Albert HH (2009) The P0 gene of sugarcane yellow leaf virus encodes an RNA silencing suppressor with unique activities. *Virology* 384: 38-50

Margis R, Fusaro AF, Smith NA, Curtin SJ, Watson JM, et al., (2006). The evolution and diversification of Dicers in plants. *FEBS Lett.* 580:2442-50

Marin E, Jouannet V, Herz A, Lokerse AS, Weijers D, Vaucheret H, Nussaume L, Crespi MD, Maizel A (2010). miR390, Arabidopsis TAS3 tasiRNAs, and their AUXIN RESPONSE FACTOR targets define an autoregulatory network quantitatively regulating lateral root growth. Plant Cell 22: 1104-1117

Meister G (2013). Argonaute proteins: functional insights and emerging roles. Nat Rev Genet 14:447-459.

Melnyk CW, Molnar A, Baulcombe DC. (2011). Intercellular and systemic movement of RNA silencing signals. EMBO J. 30:3553-63. doi: 10.1038/emboj.2011.274. Review.

Merai Z, Kerenyi Z, Kertesz S, Magna M, Lakatos L, and Silhavy D. (2006) Double stranded RNA binding may be a general plant RNA viral strategy to suppress RNA silencing. *J. Virol.* 80: 5747-5756

Merai, Z., Kerenyi, Z., Molnar, A., Barta, E., Valoczi, A., Bisztray, G., Havelda, Z., Burgyán, J., Silhavy, D., (2005). Aureusvirus P14 is an efficient RNA silencing suppressor that binds double-stranded RNAs without size specificity. J. Virol.79, 7217–7226.

Merits A, Kettunen R, Mäkinen K, Lampio A, Auvinen P, Kääriäinen L, Ahola T. (1999). Virus-specific capping of tobacco mosaic virus RNA: methylation of GTP prior to formation of covalent complex p126-m^7GMP. FEBS Lett 455(1-2), 45-48

Meyers BC, Kozik A, Griego A, Kuang H, Michelmore RW (2003). Genome-wide analysis of NBS-LRR-encoding genes in Arabidopsis. Plant Cell 15:809-834.

Mi S, Cai T, Hu Y, Chen Y, Hodges E, Ni F, Wu L, Li S, Zhou H, Long C, Chen S, Hannon GJ, Qi Y (2008). Sorting of small RNAs into Arabidopsis argonaute complexes is directed by the 5' terminal nucleotide. Cell 133:116–127.

Moissiard, G., Parizotto, E.A., Himber, C., and Voinnet, O. (2007).Transitivity in *Arabidopsis* can be primed, requires the redundant action of the antiviral Dicer-like 4 and Dicer-like 2, and is compromised by viral-encoded suppressor proteins. RNA 13: 1268-1278.

Molnár A, Csorba T, Lakatos L, Várallyay E, Lacomme C, Burgyán J. (2005). Plant virus-derived small interfering RNAs originate predominantly from highly structured single-stranded viral RNAs. J Virol. 2005 Jun;79(12):7812-8

Montgomery TA, Howell MD, Cuperus JT, Li D, Hansen JE, Alexander AL, Chapman EJ, Fahlgren N, Allen E, Carrington JC.(2008). Specificity of ARGONAUTE 7-miR390 Interaction and Dual Functionality in TAS3 Trans-Acting siRNA Formation.Cell 133:128-141

Morel JB and Dangl JL. (1997). The hypersensitive response and the induction of cell death in plants. Cell Death Differ. 4: 671-683

Morel JB, Godon C, Mourrain P, Béclin C, Boutet S, Feuerbach F, Proux F, Vaucheret H.(2002). Fertile hypomorphic ARGONAUTE (ago 1) mutants impaired in post-transcriptional gene silencing and virus resistance. Plant Cell 14: 629-639

Moussian B, Schoof H, Haecker A, Jürgens G, Laux T. (1998). Role of the ZWILLE gene in the regulation of central shoot meristem cell fate during *Arabidopsis* embryogenesis. EMBO J. 17:1799-1809

Nagy PD, Strating JR, van Kuppeveld FJ (2016). Building Viral replication Organelles: Close encounters of the Membrane Types. Plos Pathog 12: 1-6. doi: 10.1371/journal.ppat.1005912. eCollection 2016.

Nandakumar J, Shuman S, D. Lima C. (2006). RNA Ligase Structures Reveal the Basis for RNA Specificity and Conformational Changes that drive Ligation Forward. Cell 127: 71-84

Nicaise, V., and Candresse, T. (2016). Plum pox virus capsid protein suppresses plant pathogen-associated molecular pattern (PAMP)-triggered immunity. Mol. Plant Pathol. Jun 15 [Epub ahead of print].

Niehl, A., Wyrsch, I., Boller, T., and Heinlein, M. (2016). Double-stranded RNAs induce a pattern-triggered immune signaling pathway in plants. New Phytol. 211:1008-1019.

Nishikiori, M., Meshi, T., and Ishikawa, M. (2012). Guanylylation-competent replication proteins of Tomato mosaic virus are disulfide-linked. Virology 434:118-128.

Nishimura T, Molinard G , Petty TJ , Broger L , Gabus C , Halazonetis TD , Thore S, Paszkowski J. (2012). Structural Basis of Transcriptional Gene Silencing Mediated by Arabidopsis MOM1. PLoS Genet 8(2): e1002484. doi:10.1371/journal.pgen.1002484

Omarov RT, Ciomperlik JJ, Scholthof HB. (2007). RNAi-associated ssRNA-specific ribonucleases in Tombusvirus P19 mutant-infected plants and evidence for a discrete siRNA-containing effector complex. Proc.Natl.Acad.Sci. USA. 104:1714–9.10.1073/pnas.0608117104 PMID: 17244709

Osman, T. A., and Buck, K. W. (1996). Complete replication in vitro of tobacco mosaic virus RNA by a template-dependent, membrane-bound RNA polymerase. J. Virol. 70:6227-6234.

Ouyang S, Park G, Atamian HS, Han CS, Stajich JE, Kaloshian I, Borkovich KA (2014). MicroRNAs suppress NB domain genes in tomato that confer resistance to Fusarium oxysporum. PLoS Pathog 10:e1004464.

Padgett HS and Beachy RN (1993). Analysis of a Tobacco Mosaic Virus Strain Capable of Overcoming *N* Gene-Mediated Resistance. The Plant Cell 5: 577-586

Palukaitis P, García-Arenal F, Sulzinski MA, Zaitlin M. (1983). Replication of tobacco mosaic virus. VII. Further characterization os single- and double-stranded virus-related RNAs from TMV-infected plants. Virology 131:533-545

Pantaleo V, Szittya G, Burgyán J (2007) Molecular bases of viral RNA targeting by viral small interfering RNA-programmed RISC. J. Virol 81: 3797-3806

Parent, J.S., Bouteiller,N., Elmayan,T., Vaucheret,H., (2015). Respective contributions of Arabidopsis DCL2 and DCL4 to RNA silencing Plant J.81,223–232.

Park JE, Heo I, Tian Y, Simanshu DK, Chang H, Jee D, et al.,. (2011) Dicer recognizes the 5' end of RNA for efficient and accurate processing. Nature 475:201-205

Parker, J.S., Roe, S.M., and Barford, D. (2005). Structural insights into mRNA recognition from a PIWI domain-siRNA guide complex. Nature 434, 663-666.

Paul D and Bartenschlager R (2013). Architecture and biogenesis of plus-strand RNA virus replication factories. World J of Virol 2: 32-48

Pazhouhandeh, M., Dieterle, M., Marrocco, K., Lechner, E., Berry, B., Brault, V., Hemmer, O., Kretsch, T., Richards, K.E., Genschik, P., Ziegler-Graff, V., (2006). F- box-like domain in the polerovirus protein P0 is required for silencing suppressor function. Proc. Natl. Acad. Sci. USA 103, 1994–1999.

Peragine A, Yoshikawa M, Wu G, Albrecht HL, Poethig RS (2004). SGS3 and SGS2/SDE1/RDR6 are required for juvenile development and the production of trans-acting siRNAs in Arabidopsis. Genes Dev.18:2368-79.

Pfeffer S, Dunoyer P, Heim F, Richards KE, Jonard G, Ziegler-Graff V (2002) P0 of beet western yellows virus is a suppressor of posttranscriptional gene silencing. *J. Virol.* 76: 6815-6824

Plotnikova A, Baranauske S, Osipenko A, Klimasauskas S, Vilkaitis G (2013). Mechanistic insights into small RNA recognition and modification by the HEN1 methyltransferase. *Biochem J.* 453:281-290

Pontes O et al., (2006) The Arabidopsis chromatin-modifying nuclear siRNA pathway involves a nucleolar RNA processing center. Cell 126:79–92. doi:10.1016/j.cell.2006.05.031

Qi D, DeYoung BJ, Innes RW. (2012). Structure-function analysis of the coiled-coil and leucine-rich repeat domains of the RPS5 disease resistance protein. Plant Physiol. 158:1819–32

Qi, Y., Denli, A.M., and Hannon, G.J. (2005). Biochemical specialization within Arabidopsis RNA silencing pathways. Molecular cell 19, 421-428.

Qi, Y., He, X., Wang, X.J., Kohany, O., Jurka, J., and Hannon, G.J. (2006). Distinct catalytic and non-catalytic roles of ARGONAUTE4 in RNA-directed DNA methylation. Nature 443, 1008-1012.

Qi Y, Tsuda K, Glazebrook J and Katagiri F. (2011). Physical association of pattern-triggered immunity (PTI) and effector-triggered immunity (ETI) immune receptors in Arabidopsis. Molecular Plant Pathology 12: 702-708

Qu F, Ye X, Morris TJ (2008). Arabidopsis DRB4, AGO1, AGO7 and RDR6 participate in a DCL4-initiated antiviral RNA silencing pathway negatively regulated by DCL1. Proc. Natl. Acad. Sci. USA 105: 14732-14737

Qu, F (2010). Antiviral role of plant-encoded RNA-dependent RNA polymerases revisited with deep sequencing of small interfering RNAs of viral origin. *Mol Plant Microbe Interact*. 23:1248-1252

Raja P, Sanville BC, Buchmann RC, Bisaro DM (2008). Viral genome methylation as an epigenetic defense against geminiviruses. *J. Virol* 82: 8997-9007

Raja P, Wolf JN, Bisaro DM (2010). RNA silencing directed against geminiviruses: Post-transcriptional and epigenetic components. Biochimica et Biophysica Acta 1799: 337-351

Rajeswaran R and Pooggin MM. (2012). RDR6-mediated synthesis of complementary RNA is terminated by miRNA stably bound to template RNA. Nucleic Acids Research 40: 594-599

Ramanathan A, Robb GB and Chan SH. (2016). Survey and Summary. mRNA capping: biological functions and applications. Nucleic Acids Research doi: 10.1093/nar/gkw551

Ren, B., Guo, Y., Gao, F., Zhou, P., Wu, F., Meng, Z., Wei, C., Li, Y., (2010). Multiple functions of rice dwarf phytoreovirus Pns10 in suppressing systemic RNA silencing. J. Virol. 84, 12914–12923.

Ren GD, Xie M, Zhang SX, Vinovskis C, Chen XM, et al., (2014). Methylation protects microRNAs from an AGO1-associated activity that uridylates 5' RNA fragments generated by AGO1 cleavage. Proc. Natl. Acad. Sci. U.S.A. 111:6365-6370. doi: 10.1073/pnas.1405083111

Rhoades, M.W., Reinhart, B.J., Lim, L.P., Burge, C.B., Bartel, B., and Bartel, D.P. (2002). Prediction of plant microRNA targets. Cell 110, 513-520.

Rivas, F.V., Tolia, N.H., Song, J.J., Aragon, J.P., Liu, J., Hannon, G.J., and Joshua-Tor, L. (2005). Purified Argonaute2 and an siRNA form recombinant human RISC. Nature structural & molecular biology 12, 340-349.

Rodríguez-Negrete E, Lozano-Durán R, Piedra-Aguilera A, Cruzado L, Bejarano ER and Castillo AG (2013). Geminivirus Rep protein interferes with the plant DNA methylation machinery and suppresses transcriptional gene silencing. New Phytologist 199:464-475

Ruíz-Ferrer, V and Voinnet, O. (2009) Roles of plant small RNAs in biotic stress responses. *Annu Rev. Plant Biol.* 60:485-510

Rybicki E. 2015. A Short History of the Discovery of Viruses. Buglet Press.

Sahana, N., Kaur, H., Jain, R.K., Palukaitis, P., Canto, T., Praveen, S., (2014). The asparagine residue in the FRNK box of potyviral helper-component protease is critical for its small RNA binding and subcellular localization. J. Gen. Virol. 95, 1167–1177.

Saini HK, Griffiths-Jones S, Enright AJ (2007). Genomic analysis of human microRNA transcripts. Proc.Natl. Acad. Sci USA 104(45):17719-24

Sarkies P and Miska EA (2014). Small RNAs break out: the molecular cell biology of mobile small RNAs. Nature Reviews Molecular Cell Biology 15: 525-535

Schmitz-Linneweber C and Small I. (2008) Pentatricopeptide repeat proteins: a socket set for organelle gene expression. Trends Plant Sci: 13(12) 663-670

Scholthof HB, Alvarado VY, Vega-Arreguin JC, Ciomperlik J, Odokonyero D, Brosseau C, Jaubert M, Zamora A, Moffett P. (2011). identification of an ARGONAUTE for antiviral RNA silencing in *Nicotiana benthamiana*. Plant Physiol. 156:1548-55. doi: 10.1104/pp.111.178764.

Schuck J, Gursinsky T, Pantaleo V, Burgyán J, Behrens SE. AGO/RISC-mediated antiviral RNA silencing in a plant in vitro system. Nucleic Acids Res. (2013); 41(9):5090–103. 10.1093/nar/gkt193 PMID: 23535144

Schwach, F., Vaistij, F.E., Jones, L., Baulcombe, D.C.(2005) An RNA-dependent RNA polymerase prevents meristem invasion by Potato virus X and is required for the activity but not the production of a systemic silencing signal. Plant Physiol. 138:1842–1852.

Seguin[b] J, Otten P, Baerlocher L, Farinelli L, Pooggin MM (2014) MISIS: A bioinformatics tool to view and analyze maps of small RNAs derived from viruses and genomic loci generating multiple small RNAs. J Virol Methods 195: 120–122

Seguin[a] J, Rajeswaran R, Malpica-López N, Martin RR, Kasschau K, Dolja VV, Otten P, Farinelli L, Pooggin MM (2014). *De Novo* Reconstruction of Consensus Master Genomes of Plant RNA and DNA Viruses from siRNAs. *PLOS ONE* 9: 1-8

Shamandi, N., Zytnicki, M., Charbonnel, C., Elvira-Matelot, E., Bochnakian, A., Comella, P., Mallory, A. C., Lepère, G., Sáez-Vásquez, J., and Vaucheret, H. (2015). Plants Encode a General siRNA Suppressor That Is Induced and Suppressed by Viruses. PLoS Biol. 13:e1002326.

Shen, M., Xu, Y., Jia, R., Zhou, X., Ye, K., (2010). Size-independent and noncooperative recognition of dsRNA by the rice stripe virus RNA silencing suppressor NS3. J. Mol. Biol. 404, 665–679.

Shivaprasad PV, Chen H-M, Patel K, Bond DM, Santos BACM, Baulcombe DC. (2012). A microRNA superfamily regulates nucleotide binding site-leucine-rich repeats and other mRNAs. Plant Cell 24:859–74

Shivaprasad, P.V., Rajeswaran, R., Blevins, T., Schoelz, J., Meins, F., Hohn, T., Pooggin, M.M., (2008). The CaMV transactivator/viroplasmin interferes with RDR6- dependent trans-acting and secondary siRNA pathways in Arabidopsis. Nucleic acid Res. 36, 5896–5909.

Shuman S and D Lima C. (2004). The polynucleotide ligase and RNA capping enzyme superfamily of covalent nucleotidyltransferases. Current Opinion in Structural Biology 14:757-764.

Silhavy, D., Molnar, A., Lucioli, A., Szittya, G., Hornyik, C., Tavazza, M., Burgyán, J., (2002). A viral protein suppresses RNA silencing and binds silencing-generated, 21- to 25-nucleotide double-stranded RNAs. EMBO 21, 3070–3080.

Singh RK, Gase K, Baldwin IT and Pandey SP (2015). Molecular evolution and diversification of the Argonaute family of proteins in plants. BMC Plant Biology 15:23 DOI 10.1186/s12870-014-0364-6

Smith, N. A., Eamens, A. L., and Wang, M. B. (2010). The presence of high-molecular weight viral RNAs interferes with the detection of viral small RNAs. RNA 16:1062-1067.

Song, J.J., Liu, J., Tolia, N.H., Schneiderman, J., Smith, S.K., Martienssen, R.A., Hannon, G.J., and Joshua-Tor, L. (2003). The crystal structure of the Argonaute2 PAZ domain reveals an RNA binding motif in RNAi effector complexes. Nature structural biology 10,1026-1032.

Song JJ, Smith SK, Hannon GJ, Joshua-Tor L (2004). Crystal structure of Argonaute and its implications for RISC slicer activity. *Science* 305:1434–1437

Souret FF, Kastenmayer JP, Green PJ (2004). AtXRN4 degrades mRNA in *Arabidopsis* and its substrates include selected miRNAs targets. *Mol. Cell* 15: 173-183

Staskawicz, B.J., Ausubel, F.M., Baker, B.J., Ellis, J.G. and Jones, J.D. (1995) Molecular-genetics of plant-disease resistance. Science, 268, 661–667.

Stokes TL, Kunkel BN, Richards EJ. (2002). Epigenetic variation in Arabidopsis disease resistance. Genes Dev. 16:171–182.

Szittya G, Moxon S, Pantaleo V, et al., (2010). Structural and functional analysis of viral siRNAs. PLoS Pathog, 2010, 6: e1000838

Szyttya G. and Burgyán J. (2013). RNA Interference-Mediated Intrinsic Antiviral Immunity in Plants. B.R. Cullen (ed), *Intrinsic Immunity,* Current topics in Microbiology and Immunology 371:153-181.

Takeda A, Iwasaki S, Watanabe T, Utsumi M, Watanabe Y (2008). The mechanism selecting the guide strand from small RNA duplexes is different among argonaute proteins. Plant Cell Physiol 49:493–500.

Takimoto K et al., (2009). Mammalian GW182 contains multiple Argonaute-binding sites and functions in microRNA-mediated translational repression. RNA 15:1078-1089.

Tameling WIL, Vossen JH, Albrecht M, Lengauer T, Berden JA, Haring MA, Cornelissen BJC and Takken FLW (2006). Mutations in the NB-ARC domain of I-2 that impair ATP hydrolysis cause autoactivation. Plant Physiology 140:1233-1245.

Tang, G., Reinhart, B.J., Bartel, D.P., and Zamore, P.D. (2003). A biochemical framework for RNA silencing in plants. Genes Dev 17: 49-63.

Tian D, Traw MB, Chen JQ, Kreitman M, Bergelson J. (2003). Fitness costs of R-gene-mediated resistance in Arabidopsis thaliana. Nature 423:74–77.

Till S et al., (2007). A conserved motif in Argonaute-interacting proteins mediates functional interactions through the Argonaute PIWI domain. Nat. Struct. Mol. Biol. 14:897-903

Tolia NH and Joshua-Tor L (2007). Slicer and the argonautes. Nat. Chem. Biol. 1:36-43. DOI: 10.1038/nchembio848

Tomari Y, Zamore PD (2005). Perspective: machines for RNAi. *Genes Dev* 19:517–529

Tucker, M.R., Okada, T., Hu, Y., Scholefield, A., Taylor, J.M., and Koltunow, A.M. (2012). Somatic small RNA pathways promote the mitotic events of megagametogenesis during female reproductive development in Arabidopsis. Development 139, 1399-1404.

Várallyay, E., Havelda, Z., (2013). Unrelated viral suppressors of RNA silencing mediate the control of ARGONAUTE1 level. Mol. Plant Pathol. 14, 567–575.

Várallyay, E., Valoczi, A., Agyi, A., Burgyán, J., Havelda, Z., (2010). Plant virus-mediated induction of miR168 is associated with repression of ARGONAUTE1 accumula- tion. EMBO J. 29, 3507–3519.

Vargason, J.M., Szittya, G., Burgyán, J., Hall, T.M., (2003). Size selective recognition of siRNA by an RNA silencing suppressor. Cell 115, 799–811.

Vaucheret, H., Vazquez, F., Crete, P., and Bartel, D.P. (2004). The action of ARGONAUTE1 in the miRNA pathway and its regulation by the miRNA pathway are crucial for plant development. Genes & development 18, 1187-1197.

Vazquez F (2006). Arabidopsis endogenous small RNAs: highways and byways. *Trends Plant Sci* 11:460-468

Vazquez F, Vaucheret H, Rajagopalan R, Lepers C, Gasciolli V, Mallory AC, Hilbert JL, Bartel DP, Crété P. (2004). Endogenous trans-acting siRNAs regulate the accumulation of Arabidopsis mRNAs. Mol Cell.16:69-79.

Voinnet (2008). Use, tolerance and avoidance of amplified RNA silencing by plants. Trends Plant Sci. 13(7):317-28. doi: 10.1016/j.tplants.2008.05.004. Epub 2008 Jun 17.

Voinnet O (2009). Origin, biogenesis, and activity of plant microRNAs. *Cell* 136:669-687

Wang X, Zhang S, Dou Y, Zhang C, Chen X, Yu B, et al., (2015). Synergistic and Independent Actions of Multiple Terminal Nucleotidyl Transferases in the 3' Tailing of Small RNAs in Arabidopsis. PLoS Genet 11(4): e1005091. doi:10.1371/journal. pgen.1005091

Wang XB, Wu Q, Ito T, Cillo F, Li WX, Chen X, Yu JL, Ding SW (2010). RNAi mediated viral immunity requires amplification of virus-derived siRNAs in *Arabidopsis thaliana*. *Proc. Natl. Acad. Sci. U.S.A.* 107:484-489

Wang XB, Jovel J, Udomporn P, Wang Y,Wu Q, Li WX, Gasciolli V, Vaucheret H, Ding SW (2011). The 21-nucleotide, but not 22-nucleotide, viral secondary small interfering RNAs direct potent antiviral defense by two cooperative argonautes in *Arabidopsis thaliana*. Plant Cell 23, 1625-1638

Wassenegger M and Krczal G. (2006). Nomenclature and functions of RNA-directed RNA polymerases. *Trends Plant Sci* 11:142-151

Watanabe T, Honda A, Iwata A, Ueda S, Hibi T, Ishihama A. (1999). Isolation from Tobacco Mosaic Virus-Infected Tobacco of a Solubilized Template-Specific RNA-Dependent RNA Polymerase Containing a 126K/183K Protein Heterodimer. Journal of Virology 73:2633-2640

Willmann MR, Endres MW, Cook RT and Gregory BD (2011). The Functions of RNA-Dependent RNA Polymerases in Arabidopsis. The Arabidopsis Book. e0146. doi: 10.1199/tab.0146

Wilson RC and Doudna JA (2013). Molecular Mechanisms of RNA Interference. Annu. Rev. Biophys. 42: 217-239.

Wu L, Fan J, Belasco JG (2006). MicroRNAs direct rapid deadenylation of mRNA. PNAS 103: 4034-4039

Xie ZX et al., (2004). Genetic and functional diversification of small RNA pathways in plants. PLoS Biol 2:642–652. doi:10.1371/journal.pbio.0020104

Yan, K.S., Yan, S., Farooq, A., Han, A., Zeng, L., and Zhou, M.M. (2003). Structure and conserved RNA binding of the PAZ domain. Nature 426, 468-474.

Yang X and Li L. (2012) Analyzing the microRNA Transcriptome in Plants using Deep Sequencing Data. Biology 1(2): 297-310

Yang Z, Ebright YW, Yu B, Chen X (2006). HEN1 recognizes 21-24-nt small RNA duplexes and deposits a methyl group onto the 2'OH of the 3' terminal nucleotide. Nucleic Acids Res 34: 667-675

Yi R, Qin Y, Macara IG, Cullen BR. (2003). Exportin-5 mediates the nuclear export of pre-microRNAs and short hairpin RNAs. Genes Dev 17: 3011–3016.

Yin S, Ho K, Shuman S. (2003). Structure-Function analysis of T4 RNA Ligase 2. The Journal of Biological Chemistry 278:17601-17608

Yoshikawa M, Peragine A, Park MY, Poethig RS. (2005). A pathway for the biogenesis of trans-acting siRNAs in Arabidopsis. Genes Dev. 19:2164–75

Yu B, Yang Z, Li J, Minakhina S, Yang M, Padgett RW, Steward R and Chen X (2005). Methylation as a crucial step in plant microRNA biogenesis. *Science* 307:932-935

Yu D, Fan B, MacFarlane SA, Chen Z (2003). Analysis of the Involvement of an Inducible Arabidopsis RNA-dependent RNA Polymerase in Antiviral Defense. MPMI 16: 206-216

Zhai, Y., Bag, S., Mitter, N., Turina, M., Pappu, H.R., (2014). Mutational analysis of two highly conserved motifs in the silencing suppressor encoded by tomato spotted wilt virus (genus Tospovirus, family Bunyaviridae). Arch. Virol. 159, 1499–1504.

Zhai J, Jeong DH, De Paoli E, Park S, Rosen BD, Li Y, Gonzalez AJ, Yan Z, Kitto SL, Grusak MA, Jackson SA, Stacey G, Cook DR, Green PJ, Sherrier DJ, Meyers BC (2011). MicroRNAs as master regulators of the plant NB-LRR defense gene family via the production of phased, trans-acting siRNAs. *Genes Dev*. 25: 2540-2553

Zhai J and Meyers BC (2012). Deep Sequencing from *hen1* Mutants to identify Small RNA 3' Modifications. *Cold Spring Harbor Symposia on Quantitative Biology*, Volume LXXVII

Zhai J, Zhao Y, Simon SA, Huang S, Petsch K, Arikit S, Pillay M, Ji L, Xie M, Cao X, Yu B, Timmermans M, Yang B, Chen X and Meyers BC (2013). Plant microRNAs display differential 3' truncation and tailing modifications that are ARGONAUTE 1 dependent and conserved across species. *The Plant Cell* 25: 2417-2428

Zhang[a] X, Henriques R, Lin S, Niu Q, and Chua N (2006). *Agrobacterium*-mediated transformation of *Arabidopsis thaliana* using the floral dip method. Nature Protocols 1:1-6

Zhang X, Xia J, Lii YE, Barrera-Figueroa BE, Zhou X, et al., (2012). Genome-wide analysis of plant NAT-siRNAs reveals insights into their distribution, biogenesis and function. Genome Biol. 13:R20

Zhang[b], X., Yuan, Y.R., Pei, Y., Lin, S.S., Tuschl, T., Patel, D.J., Chua, N.H., (2006). Cucumber mosaic virus-encoded 2b suppressor inhibits Arabidopsis Argonaute1 cleavage activity to counter plant defense. Genes Dev. 20, 3255–3268.

Zhang, X., Zhang,X., Singh,J., Li,D., Qu,F., (2012). Temperature-dependent survival of turnip crinkle virus-infected Arabidopsis plants relies on an RNA silencing-based defense that requires dcl2, AGO2, and HEN1.J.Virol.86,6847–6854.

Zhang X, Zhao H, Gao S, Wang W, Katiyar-Agarwal S, Huang H, Raikhel N and Jin H. (2011). Arabidopsis Argonaute 2 regulates innate immunity via miRNA393*-mediated silencing of a Golgi-localized SNARE gene, MEMB12. Mol Cell 42:356–366.

Zhang Y, Dorey S, Swiderski M, Jones JD (2004). Expression of RPS4 in tobacco induces an AvrRps4-independent HR that requires EDS1, SGT1 and HSP90. Plant J 40:213-224.

Zhao Y, Yu Y, Zhai J, Ramachandran V, Dinh TT, Meyers BC, Mo B and Chen X (2012). The *Arabidopsis* nucleotidyl transferase HESO1 uridylates unmethylated small RNAs to trigger their degradation. *Curr. Biol.* 22:689-694

Zheng X, Zhu J, Kapoor A, Zhu JK. (2007). Role of Arabidopsis AGO6 in siRNA accumulation, DNA methylation and transcriptional gene silencing. EMBO 26:1691-1701

Zhu, S., Jeong, R.D., Lim, G.H., Yu, K., Wang, C., Chandra-Shekara, A.C., Navarre, D., Klessig, D.F., Kachroo, A., Kachroo, P., (2013). Double-stranded RNA-binding protein 4 is required for resistance signaling against viral and bacterial pathogens. Cell Rep. 4, 1168–1184.

Zipfel C, Robatzek S, Navarro L, Oakeley EJ, Jones JD, Felix G, Boller T: Bacterial disease resistance in Arabidopsis through flagellin perception. Nature (2004), 428:764-767.

Zvereva AS and Pooggin MM, (2012). Review. Silencing and Innate Immunity in Plant Defense against Viral and Non-Viral Pathogens. Viruses 4, 2578-2597

Zvereva, A. S., Golyaev, V., Turco, S., Gubaeva, E. G., Rajeswaran, R., Schepetilnikov, M. V., Srour, O., Ryabova, L. A., Boller, T., and Pooggin, M. M. 2016. Viral protein suppresses oxidative burst and salicylic acid-dependent autophagy and facilitates bacterial growth on virus-infected plants. New Phytol. 211:1020-1034.

Section XI. Supplementary Material

Supplementary Dataset S1, S2 and S3 (Malpica-López et al, MPMI. doi: 10.1094/MPMI-07-17-0164-R).

Supplementary Dataset S1.xlsx

Supplementary Dataset S2.xlsx

Supplementary Dataset S3 .xlsx

Supplementary Table S1. DNA oligonucleotide probes, PCR primers and synthetic gene fragments

Name original	Detects	(Gene/region)	Sequence (5' to 3')
***A. thaliana* genome sRNA specific probes:**			
miR160a_as	**miR160**	**miRNA**	**TGGCATACAGGGAGCCAGGCA**
miR168a_as	**miR168**	**miRNA**	**TTCCCGACCTGCACCAAGCGA**
miR173_as	**miR173**	**miRNA**	**GTGATTTCTCTCTGCAAGCGAA**
miR173*_as	**miR173***	**miRNA***	**CTTTCGCTTACACAGAGAATC**
miR403a_as	**miR403**	**miRNA**	**CGAGTTTGTGCGTGAATCTAA**
miR472_as	**miR472**	**miRNA**	**GGTATGGGCGGAGTAGGAAAAA**
miR472*_as	**miR472***	**miRNA***	**GATTTTGCCTACTTCGACCAT**
siR255_as	**siR255**	**TAS1a/b/c siRNA**	**TACGCTATGTTGGACTTAGAA**
siR255*_as	**siR255***	**TAS1a/b/c siRNA***	**TATTCTAAGTCCAACATAGCG**

siR1003 as	siR1003	5S rRNA siRNA	ATGCCTATGTTGGCCTCACGGTCT
Met_tRNA_as	Met-tRNA	tRNA	TGGTATCAGAGCCAGGTTTCGATCC

***N. benthamiana* genome sRNA specific probes:**

miR160a_as	miR160	miRNA	TGGCATACAGGGAGCCAGGCA
nbmiR482a_as	miR482	miRNA	TAGGAATGGGTGGAATTGGAAA
nbmiR482a_star_as	miR482*	miRNA*	GCTTTCCAACCCACCAATCCC

***N. benthamiana* GFP transgene-specific probes**

NOSterm_s	3'UTR a/sense siRNAs	CAATAAAGTTTCTTAAGATTGAATCCTGTTGCCGGTCTTGCG
NOSterm_as	3'UTR a/sense siRNAs	CGCAAGACCGGCAACAGGATTCAATCTTAAGAAACTTTATTG

β-elimination internal control RNA-specific probe:

GFP_22ntRNA_as	non-methylated GFP RNA	AGAAGAACGGCATCAAGGTGAA

ORMV genome-specific probes for long RNA blot hybridization:

OrmvCP_qPCR_s	ORMV CP antisense	GTACCAGTATTTCGCAGCGATGTG
OrmvCP_qPCR_as	ORMV CP sense	GTATCTCTTGCCGCTTGAGTTTGG

Arabidopsis genome-specific probes for long RNA blot hybridization:

AGO1_as	AGO1 mRNA	CCACTGTCTGATGTCTCTGGCTCCATGTAGAATC
AGO2_as	AGO2 mRNA	GAGATTACAAATTCGTTTCAACACACCAAAACC
RPS5_as	RPS5 mRNA	CTCCACCGCCACCTGGATGAAGGTAAGAAAC
RPS4_as	RPS4 mRNA	CTCTGCTTCTTCTTTGGCCGTCCATTATCCATTC

ORMV genome specific probes for small RNA blot hybridization:

OrmvCP_qPCR_s	ORMV CP antisense siRNAs	GTACCAGTATTTCGCAGCGATGTG
Mixture of 3 oligos	ORMV p125 antisense siRNAs	
ormv5_1s		GCACGCTCGAGACGCCCTAAGGTCCAT
ormv5_2s		AGGCCGTACACTCCCTAGCGGGTGGTC
ormv5_3s		CGCTGCGCACCTTTTCAAGGGACGCGA

ORMV qPCR primers

OrmvRep_qPCR_s	ORMV p125 sense	TGCCTCATTGTCAGCTACAGTCTC
OrmvRep_qPCR_as	ORMV p125 antisense	TAACCAGCGTCCTCTTCTCACATC
OrmvMP_qPCR_s	ORMV MP sense	CTGGCTCTGGAGGTGGTTTCTG
OrmvMP_qPCR_as	ORMV MP antisense	CTTCGACGTTCGGATCATTCACAG
OrmvCP_qPCR_s	ORMV CP sense	GTACCAGTATTTCGCAGCGATGTG
OrmvCP_qPCR_as	ORMV CP antisense	GTATCTCTTGCCGCTTGAGTTTGG

PCR primers to introduce the ORMV p125 stop codon mutation:

p126_stopsup_s	ORMV p125 stop sense	TCGGGTACCCAATAcCAATTACAGATCGACACAGTG
p126_stopsup_as	ORMV p125 stop antisense	GTCGATCTGTAATTGgTATTGGGTACCCGACTCTAC
p180_ClaI_s	p125 stop sense upstream	AGGTTGTTTATCGATGAGGGATTAATGCTG
p180_XmaIII_as	p125 stop a/sense downstream	GAAAACCGGCCGTTCTTTCGGCACTTGCAC

Gateway primers to generate vectors expressing ORMV p125 and/or p182 proteins:

AttB1_Rep_s	ORMV p125 start sense	ggggacaagtttgtacaaaaaagcaggctACAcCATGGCACAATTTCAACAAACAG
AttB2_p126_as	ORMV p125 stop antisense	ggggaccactttgtacaagaaagctgggtCCTATTGGGTACCCGACTCTACCT
AttB2_p180_as	ORMV p182 stop antisense	ggggaccactttgtacaagaaagctgggtcTCAAACAAAAAACAAATCTTTAAACAACC

PCR primers for genotyping transgenic lines:

CaMV35Spro_#1	CaMV 35S promoter	CGCGTCGAGATGCTAAAT

Ormv141_as	**ORMV p125 ORF**	**CGCGTCGAGATGCTAAATC**
Ormv323_as	**ORMV p125 ORF**	**AGATACTCCAACTCAAGAGTCCTTAGACCA**

Synthetic fragments to repair the pORMV infectious clone:

>Ormv_NarI_EcoNI

**ggcgccTTAATACGACTCACTATAGTTTTATTTTTATTGCAACAACAACAACAAATTACAATAACAACAAAACAAATACAAACAACAACAACATGGCACAATTTCAACAAACAGTAAACATGCAA
ACATTGCAGGCTGCCGCGGGGCGCAACAGCCTGGTGAATGATTTAGCATCTCGACGCGTTTATGATAATGCTGTCGAGGAGCTAAATGCACGCTCGAGACGCCCTAAGGTCCATTTCTCCAAATC
AGTGTCTACGGAACAGACGCTGTTGGCTTCAAACGCTTATCCGGAGTTTGAGATTTCCTTTACTCATACCCAACAGGCCGTACACTCCCTAGCGGGTGGTCTAAGGACTCTTGAGTTGGAGTATC
TCATGATGCAAGTTCCGTTCGGTTCTCTAACGTACGATATCGGTGGTAACTTCGCTGCGCAccttttcaagg**

>Ormv_NcoI_PstI

**ccatggTTACTAATAACGTGGTTGTTAAAGGTTTGAGGGAAAAAGTCATCGCTGTGAATGATCCGAACGTCGAAGGTTTCGAAGGTGTGGTTGACGATTTCGTCGATTCGGTTGCTGCATTCAAG
GCGATTGACAGTTTCAGGAAGAAAAAGAAAAGGATTGGAGGAAGGGATGTAAATAGTAATAAGTATAGATATAGACCGGAGAGATACGCCGGTCCTGATTCGTTACAATATAAAGAAGAAAATGG
TTTACAACATCACTAGCTCGAATCAGTACCAGTATTTCGCAGCGATGTGGGCAGAGCCCACAGCGATGCTTAACCAGTGCGTGTCTGCGTTGTCGCAGTCGTACCAAACTCAAGCGGCAAGAGAT
ACTGTTAGACAGCAGTTCTCTAACCTTCTGAGTGCGATTGTGACACCGAACCAGCGGTTTCCAGAAGCAGGATACCGGGTGTATATTAATTCAGCAGTTCTAAAACCGTTGTACGAGTCTCTCAT
GAAGTCCTTTGATACTAGGAATAGGATCATTGAAACTGAAGAAGAGTCGCGTCCATCGGCTTCCGAAGTAGCTAATGCAACACAACGTGTTGATGATGCGACCGTGGCCATCAGGAGTCAAATTC
AGCTTTTGCTGAACGAGCTCTCCAACGGACATGGTCTGATGAACAGGGCAGAGTTCGAGGTTTTATTACCTTGGGCTACTGCGCCAGCTACATAGGCGTGGTGCACACGATAGTGCACAGTGTTT
TTCTCTCCACTTAAATCGAAGAGATATACTTACGGTGTAATTCCGTAAGGGTGGCGTAAACCAAATTACGCAATGTTTTAGGTTCCATTTAAATCGAAACCTGTTATTTCCTGGATCACCTGTTA
ACGTACGCGTGGCGTATATTACAGTGGGAATAACTAAAAGTGAGAGGTTCGAATCCTCCCTAACCCCGGGTAGGGGCCCATGCATctgcag**

Supplemental Figure Legends

Supplementary Fig. S1. Infectivity tests and molecular analysis of the p125-deficient virus in *N. benthamiana*, *A. thaliana* and its mutant lines with impaired siRNA biogenesis.

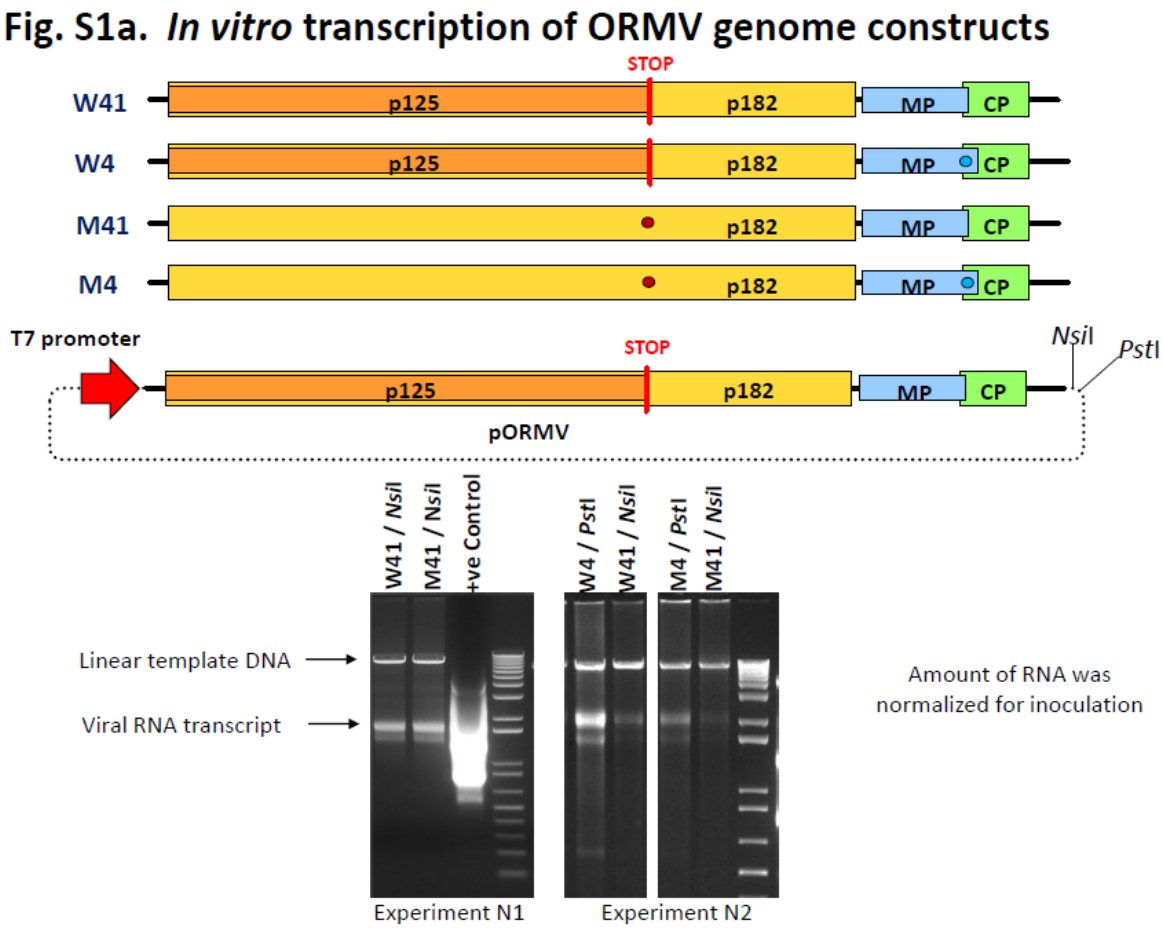

Fig. S1a. *In vitro* transcription of ORMV genome constructs. The top panel contains linear diagrams of the genome organization of each ORMV construct, depicting the p125, p182, movement protein (MP) and coat protein (CP) ORFs, and a diagram of a prototypical ORMV genome construct in the context of a circular plasmid (pORMV). The leaky stop codon of p125 is shown as a vertical red line in the two p125-expressing constructs (W41 and W4) and the mutated p125 stop codon is shown as a red circle in constructs M41 and M4. The T-to-G substitution at position 5612 (which eliminates the original MP stop codon, elongating the protein by an additional 19 amino acids) is shown as a blue circle in constructs W4 and M4. The location of the T7 promoter for *in vitro* transcription and of the restriction sites (*Nsi* I and *Pst* I) used to linearize the constructs before *in vitro* transcription are also shown. The bottom panel shows an analysis by non-denaturing agarose gel electrophoresis

of two *in vitro* transcription experiments (N1 and N2) using the linearized constructs, indicating the positions of the linear template DNA and viral RNA transcripts with arrows. The positive control was an *in vitro* transcription reaction from the linear plasmid pTRI-Xef, provided by the kit supplier (Ambion).

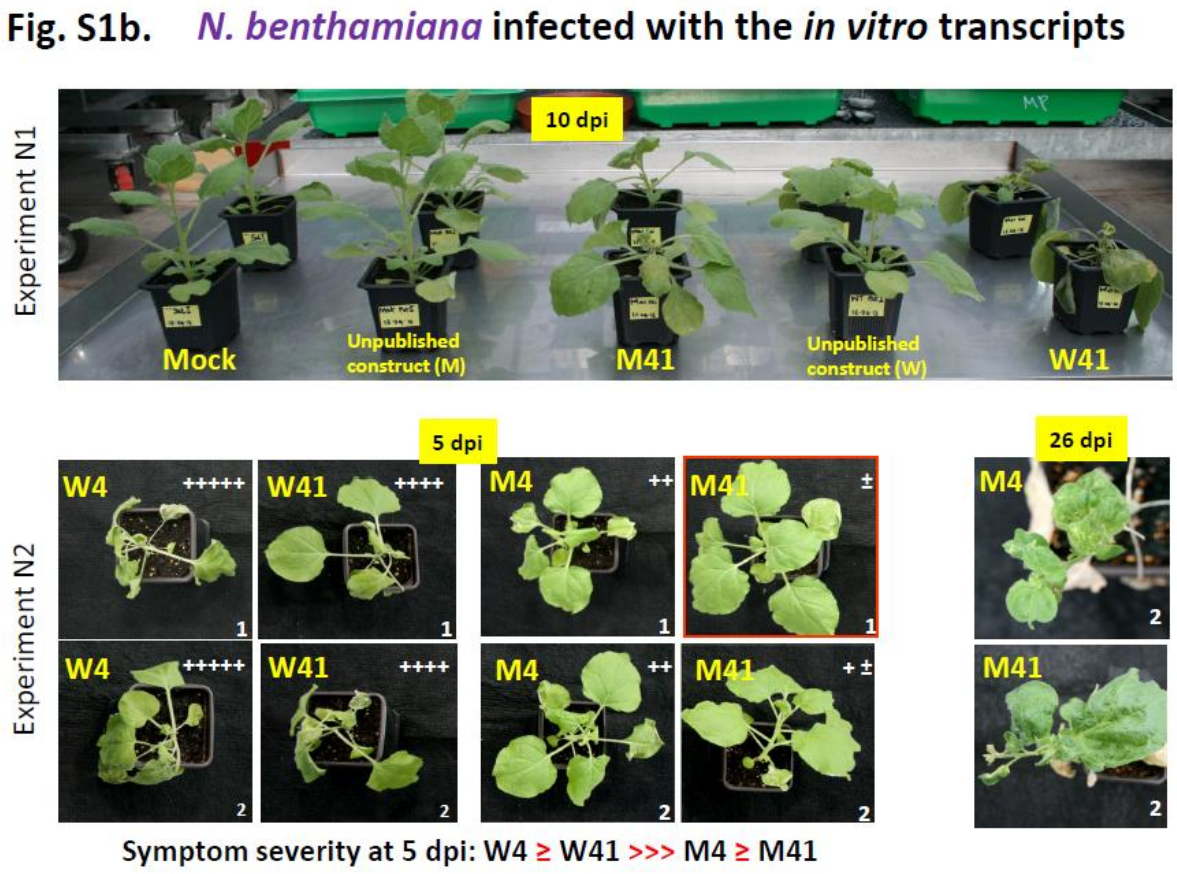

Fig. S1b. Infection of *N. benthamiana* with *in vitro* transcripts. The figure shows the disease symptoms caused by infection with *in vitro* transcripts from two different experiments (N1 and N2). *N. benthamiana* plants (two per construct) were inoculated with *in vitro* transcripts from wild-type (W41 or W4) or mutant (M41 or M4) ORMV constructs. The symptoms of viral infection at 5, 10 and 26 dpi are shown, indicating their relative severity. Note that after stem necrosis and tilting at 5 dpi, systemic tissue death had occurred in all plants infected with W41 or W4 by 26 dpi (not shown). In experiment N2, one of the two plants inoculated with M41 (plant 1)

remained asymptomatic up to 26 dpi (not shown), even though plant 2 and both plants inoculated with M4 had developed disease symptoms by that date. In both cases, the figures shows only plant 2 of both conditions at 26 dpi.

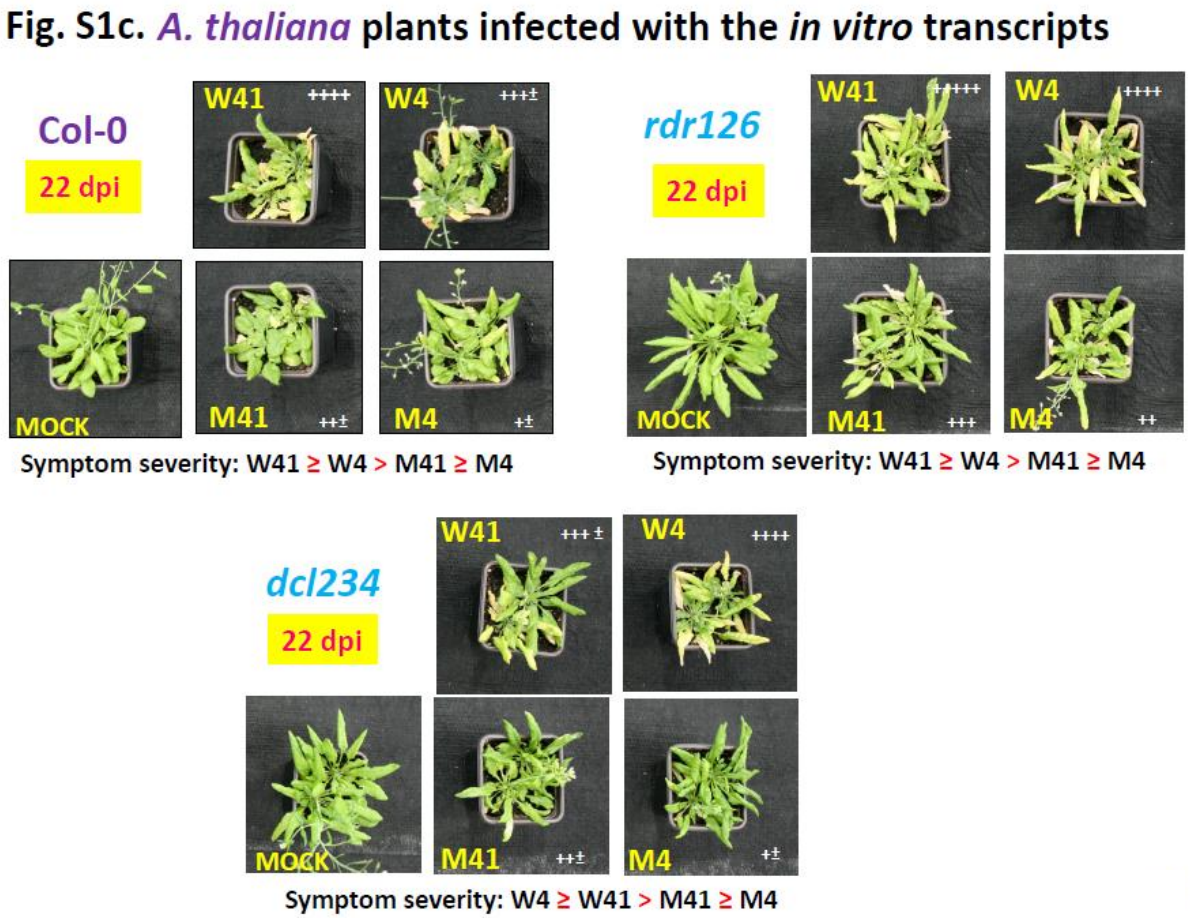

Fig. S1c. Infection of *A. thaliana* with *in vitro* transcripts. Disease symptoms caused in Col-0, *rdr126* and *dcl234* plants by infection with *in vitro* transcripts. Each *A. thaliana* line (two plants per construct) was inoculated with *in vitro* transcripts from wild-type (W41 or W4) or mutant (M41 or M4) ORMV constructs. The figure shows the symptoms of viral infection at 22 dpi for one representative plant per construct, together with the relative severity of disease symptoms.

Fig. S1d. RT-PCR amplification and sequencing of the viral RNA

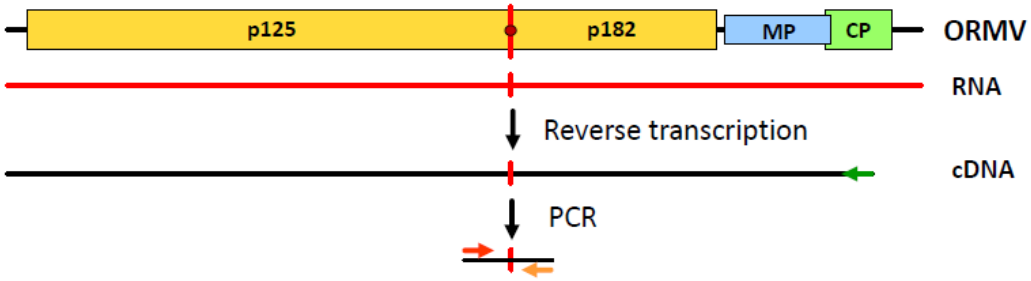

	Type	Transcript	Col-0 22 dpi	*rdr126* 22 dpi	*dcl234* 22 dpi	N. b. 5 dpi	N. b. 26 dpi
W41	Original	TAG CAA	TAG CAA	TAG CAA	TAG CAA	TAG CAA	-
W4	Original	TAG CAA	TAG CAA	TAG CAA	TAG CAA	TAG CAA	-
M41	Mutated	TAC CAA	TAA CAA (Major)	TAA CAA (Major)	TAA CAA (Major)	TAC CAA	TAC CAA (Minor rev)
M4	Mutated	TAC CAA	TAA CAA (Major)	TAA CAA (Major)	TAA CAA (Major)	TAC CAA	TAC CAA (Minor rev)

Fig. S1d. RT-PCR amplification and sequencing of viral RNA to examine the stability of the mutated stop codon of p125 *in planta*. RT-PCR analysis of viral RNA prepared from *A. thaliana* and *N. benthamiana* plants inoculated with wild-type or mutant viral constructs. The top panel shows a diagram of the ORMV genome, the positive sense genomic RNA transcribed from the ORMV constructs and replicated in infected plants (red line), the location of the primer (short green arrow) used to generate the cDNA (black line) and the location of the primers (orange and red arrows) used to generate a PCR amplicon containing the p125 stop codon (original, mutated, or reverted). The table below summarizes the RT-PCR sequencing results (shown in Fig. S1e,f). For each construct (W41, W4, M41, M41) the columns show the sequence context of the p125 stop codon (underlined) in the constructs used for *in vitro* transcription and the actual sequence of the codon obtained by sequencing of the viral RNA from the infected plants at 22 dpi for *A. thaliana* (Col-0) and its mutant

lines (*rdr126* and *dcl234*) and at 5 and 26 dpi for *N. benthamiana* (N.b.). Major and minor reversions of the p125 stop codon mutation are marked in red and orange.

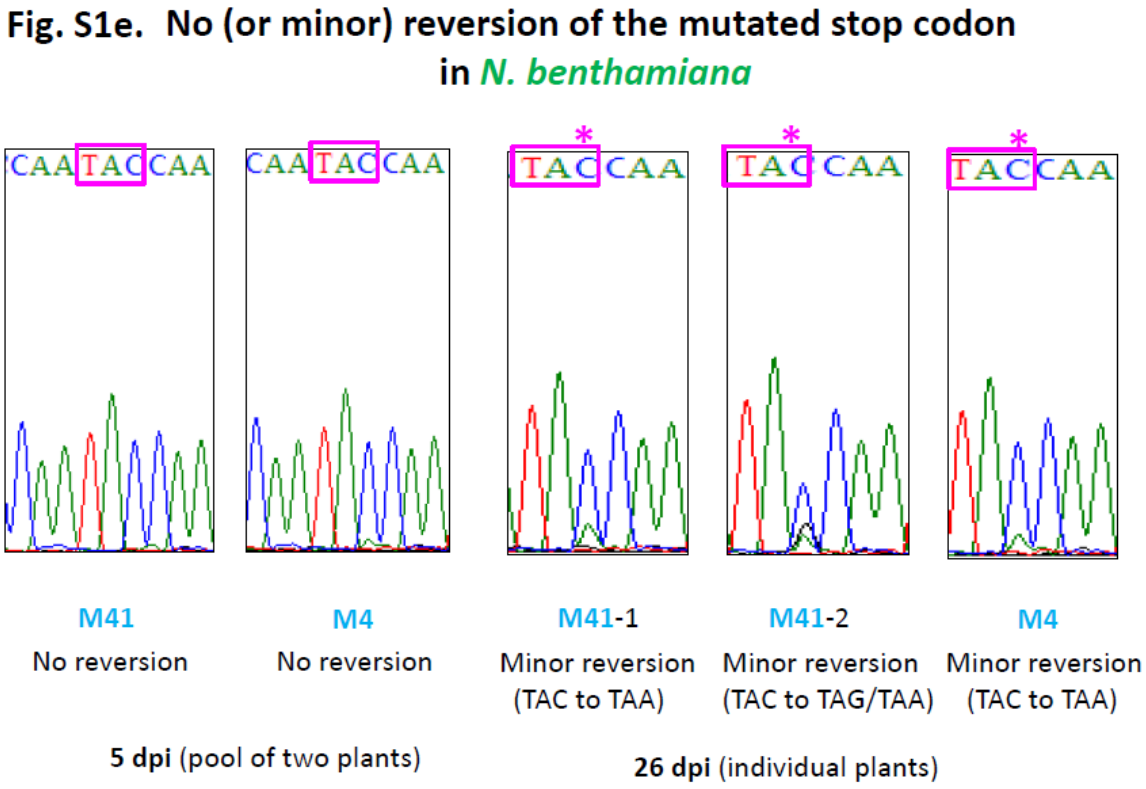

Fig. S1e. No (or minor) reversion of the mutated stop codon in *N. benthamiana*. Partial sequencing electrophoretograms of cDNA-PCR amplicons from viral RNA of *N. benthamiana* plants inoculated with the mutant ORMV constructs (M41 and M4) at 5 dpi and 26 dpi. The mutated stop codon of p125 is boxed and the peak showing a minor reversion to the stop codon is labeled with an asterisk.

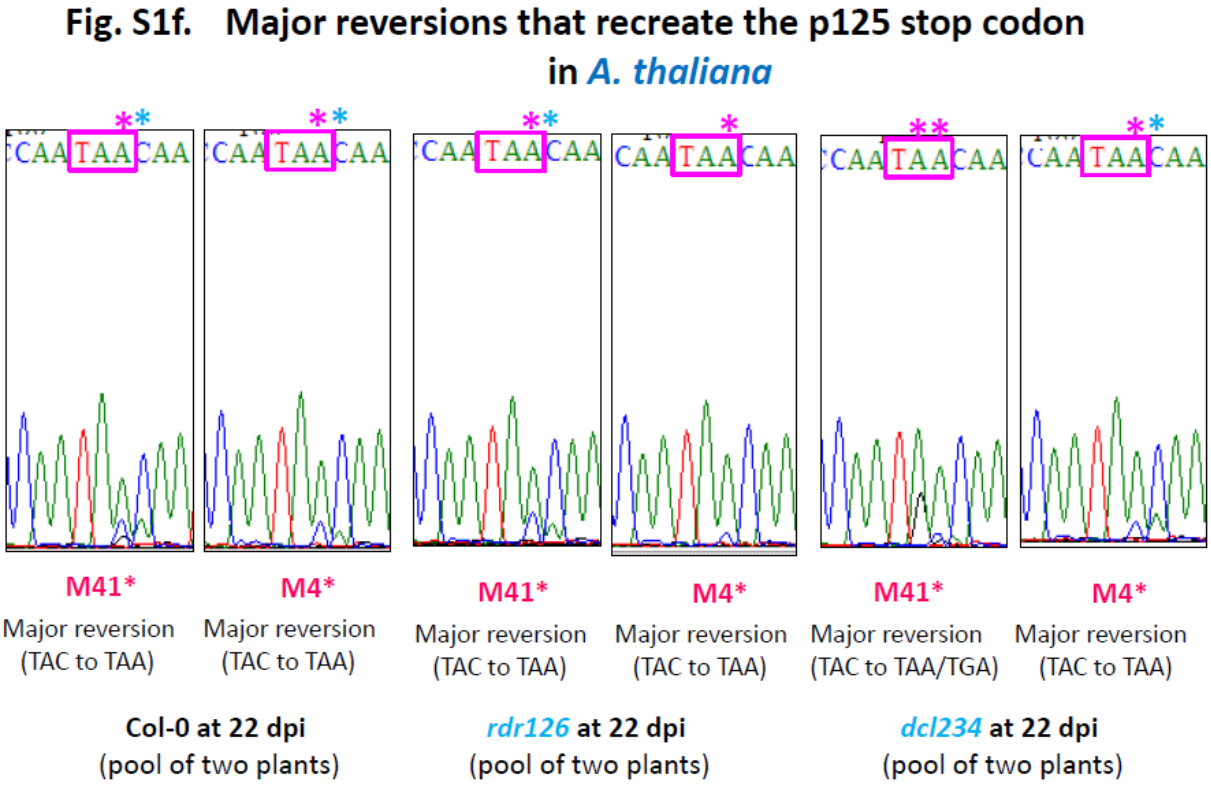

Fig. S1f. Major reversions recreating the mutated stop codon of p125 in *A. thaliana*. Partial sequencing electrophoretograms of cDNA-PCR amplicons from viral RNA of *A. thaliana* plants (Col-0, *rdr126* and *dcl234*) inoculated with the mutant ORMV constructs (M41 and M4) at 22 dpi. The mutated stop codon of p125 is boxed and the peak showing a major reversion to the stop codon is labeled with an asterisk.

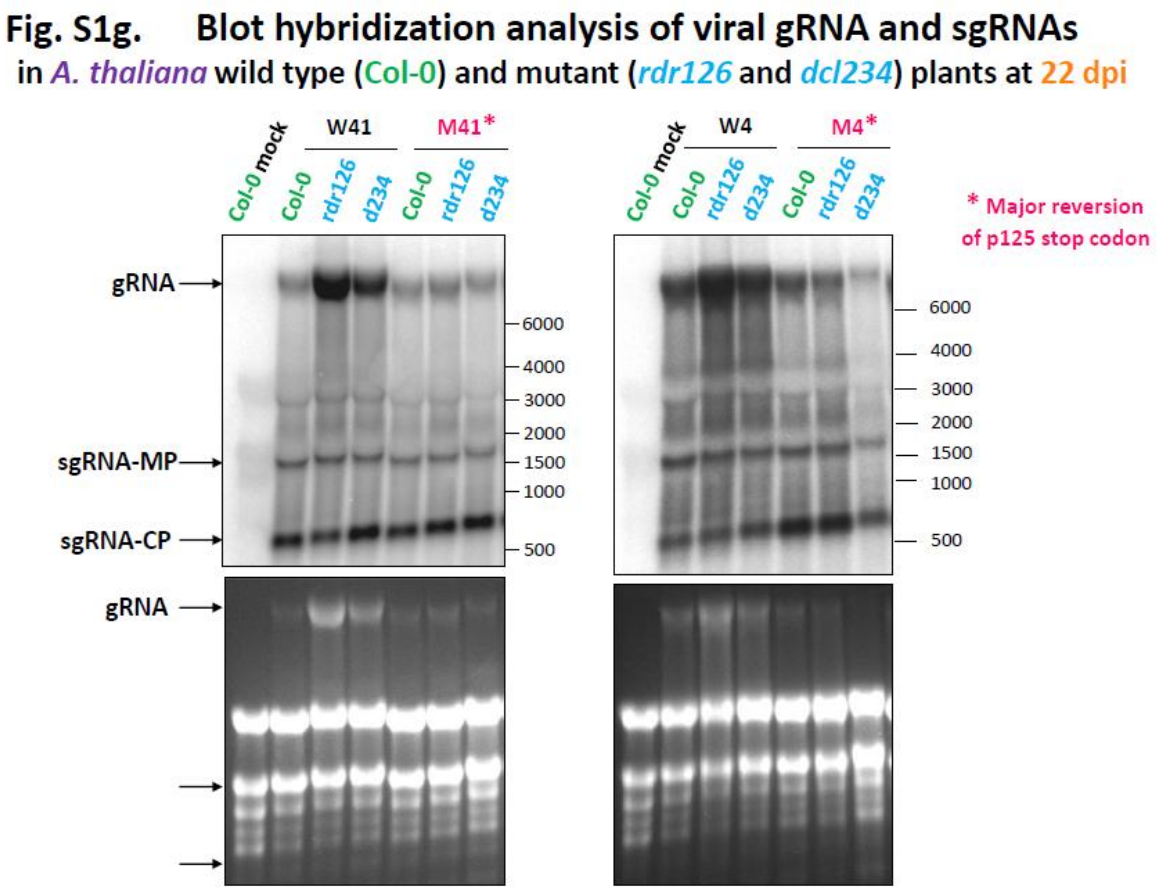

Fig. S1g. Blot hybridization analysis of 22 dpi viral gRNAs and sgRNAs in *A. thaliana* plants (Col-0, *rdr126* and *dcl234*) inoculated with *in vitro* transcripts from ORMV constructs (W41, W4, M41, M4). The top panels show long RNA analysis (in denaturing 1% agarose gels) of total RNA samples from a pool of two plants per construct. The blots show viral positive-sense RNAs (gRNA, sgRNA-MP, sgRNA-CP) detected by a probe specific for the CP region of the ORMV genome. The EtBr-stained gels used for the blots are shown below as loading controls. The positions of the gRNA, sgRNA-MP and sgRNA-CP are marked with arrows. Note that by 22 dpi, stop codon revertants had overtaken the initial population of mutant viruses (M41 and M4) in all the lines (Col-0, *rdr126* and *dcl234*, see Fig. S1f), thereby restoring p125 expression (see Fig. 1f).

Fig. S1h. Blot hybridization analysis of viral and endogenous sRNAs in *A. thaliana* wild type (Col-0) and mutant (*rdr126* and *dcl234*) plants at 22 dpi

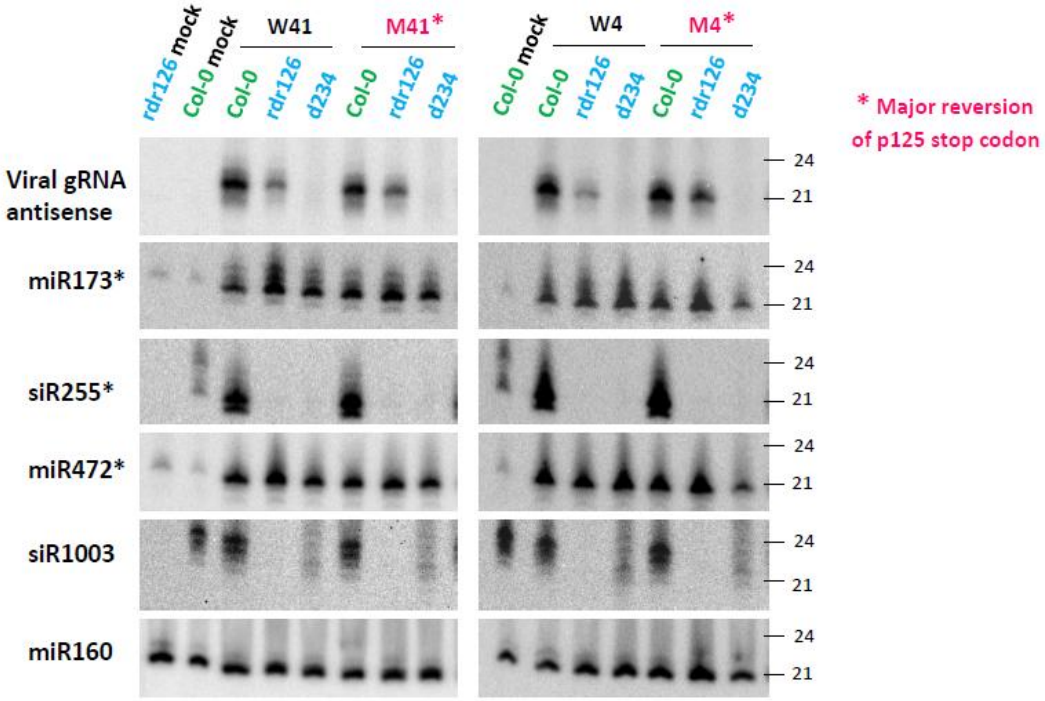

Fig. S1h. Blot hybridization analysis of 22 dpi viral and endogenous sRNAs from *A. thaliana* Col-0, *rdr126* and *dcl234* inoculated with *in vitro* transcripts from ORMV constructs (W41, W4, M41, M4). The panels show high-resolution sRNA analysis (15% PAGE) of total RNA samples from a pool of two plants per construct. The blots were successively hybridized with DNA oligonucleotide probes specific for viral antisense siRNAs derived from the ORMV p125 region as well as for plant miRNA (miR160), rasiRNA (siR1003), miRNA* (miR173*, miR472*) and tasiRNA * (siR255*) species. Note that by 22 dpi the stop codon mutation of viruses M41 and M4 has been fully reverted (see Fig. S1f), thereby restoring p125 expression (see Fig. 1f).

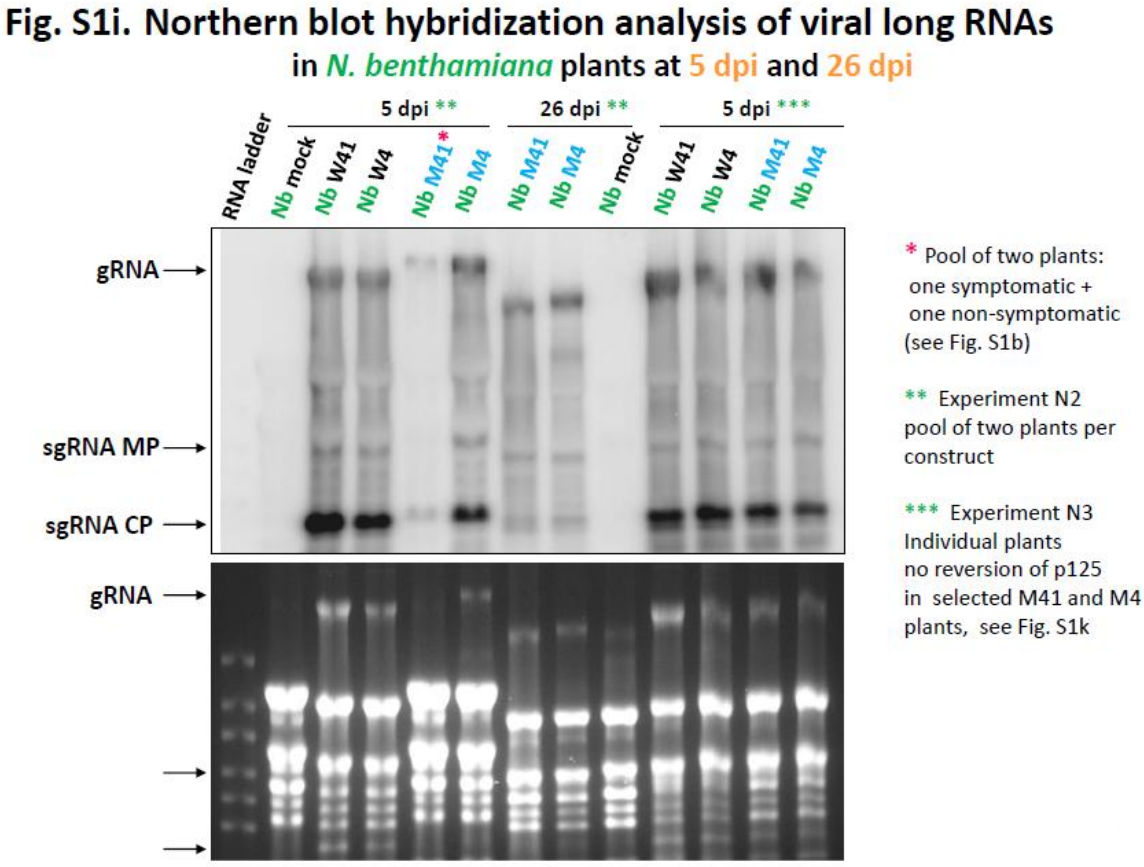

Fig. S1i. Blot hybridization analysis of 5 and 26 dpi viral long RNAs from *N. benthamiana* plants inoculated with *in vitro* transcripts from ORMV constructs (W41, W4, M41, M4). The top panel shows a long RNA blot (1% agarose denaturing gel electrophoresis) of total RNA samples from two experiments: in experiment N2, the RNA was extracted from a pool of two plants, while in experiment N3 it was extracted from individual plants selected on the basis of the Western blot data shown in Fig. S1k (plants indicated with black asterisks). The blots show ORMV positive-sense RNAs (gRNA, sgRNA-MP, sgRNA-CP) detected by a probe specific for the CP region of the ORMV genome. The EtBr-stained gel used for the blot is shown below as a loading control. The position of the gRNA, sgRNA-MP and sgRNA-CP species are marked with arrows. Note that in experiment N2 one of the two plants of pool M41 was asymptomatic (Fig. S1b, plant 1) and had not developed disease symptoms at 26 dpi.

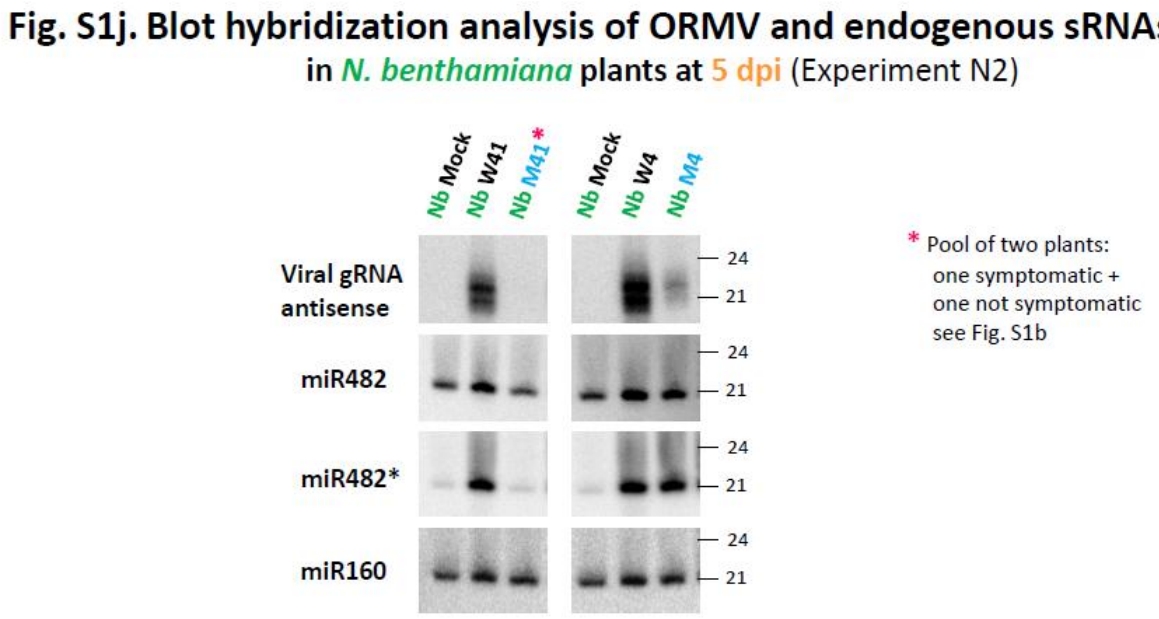

Fig. S1j. Blot hybridization analysis of 5 dpi viral and endogenous sRNAs from *N. benthamiana* plants inoculated with *in vitro* transcripts from ORMV constructs (W41, W4, M41, M4). The panels show high-resolution sRNA blots (15% PAGE) of total RNA samples from experiment N2 (pool of two plants per construct), hybridized successively with DNA oligonucleotide probes specific for the viral antisense siRNAs derived from ORMV p125 region, plant miRNAs (miR160 and miR482) and the * species of miR482 (miR482*). Note that in experiment N2 one of the two plants of pool M41 was asymptomatic (Fig. S1b, plant 1) and had not developed disease symptoms at 26 dpi.

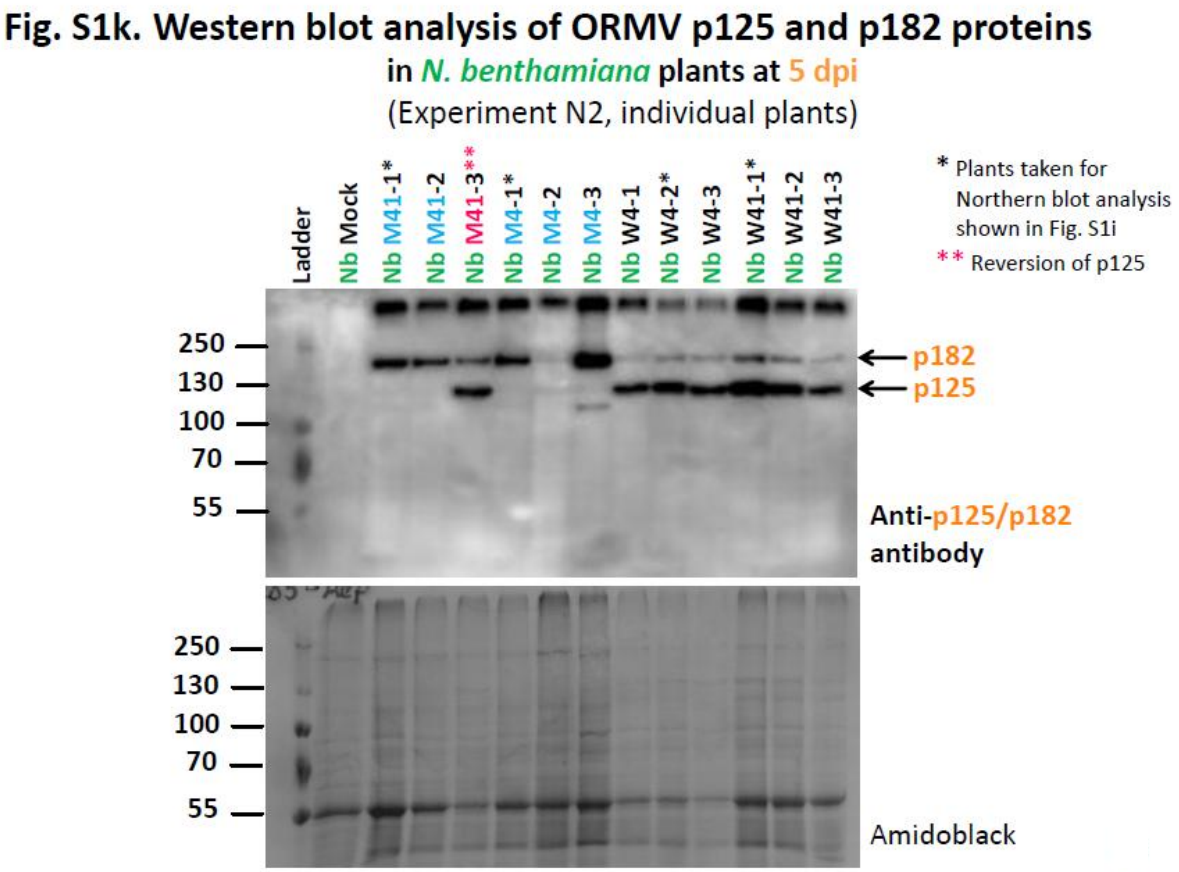

Fig. S1k. Western blot analysis of ORMV p125 and p182 proteins. Total protein samples were obtained from upper (systemic) leaf tissues of individual *N. benthamiana* plants at 5 dpi following inoculation with *in vitro* transcripts of the viral constructs M4, M41, W4 or W41 (3 plants per construct) and separated in a 9% SDS-PAGE gel. ORMV p182 and p125 were detected with a primary anti-p125 antibody (see Material and Methods). The AmidoBlack-stained membrane is shown below as a loading control. Note that in plants inoculated with W4- and W41-derived transcripts, both proteins were present (although p125 constituted the most abundant species of the two), while in plants inoculated with M4- and M41-derived transcripts only p182 was present, with the exception of plant M41-3 (indicated with red asterisks), where stop codon revertants overtook the mutant population and restored p125 expression. The black asterisks indicate the individual plants taken for the RNA blot hybridization shown in Fig S1i (Experiment N3).